NATIONAL ACADEMY OF SCIENCES OF UKRAINE
Palladin Institute of Biochemistry

BIOTECHNOLOGIA ACTA

Vol. 14, No 4, 2021

BIMONTHLY

Editorial address:
Palladin Institute of Biochemistry of the NAS of Ukraine, 9 Leontovich Street, Kyiv, 01601, Ukraine;
Tel.: +3 8 044–235–14–72; ***E-mail:*** biotech@biochem.kiev.ua; ***Web-site***: www.biotechnology.kiev.ua

According to the resolution of the Presidium of the National Academy of Sciences of Ukraine from 27.05.2009 №1-05 / 2 as amended on 25.04.2013 number 463 Biotechnologia Acta has been included in High Attestation Certification Commission list of Ukraine for publishing dissertations on specialties "Biology" and "Technology".

Certificate of registration of print media КВ series №19650-9450ПР on 01.30.2013

Literary editor — H. **Shevchenko**; Computer-aided makeup — **O. Melezhyk**
Authorized for printing 30.08.2021, Format — 210×297. Paper 115 g/m^2. Gaqrn. SchoolBookC. Print — digital. Sheets 11.6. An edition of 100 copies. Order 4.6. Make-up page is done in Palladin Institute of Biochemistry of the National Academy of Sciences of Ukraine. Print — **O. Moskalenko** FOP

NATIONAL ACADEMY OF SCIENCES OF UKRAINE
Palladin Institute of Biochemistry

BIOTECHNOLOGIA ACTA

Scientific journal

Bimonthly

Vol. 14, No 4, 2021

REVIEWS

Kryvoshlyk I., Skivka L.
Circulating tumor cells: where we left off? 5

Krasnopolsky Yu. M., Pylypenko D. M.
Biotechnological research in the creation and production of antirabic vaccines 28

Aralova N. I., Klyuchko O. M., Mashkin V. I., Mashkina I. V., Radziejowski Paweł, Radziejowska Maria
Mathematical model for the investigation of hypoxic states in the heart muscle at viral damage 38

EXPERIMENTAL ARTICLES

Yaroshko O. M., Kuchuk M. V.
Transient expression of reporter genes in cultivars of *Amaranthus caudatus* L. 53

Sych N. V., Kotyns'ka L. I., Vikarchuk V. M., Farbun I. A.
On the possibility of using carbon enterosorbents to normalize cholesterol metabolism 64

Hovorukha V. M., Havryliuk O. A., Bida I. O., Danko Ya. P., Shabliy O. V., Gladka G. V., Yastremska L. S., Tashyrev O. B.
Two-stage degradation of solid organic waste and liquid filtrate 70

Sabliy L., Zhukova V., Konontsev S., Obodovych O., Sydorenko V.
Problems of soapstock treatment of vegetable oil productions and their solutions 80

НАЦІОНАЛЬНА АКАДЕМІЯ НАУК УКРАЇНИ
Інститут біохімії ім. О. В. Палладіна

BIOTECHNOLOGIA ACTA

Науковий журнал

Том 14, № 4, 2021

ОГЛЯДИ

Кривошлик І., Сківка Л.
Циркулювальні пухлинні клітини: на чому ми зупинилися? 5

Краснопольський Ю. М., Пилипенко Д. М.
Біотехнологічні дослідження при створенні
та у виробництві антирабічних вакцин 28

Аралова Н. І., Ключко О. М., Машкін В. І., Машкіна І. В., Radziejowski Paweł, Radziejowska Maria
Математична модель для дослідження гіпоксичних станів серцевого мяза
за вірусного ураження 38

ЕКСПЕРИМЕНТАЛЬНІ СТАТТІ

Ярошко О. М., Кучук М. В.
Транзієнтна експресія репортерних генів у сортах *Amaranthus caudatus* L. 53

Сич Н. В., Котинська Л. Й., Вікарчук В. М., Фарбун І. А.
Про можливість використання вуглецевих ентеросорбентів
для нормалізації холестеролового метаболізму 64

Говоруха В. М., Гаврилюк О. А., Біда І. О., Данько Я. П., Шаблій О. В., Гладка Г. В., Ястремська Л. С., Таширев О. Б.
Двоступенева деградація твердих органічних відходів та рідкого фільтрату 70

Саблій Л., Жукова В., Кононцев С., Ободович О., Сидоренко В.
Проблеми очищення мильних соапстоків олійних виробництв
та їх вирішення 80

UDC 576.522; 576.523; 576.385.5; 571.27; 616-006
https://doi.org/10.15407.biotech14.04.005

CIRCULATING TUMOR CELLS: WHERE WE LEFT OFF?

I. KRYVOSHLYK, L. SKIVKA

ESC "Institute of Biology and Medicine" Taras Shevchenko National University of Kyiv, Ukraine

E-mail: skivkalarysa964@gmail.com

Received 27.06.2021
Revised 12.07.2021
Accepted 31.08.2021

Cancer metastasis and recurrence are the leading causes of cancer-related death. Tumor cells which leave the primary or secondary tumors and shed into the bloodstream are called circulating tumor cells (CTC). These cells are the key drivers of cancer dissemination to surrounding tissues and to distant organs. The use of CTC in clinical practice necessitates the deep insight into their biology, as well as into their role in cancer evasion of immune surveillance, tumor resistance to chemo- radio- and immunotherapies and metastatic dormancy.

Aim. The purpose of the work was to review the current knowledge on the CTC biology, as well as the prospects for their use for the diagnosis and targeted treatment of metastatic disease.

Methods. The work proposed the integrative literature review using MEDLINE, Biological Abstracts and EMBASE databases.

Results. This review summarizes and discusses historical milestones and current data concerning CTC biology, the main stages of their life cycle, their role in metastatic cascade, clinical prospects for their use as markers for the diagnosis and prognostication of the disease course, as well as targets for cancer treatment.

Conclusions. Significant progress in the area of CTC biology and their use in cancer theranostics convincingly proved the attractiveness of these cells as targets for cancer prognosis and therapy. The effective use of liquid biopsy with quantitative and phenotypic characteristics of CTCs is impeded by the imperfection of the methodology for taking biological material and by the lack of reliable markers for assessing the metastatic potential of CTCs of various origins. The variety of mechanisms of tumor cells migration and invasion requires the development of complex therapeutic approaches for anti-metastatic therapy targeting CTCs. Efforts to address these key issues could help developing new and effective cancer treatment strategies.

Key words: circulating tumor cells; circulating tumor microembols; metastasis; epithelial-mesenchymal transition; minimal residual disease.

Cancer is the second leading cause of death in the world after cardiovascular diseases. Experts estimate that cancer rates have risen to 2.7 million cases (all types of cancer except non-melanoma skin cancer) and led to 1.3 million deaths in 2020 in the European Union [1]. The Cancer Statistics 2020, published in the peer-reviewed journal of the American Cancer Society CA: A Cancer Journal for Clinicians, reported 180,690 cancer cases and 6,065,20 deaths, which is about 4,950 cases and more than 1,600 deaths daily [2]. In Ukraine, incidence of cancer per 100 000 population is ~384.7 cases according to the data from Bulletin of National Cancer Registry of Ukraine (No 21).

The main cause of death in ~80% of cancer cases is the development of relapses and metastases. This actualizes the search for reliable markers for the assessment and prediction of the course of oncological pathology, as well as for the development of methods and means of prevention and treatment of cancer recurrence and metastatic

disease. Attractive candidates for the role of such markers are tumor cells that separate from the primary node and circulate in the blood and lymphatic vessels — the circulating tumor cells (CTC). That is why CTC are called “pioneers” of tumor origin, which are responsible for the metastatic spread of cancer.

The study of the CTC biology is important both in terms of improving the knowledge about the biology of cancer, and applying the acquired knowledge in clinical practice for the development of targeted treatments for cancer. The problem of studying the CTC dates back to antiquity, i.e., since the time of Hippocrates, when such pathology as cancer was first established, the search for effective treatments of which is still relevant today. The importance and prospects of this scientific area is evidenced by the long period of its study with the growing number of publications in the scientific literature and the involvement of specialists in various fields of biology and medicine: from cytologists, geneticists and biochemists to biophysicists, molecular biologists and immunologists.

This review summarizes and discusses historical milestones and current data concerning CTC biology, the main stages of their life cycle, the significant role of CTC in metastasis, the methods of their study and clinical prospects for their use as markers for the diagnosis and prognostication of the disease course, as well as targets for cancer treatment.

Historical milestones in the study of circulating tumor cells

The ability of a malignant neoplasm to spread systematically was first mentioned in ‘Humoral Theory’ of Hippocrates — the “father of medicine”, who described not only the term “cancer” but also singled out its ability to grow, be surrounded by blood vessels, and its immune infiltration (Fig. 1) [3].

The long period from the death of Hippocrates to the Middle Ages was famous for a number of works devoted to the study of tumors and the problem of cancer treatment, which are still questionable in their usefulness. It was not until the middle of the 18th century that Henri Le Dran (1685–1770), a leading French physician, realized that cancer was not only a systemic disease, as Hippocrates believed, but was local with gradual progression. In 1757, Le Dran suggested that

Fig. 1. **Chronological periodization on the study of circulating tumor cells from ancient times to the present**

From left to right: Hippocrates (460–370 BC), Henri Le Dran (1685–1770), Joseph Récamier (1774–1852), Bernhard von Langenbeck (1810–1887), Rudolf Virchow (1821–1902), Karl Thiersch (1822–1895), Thomas Ramsden Ashworth (bef. 1830–1876), H. C. Engell (1921–2011), Judah Folkman (1933–2008), Lance A. Liotta (born July 12, 1947), Peter C. Nowell (1928–2016), Napoleone Ferrara (born 26 July 1956), Pantel Klaus (born 3 August 1960), new era of CTC research, which is characterized with the most sensitive methods of detection (1998–currently). Red threshold signifies a big step towards understanding a significance of tumor angiogenesis

surgery should take place before the tumor could metastasize through the lymphatic system and affect other parts of the body [4].

Recamier (1829) and later Thiersch (1865) were among the first to report the invasion of malignant cells into the veins and lymphatic vessels of a patient with basal cell carcinoma of the skin (BCC). In 1841, Langenbeck's experimental data obtained by microscopy provided conclusive evidence for the presence of tumor cells in the bloodstream.

In 1858 Virchow's generally accepted theory emerged. It explained metastasis by tumor emboli arrest in the vascular network. Eleven years later, Thomas Ashworth, who performed an autopsy on a patient who had died of metastatic cancer, reported the presence of circulating cells in his subcutaneous vein, similar in morphology to the primary tumor cells. This observation provided further evidence of the ability of individual tumor cells to migrate to blood vessels etc. [5–9].

The work of Engell et al., 1955 on the detection of tumor cells in peripheral blood in cancer patients, is considered to be more "mature" in this scientific direction. This research group found that in 61% of cases of tumor cells in blood samples, their presence was associated with a low degree of tumor differentiation (≤ G3). Because 51% of patients who survived 5 to 9 years after tumor resection had circulating tumor cells, Engell suggested that "these cells must spread into the bloodstream before or during surgery" [10].

The next step in the progress of the theory of circulating tumor cells was the elaboration of experimental models of metastasis in the 70s of the previous century. However, metastases were generally considered at this time as a late event in the development of epithelial tumors. Subsequently, Pantel et al. [11, 12] using the methods of immunohistochemistry, concluded that there is a common phenomenon of early spread of isolated tumor cells for non-small cell lung cancer. In addition, this scientific group has shown that in carcinomas of the breast and gastrointestinal tract, most disseminated tumor cells in the bone marrow of patients are at rest.These scientists also performed an important observation on the detection in histological specimens of tumors of lung cancer patients without metastases. It was found out that a significant proportion of cytokeratin-positive cells were present compared with specimens of patients with metastases.

A rather interesting theory was proposed by Nowell (1976), known as the "model of somatic evolution" [13]. According to this model, metastatically competent disseminated cells are considered as central players in the extremely complex phenomenon of metastasis, where genetic variability and selection of the most aggressive and adapted clones in tumor tissue determines the consistent of the population of malignantly transformed cells and the ability of individual representatives to spread.

Further in a series of pioneering experiments, Folkman et al. [14, 15] identified the critical role of angiogenesis in the metastatic cascade. Folkman himself theorized that tumors need constantly new blood vessels, and thus trigger certain mechanisms of their formation to provide rapidly proliferating cell mass with the necessary oxygen and nutrients. This was the beginning of a scientific field devoted to the study of tumor angiogenesis. However, the scientist's ideas were not approved by the scientific community until in 1980 when Napoleone Ferrara, a scientist at the biotechnology company Genentech, discovered the vascular endothelial growth factor (VEGF), a cytokine that stimulates the formation of new blood vessels.

Folkman's scientific research was continued by Liotta, who proved that there is a balance between factors that stimulate angiogenesis and inhibits this process. They are both secreted by the tumor cells themselves and cells of the tumor microenvironment. By modeling a course of fibrosarcoma in mice daily, the scientist observed a linear correlation between the density of perfusion vessels and a growth of the proportion of tumor embolus cells (four or more). The studies above have shown that vascularization of tumor tissue and the concomitant process of tumor complexes entering the bloodstream are closely related and critical events in the initiation of metastasis [16, 17].

These and many other experimental works and clinical observations have initiated a new era in the study of malignant tumors, associated with the investigation of the origin, phenotypic and functional characteristics, detection methods and clinical significance of CTC.

Epithelial-mesenchymal transition in the life story of the circulating tumor cells

Tumor is a localized mass of malignant cells that contains transformed cancer cells, stromal cells, and cells that infiltrate the tumor. In the process of malignancy, tumor cells acquire a number of common properties: the potential to proliferate in the absence of

exogenic growth factors, the ability to resist pro-apoptotic stimuli, the capacity to stimulate angiogenesis, etc.

Genetic instability of tumor cells is caused by constant errors in chromosome segregation during mitosis, as well as external selective pressure of the microenvironment, including immune surveillance with the need to adapt to it. By acting together, these factors create a basis for the formation of a heterogeneous population of primary tumor cells [18, 19].

Different cells in such heterogeneous population are specialized on the development of one or another tumor property, which determines their fate in the pathological process. For example, an exceptional ability to proliferate locally using autocrine signals guarantees a tumor cell the fate of the cell that creates a mass of the primary tumor, i.e., the destiny of the bulk tumor cell.

A small part of the cells of the heterogeneous population of the primary tumor in a course of their development acquires completely different properties. They lose intercellular contacts, but instead gain the ability to invade the local microenvironment, they intravasate into blood and lymphatic vessels, from which these cells extravasate back into the tissue. Such characteristics are typically unsuitable for local clonal expansion, that is why these cells became 'travelers', or CTCs, due to their feature to initiate foci of tumor growth at a distance from the primary tumor. One of the key events in the life cycle of the CTC is the epithelial-mesenchymal transition (EMT), which was identified by Hanagan and Weinburg as one of cancer features [20].

EMT was discovered in 1982 by Greenberg and Hay [21]. It is the process of a complete loss of the epithelial features and an acquisition of a mesenchymal phenotype by former epithelial cells.

Epithelial cells are characterized by a flat, cubic, cylindrical shape, they are also distinguished by polarity, that is the part of the cell which is located in the area of contact with the basement membrane, differs in a structure from the apical part. The epithelial cells are connected by tight junctions (TJs), gap junctions, adhesive (containing a stretched actin belt) and desmosomal contacts, which cause both linearization of location and tight fit of cells to each other [22].

In contrast to epithelial cells, mesenchymal cells are spindle-shaped and are connected by weak integrin focal contacts with the glycoprotein matrix. At the same time, the mesenchymal morphology of cells guarantees their ability to move. In order to migrate elsewhere, the cell must first get through the surrounding tissues, and then appear in the delocalized areas of the basement membrane. Movement in such conditions is used with the help of specialized structures — invadopodia, which are formed as the result of a membrane's evagination (protrusion) [23].

Despite the detailed description of morphological and functional differences between epithelial and mesenchymal cells, a precise list of phenotypic characteristics that distinguish these cells still remains unformed, and the existing one is contradictory [24].

During EMT activation, epithelial cells lose apico-basal polarity due to spontaneous polymerization of actin fibers and the movement of microtubules. This process requires a rupture of cellular connections (occlusal and adhesive contacts), delocalization of proteins and subsequent reorganization of the cytoskeleton to obtain cellular plasticity [25–27].

Such rearrangements occur when a signal is received from Rho and Rac1 proteins belonging to the GTPase family, which are localized in the posterior and anterior parts of the cell, respectively. Activation of Rac1 mediates cell polarization and lamellipodia formation, while high Rho GTPase concentrations increase the level of actomyosin contractility [28, 29]. Further events are followed by the expression of mesenchymal markers — vimentin, N-cadherin, F-actin, nuclear beta-catenin and others, whereas such markers as cytokeratins 8, 18 and 19, E-cadherins, Mucin-1, occludins, desmoplakinins are thought to be purely epithelial (Fig. 2). Although EMT is subject to a general program, this process is characterized by flexibility and variability, depending on cell type, tissue microenvironment, and the extremely complex multicomponent and closely interconnected set of transcriptional and posttranscriptional, translational and posttranslational signaling pathways, including Hadgehog-, Wnt-, TGF-β-, bone morphogenetic protein (BMP)–, SMAD-depending (and independing), etc. [30]. EMT is a reversible process. The reverse process is called mesenchymal-epithelial transition (MET) [31–33]. Normally, MET is characteristic of pluripotent stem cells [34, 35].

The problem of signaling, which regulates EMT, still remains the least studied. However, today, depending on the biological conditions in which epithelial-mesenchymal transition occurs, there are three functional subtypes of this process. The first is associated

with embryogenesis (gastrulation period), implantation and organ development in Vertebrates. This type of EMT results on theformation of different types of cells, which can be exposed to MET with the derivation of secondary epithelial cells during embryogenesis. Distinctive features of this type of EMT are the absence of fibrosis and cell invasion.

The second type of EMT is associated with wound healing, tissue regeneration and fibrosis of the internal organs. The result of EMT of this type, is formation of fibroblasts and other related cells, which are necessary for tissue repair after wounds and inflammatory injuries. This type of EMT is characterized by the presence of fibrosis, but not invasion. The third type of EMT is inherent in the tumor process, during which the generated cells retain epithelial features simultaneously with the acquisition of mesenchymal characteristics, as well as tumor cells of the mesenchymal type as the consequence. Distinctive features of EMT of this type are invasion and metastasis [36, 37].

The study of the third type of EMT revealed new changes that are induced by this process, but which are not always observed (inhibition of epithelial phenotype gene expression with simultaneous increase in mesenchymal gene expression and resistance to apoptosis and cellular aging), and the fact that EMT is a dynamic process with the existence of intermediate metastable states.

The third type of EMT is associated with oncogenesis. It can be considered as an aberrant variant of this process. In this pathological condition, the ability of mesenchymal tumor cells to avoid activation of anoikis (process of apoptotic cell death that occurs due to insufficient cell-matrix interaction) and immune surveillance are associated with genes activated by EMT [38–40].

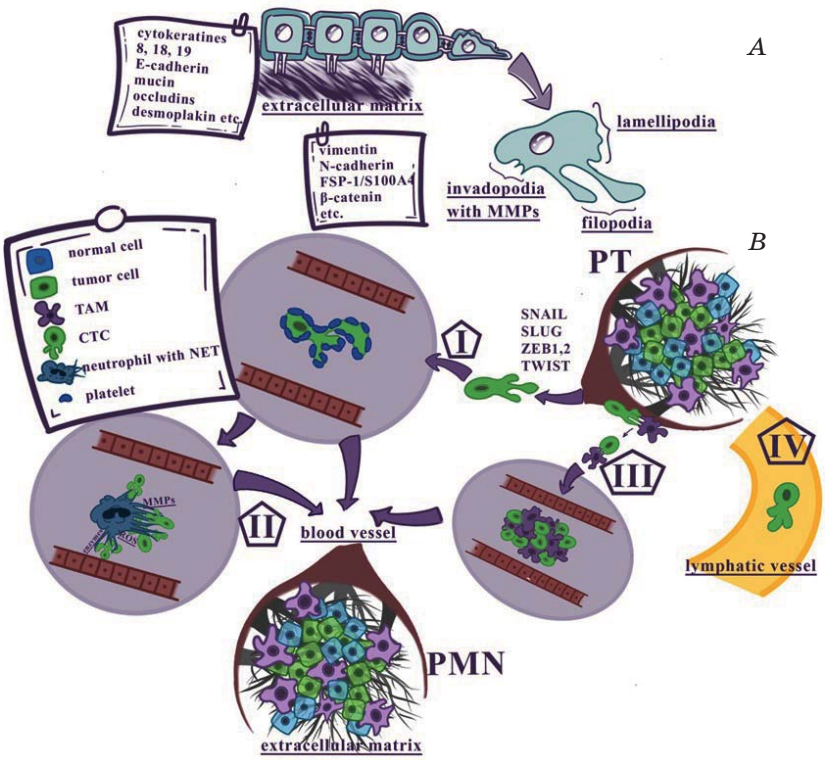

Fig. 2. **The epithelial-mesenchymal transition (EMT) and CTC strategies for the dissemination:**
A — in health condition (embryogenesis, implantation and organ development), epithelial cells lose their phenotypic markers and connections with the cell matrix, and gradually acquire mesenchymal phenotype and form membrane invaginations for the ability to move freely; *B* — incancer, tumor cell high mutagenesis along with signals from the microenvironment create the necessary prerequisites for the EMT and tumor cell dissemination using different strategies: *I* — single CTC moves independently and uses platelets to create protective shield; *II* — Single CTCs can use NET extrusion by activated neutriphils in order to create circulating tumor microemboli (CTM) straight in the blood; III — CTM can be formed within the primary tumor before entering the blood flow. In order to move freely throughout small blood vessels, cells in the microemboli "line up" in the chain without losing adhesive bonds; IV — CTC can also disseminate throug the lymphatic vessels; MMP — matrix metalloproteinases; NET — neutrophil extracellular trap; ROS — reactive oxygen species; PMN — perivascular metastatic niche; PT — primary tumor

The course of EMT during tumor progression is supported by the involvement of cytokines (VEGF, PDGF and TGF-β), which are secreted by cells of the microenvironment, including tumor-associated macrophages (TAM) — resident tumor macrophages polarized to the M2 phenotype. It is now known that TAMs are activators of malignant progression of the primary tumors. They are involved in the activation of metastasis and make a significant contribution to the adhesive integrity of the tumor stroma. A distinctive feature of TAM with this capacity permitting is the high level of expression of the transcription factor ZEB1, which provides activation of tumor metabolic pathways of these phagocytes [41–43].

Transcription factors ZEB1, ZEB2, TWIST1, Snail, Slug, SIX1, E47, ELF5, FOXC2, GRHL2, p53, p63 etc. of the tumor cells are components of signaling pathways involved in the process of their epithelial-mesenchymal transition. After phosphorylation by protein kinases, these transcription factors and the corresponding co-regulators inhibit the expression of epithelial phenotype genes in the tumor cells. This leads to the formation of a mesenchymal phenotype with reduced expression of epithelial adhesion molecules (EpCAM) and cytokeratins (CK), promotes invasion, dedifferentiation and the ability to intravasate into lymphatic and blood vessels [44]. This is how the CTC population appears.

In addition to transcription factors, anothertrans-regulatory elements — miRNA — also participate in complex EMT phenomenon. Moreover, transcription factors interact with miRNA in this sophisticated process, and can create a feedback or feed-forward loop providing cross-gene regulation network [45]. Deep insight into this network may provide a new therapeutic opportunity in cancer treatment.

The primary tumor contains cells that are at different stages of EMT with diverse invasive, metastatic properties and various degrees of differentiation. Tumor cells at varied stages of EMT are localized in different microenvironments and in contact with different stromal cells. In particular, cells with the most pronounced mesenchymal phenotype proliferate near endothelial cells and immune cells with an inflammatory metabolic profile.

Tumor cells at this stage secrete large amounts of chemokines to recruit immune cells and stimulate angiogenesis, thus contributing to the formation of a unique inflammatory and highly vascularized niche. The most effective in the circulation, as well as in the colonization of the distant metastatic niche and the development of metastases, are CTC, which express a mixture of epithelial and mesenchymal phenotypic markers (EMT-CTC) [46].

The life cycle of the CTC requires from them an extreme stress resistance, which is provided by the special genetic, phenotypic and metabolic properties of these cells.

The unique properties of CTC

By definition, CTC are a type of malignant cells that separate from both primary tumor that exists in a body and reaches a few millimeters, and the secondary tumor [47]. CTC enter the blood or lymph through the dense walls of blood vessels, spreading further to other parts of the human body, which become secondary foci of tumor growth [48].

There are different biological phenotypes of CTC: epithelial, mesenchymal, stem cell-like or cells with a mixed phenotype, depending on the stage of EMT [49, 50].

CTC has certain characteristics regardless of the stage of EMT, which distinguish them from stationary tumor cells and allow them to perform their assigned functions of dissemination of the tumor process under the action of numerous stressors:

- ability to separate from tumor tissue;
- ability to resist anoikis activation after separation;
- ability to migrate to blood and lymph vessels;
- ability to maintain viability under hemodynamic stress;
- ability to avoid immune surveillance;
- ability to attach and proliferate in a new tissue microenvironment.

Where do cells with such an exceptional set of properties in the composition of tumor tissue come from? According to the generally accepted hypothesis, CTC originate from stem tumor cells (Cancer Stem Cells, CSC) and differ from them in some features acquired as a result of unique mutations [51, 52].

The circulating tumor cells inherit from the CSC an ability to self-renewal and remain dormant (anabiosis can last from several years to decades), as well as the ability to differentiate into cells with different phenotypes, which enables them to initiate tumor growth in the secondary location. There are several mechanisms for acquiring the following unique properties by CTC:

- genetic or internal mechanisms (high level of mutagenesis with aberrant gene

expression, redistribution of gene expression induced by EMT, "stem-like" properties inherited from CSC);

• influence of the tissue microenvironment of the primary tumor (tumor-associated hypoxia, tumor exosomes, cytokine profile produced by TAM, myeloid-derived suppressor cells (MDSC) and tumor-associated fibroblasts (TAF));

• influence of circulating blood microenvironment (immunosuppressive, promigatory cytokine profile, interaction with platelets, neutrophils, monocytes, natural killer cells (NK), regulatory T cells (Treg), etc.);

• clustering.

Increased mutagenesis and aberrant gene expression in circulating tumor cells result in overexpression of dormancy-related genes, genes associated with increased survival (e. g., survivin gene), and immunosuppressive genes (e. g., PDL-1) [53]. Recently, special attention has been paid to the influence of the circulating blood microenvironment and clustering of CTC.

An important event happens when CTC, by undergoing hemodynamic pressure in the circulating blood, change their metabolism. It is followed by increased generation of reactive oxygen species (ROS) [54, 55]. ROS-dependent signaling enhances the expression of antioxidant enzymes (superoxide dismutase, catalase and glutathione peroxidase), and promotes the transmission of mitogenic signals, which contribute together to the survival of the circulating tumor cells under stress. In addition, ROS have an immunosuppressive effect and promote the differentiation of naive T cells to Treg, and immature myeloid cells — to MDSC [56].

Despite the stress resistance acquired upon mutations and aberrant gene expression, CTC still need to secure movement to the tissue niche and form metastases in the aggressive microenvironment of circulating blood. EMT gives CTC the ability to separate from the primary tumor and to invade surrounding tissue using so-called mesenchymal movement pattern, which involves the destruction of the extracellular matrix. Vasoactive mediators, such as VEGF, produced by microenvironmental cells, in particular TAM, increase vascular permeability, which promotes intravasation of the circulating tumor cells. TAM reconstruct the ECM, which facilitates the movement of CTC to the vessel [57]. Taken together, all this leads to a single CTC entering the bloodstream. Besides, tumor cells that have already passed through EMT but are encounting microenvironmental or xenobiotic stress (e.g. cytotoxic agents), can use mesenchimal-amoeboid transition (MAT) in order to evade the stress. MAT is the most primitive and most efficient movement mechanism, that does not involve destruction of the extracellular matrix and is based on highly deformable cell morphology. This tumor cell migration plasticity allows them to adapt to different environmental conditions and to disseminate to long distance [58, 59]. It is logical to assume that the simultaneous effect on mesenchymal and amoeboid motility may be more effective in preventing the process of metastasis [61].

The cells that have separated from the tumor mass and move alone have a higher migration rate, but they are effectively attacked by the immune surveillance system, experience greater hemodynamic pressure and have an increased risk of anoikis activation [61]. Due to this, less than 0.1% of single CTCs remain viable 1–2.5 h after circulation. The mechanism to avoid such rapid death is the clustering of circulating tumor cells — the formation of dense conglomerates of cells, or tumor microemboli, which include a minimum of 3, maximum 100, usually — 20–30 cells.

Currently, it is supposed that CTC microemboli can be either formed with in the primary tumor before entering the blood flow or within the circularly system [62]. At the same time, the rather large size of the cluster set up before entering the circulatory system does not prevent it from moving freely throughout small blood vessels due to the ability of cells in the microemboli to "line up" in the chain without losing adhesive bonds (Fig. 2). Intercellular bonds in circulating tumor microemboli (CTM) are formed by placoglobin (γ-catenin, which is a member of the Armadillo family of proteins and a paralog of β-catenin, an intracellular component of adhesive and desmosomal contacts), which also provides additional stress resistance of clusters during their transit into the blood [63, 64].

The composition of the microemboli is heterogeneous at the genetic, transcriptomic, proteomic and metabolic levels and contains not only tumor cells but also tumor stroma cells, such as TAM [65]. The latter make a significant contribution to the adhesive integrity of the structure. The formation of CTM is also possible in the circulatory system. Circulating neutrophils become important partners of the tumor cells in this structure. It concerns those neutrophils which are activated before NET extrusion or NETosis — the release of a network

containing mitochondrial or nuclear DNA, and the components like antimicrobial peptides, reactive oxygen species, enzymes, etc. into the extracellular space [66–68].

In spite of the large number of works concerning the study of the role of stromal cells in CTM, both the list of functions and phenotype of these cells have been insufficiently studied [69]. A crutial role in the structure of CTM is played by platelets that surround them in the form of the so-called "shield". Thrombocytes provide protection against the recognition of tumor cells by immunocompetent cells, prevent their lysis by NK cells.

When CTM moves, it is later "stuck" in the capillaries, which serve as a kind of "catcher" of malignant cells, platelets lead to a state of hypercoagulation and the formation of vascular thrombi, which are a hallmark of hematogenous spread of malignant tumors. In addition, the release of platelet granules, which contain vasoactive, antiapoptic and other biologically active mediators, is a way of apoptotic resistance of CTM cells, promotes their survival and increases metastatic potential many times [70, 71].

The movement of single CTC in the circulating system can be identified with the movement of cars during a rally, where the winner is the one who overcomes the path "from point A to point B", which is not always associated with a high level of safety. Coordinated CTM migration is reminiscent of car traffic provided that the prescribed traffic rules are followed and a mandatory stop at the red light — it is slower but secured by coordinated community action and provides more guarantees of reaching the final destination (Fig. 3).

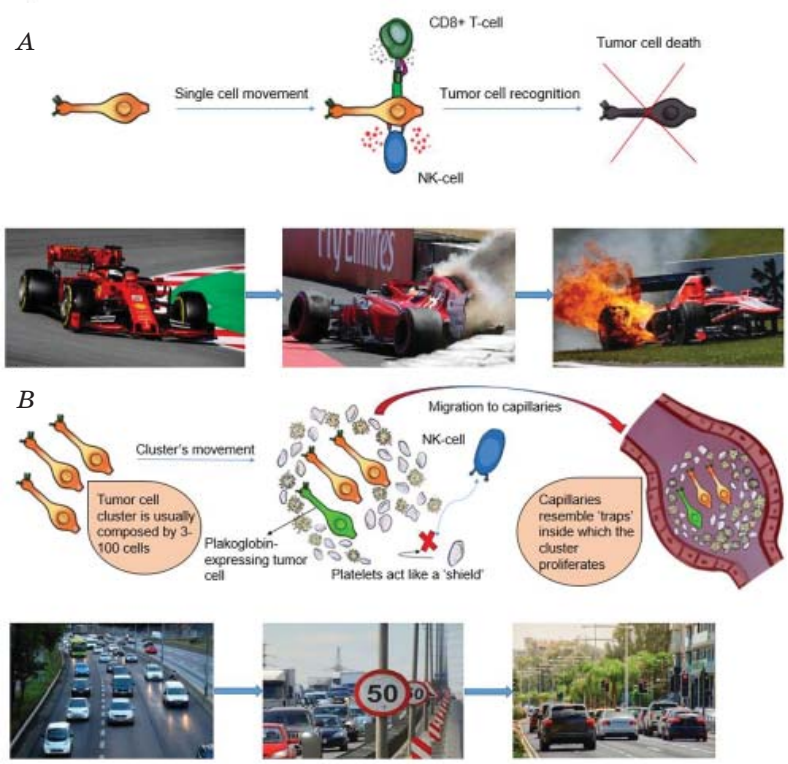

Fig. 3. **Interpretation of the movement of single circulating tumor cell vs tumor microemboli:**
A — The circulating tumor cell, which was recently shed from a primary tumor and actively moves through the blood flow has lack of survival mechanisms and thus successfully recognizes and attacks by the main cells of immune antitumor surveillance (CD8+T-cells and NK cells). This way the majority of single-moving CTC risk to be either subjected to the mechanical damage or anoikis in the blood circulation.The same events are happening when audience watches live streaming of Formula 1. It is often questionable whether a F1 car can survive a rally stage, because driving at the high speed enhances probability of the car crash. *B* — the circulating tumor microemboli have high potency to survival during the transit in the blood stream due to molecular and cellular mechanisms. Being coated with thrombocytes, CTM are endowed with an ability to avoid direct attack of NK-cells and continue their migration to the capillaries. But this unimpeded access has the other side, since small vessels own a bandwidth limit. This results in CTM being stuck inside the capillary. The circulating tumor microemboli movement resembles the car traffic at a steady speed where stopping at a red light is the basic law of survival according to main principle — 'run silent, run deep'

The formation of microemboli gives CTC the properties of "stemness" — maintaining a differentiated phenotype, the ability to divide and self-renewal through overexpression of transcription factors Hadgehog, Wnt, TGF-β and chemokine CXCL12. Binding sites for transcription factors associated with "stemness" and proliferation are specifically hypomethylated in CTC clusters, including binding sites for OCT4, NANOG, SOX2, and SIN3A [72, 73].

The initiation of metastasis, which is marked by the appearance of CTC in the circulation, is associated with a significant increase in the number of NK — important effector cells of antitumor surveillance. CTM clasterization significantly contributes to their resistance to NK cytotoxicity. CTC themselves and partner cells of the microenvironment in CTM produce a significant amount of immunosuppressive mediators, such as IL-10, prostaglandin E2, etc., which inhibit the expression of activator immunoglobulin NK receptors responsible for their antitumor activation [69, 74].

CTM formation is accompanied by overexpression of CD44, a non-kinase transmembrane glycoprotein. CD44 binds to hyaluronan within a tissue metastatic niche and activates numerous signaling pathways associated with activation of proliferation, survival of circulating tumor cells, and alteration of their cytoskeleton which enhances invasive movement [66]. This allows the CTC to acquire the status of disseminated tumor cells (DTC) and to initiate the next stage of their life cycle — the formation of a metastatic tumor foci.

Disseminated tumor cells

A small population of tumor cells, including CTC and disseminated tumor cells (DTC), which persists in the patient in a state of complete morphological remission after treatment, causes the so-called minimal residual disease (MRD) [75]. DTC are responsible for the post-extravasation stage and can be found in distal organs and all the tissues, including bone marrow [76].

DTC are a heterogeneous population of cells that share both epithelial and mesenchymal characteristics. DTC can be found singly or as clusters formed of 10–20 cells [77]. The peripheral blood sample, due to the fact that the DTC is an extremely rare component, contains at most 1 disseminated tumor cell per 1 ml [78]. The main morphological characteristics of the DTC are a large nucleus with granulation or stippling, strong or uneven staining for cytokeratin and cytokeratin filaments [79].

Circulating throughout the body, DTC are able both to enter and exit target organs without initiating tumor growth [80]. In order to form micrometastases ranging in size from 0.2 to 2 mm in tissues and organs remote from the primary location, DTC must adapt to the microenvironment of the metastatic niche [81, 82].

The microenvironment of the tumor consists of cellular and extracellular components. In the growth zone of the primary formation, the fraction of tumor cells is about half mass of the tumor, the rest are non-malignant cells of the microenvironment. In areas of metastasis, the proportion of tumor cells is incomparably little in relation to the number of non-malignant tissue elements, so the DTC face an extremely difficult task to adapt to such a potentially aggressive microenvironment. Given this, 80% of DTC are able to survive extravasation, 3% can reach the stage of micrometastases, and less than 0.02% are able to form secondary foci of metastasis [83].

DTC have a potential to reach any organ or tissue. However, recurrence of tumor growth usually develops in a limited number of tissues and organs. Moreover, different types of tumors are characterized by metastasis only in certain organs and tissues, which are probably suitable for the formation of the most favorable metastatic niche.

The perivascular metastatic niche (PMN) microenvironment, where DTC from the circulations arrive, is evolutionarily adapted to sustain the viability of stem tissue elements of the adult organism for a long time [84]. Evolutionarily formed physiological features of PMN are successfully used by DTC. These cells stay in a long latent period with subsequent reactivation of tumor growth. DTC form a direct link with stromal cells, which are a valuable reservoir of potentially promethastatic soluble mediators [85, 86].

The largest number of studies in this regard concerns DTC detected in the bone marrow and the role of their microenvironment for the persistence, latent phase and further reactivation of these cells [87–89]. In addition to the bone marrow, investigations of tissue metastatic niche often involve the brain and lungs. The long-term survival of DTC in the bone-marrow depends on the formation of gap junctions with osteogenic niche cells that is osteoblasts. The

one of the functions of osteoblasts is to serveas a calcium reservoir for the future activation of DTC from dormancy [90, 91].

In the brain, DTC occupy the tissue niche of pericytes or Rouget cells: they disrupt the blood–brain barrier (BBB) and migrate along the surface of brain capillaries in the space between pericytes. Brain DTC resemble pericytes in their morphology [92, 93]. In the lungs, airway smooth muscle cells become forced DTC partners in the colonization of this metastatic niche [94, 95].

In all instances, the extracellular matrix molecules play a key role in the successful homing of DTC in the metastatic niche [96]. DTC of various origins are characterized by overexpression of certain adhesion molecules, which determine their affinity for cells in the metastatic niche, that overexpress the corresponding ligands. For example, airway myocytes overexpress collagen III, the receptor for which (CD167a), in turn, is overexpressed in tumor cells characterized by pulmonary metastases [97].

It should be noted that an important factor in successful DTC homing is MET. DTCs that complete MET with coordinated re-expression of E-cadherin may occupy distant organs, form small preangiogenic metastases, or larger vascularized metastases [98–100].

After successful homing in a metastatic tissue niche, DTC enter a state of metastatic dormancy in which they can remain for a very long period of time in order to survive and relapse, sometimes decades later. Metastatic dormancy precedes the development of a secondary tumor. Its main features are growth arrest and resistance of malignant cells to therapy [81, 101].

Maintenance of metastatic dormancy is ensured by three important components: angiogenic dormancy, immune-mediated dormancy and intrinsic latency mechanisms of the DTC. Angiogenic mechanisms are largely regulated by hypoxia in the DTC microenvironment. The hypoxic environment of the metastatic niche causes overexpression of HIF1α and activation of the tumor angiogenesis [102].

Immune-mediated mechanisms include the possibility of the DTC to avoid immune surveillance (recognition and killing by cytoxic CD8 + T cells and natural killers) by mechanisms that are still at the research stage [103]. The internal mechanism of DTC latency is their “arrest” in the G0 phase with the full stop of proliferation. This process occurs without enhancing cell death [104].

The question of how these three programs, which form the preconditions for the development of tumor recurrence, relate over time and which of them is of paramount importance and, therefore, should become the main target for the development of approaches for the prevention and treatment of cancer recurrence, remains open. A key feature of DTC in metastatic dormancy is their ability to maintain a high degree of epigenetic and transcriptional plasticity and to reactivate various programs in order to stop growth and survive.

Successful homing, dormancy, and lack of proliferation make DTC insensitive to chemotherapeutic factors. Additional resistance of DTC to cytotoxic agents is provided by integrin signaling, which is ensured by close contacts with the corresponding extracellular matrix ligands in PMN. All of this allows the DTC to survive for a long time at dormancy state in a colonized metastatic niche.

Later, the life story of DTC passes to the stage of an exit from the state of dormacy and activation of tumor growth. The triggers for the transition of dormant DTC to the phase of tumor growth activation is still unknown. Some assumptions are made about the existence of internal and external DTC reactivation triggers. One of the hypothetical internal triggers for the DTC to exit metastatic dormancy is their overexpression of CD36 — a fatty acid translocase and one of the macrophage scavenger receptors capable of binding collagen and thrombospondin [105]. Cumulative absorption of fatty acids involving CD36 provides a substrate for β-oxidation of lipids, a highly efficient method of generating ATP required DTC to exit from dormancy [106].

An important external trigger for DTC reactivation is tissue inflammation, which in turn can be triggered by a variety of events and factors. Inflammation is known to be accompanied by recruiting into the area of its development the circulating myeloid cells (neutrophils, monocytes, etc.), which causes the remodelling of the ECM and the activation of dependent signaling of DTC in a dormant state.

These signaling cascades cause the activation of DTC proliferation and their metabolic activation. This is accompanied by the transformation of the state of immune balance in the metastatic niche (when the cytotoxic activity of antitumor immune effectors inhibits the growth of the tumor nodule) to the so-called immune editing —

changing the metabolic profile of immune cells from antitumor to pro-tumoral. Immune editing results in the formation of a tumor microenvironment, which promotes not only the growth of the tumor nodule, but also provides further drug resistance of tumor cells. For instance, smoking or bacterial infection in the lungs with lipopolysaccharide exposure causes the recruitment of neutrophils with activation of the NET extrusion. Neutrophil elastase, matrix metalloproteases and other enzymes that are part of NET mediate the ECM remodeling followed by the activation of laminin III and α3β1 integrin-dependent DTC signaling pathways, which increased a proliferative activity of these cells [77, 107].

The study of numerous unexplored issues in the life cycle of CTC and further DTC requires the development of adequate model systems that will reproduce the entire metastatic cascade *in vivo* in the patient's with the maximum proximity.

Preclinical models in the study of CTC

Preclinical models for the study of CTC can be divided into two categories: isolation and cultivation of CTC *ex vivo*, followed by the investigations of their biology and drug susceptibility testing; modeling the behavior of CTC in the metastatic cascade using murine models [108, 109].

Ex vivo technologies are a good alternative to animal models, which are time- and labor-consuming, as well as quite costly. This type of clinical study was introduced to study the biology of the metastatic cascade in colon cancer, as well as breast, prostate and lung cancer. However, this methodology has also a number of disadvantages and limitations [68, 110].

The CTC are present in small amounts in the peripheral blood — approximately 1 CTC per 7.5 ml of blood sample volume in patients with metastatic cancer [111]. According to other estimates, the frequency of CTC ranges from 1 to 10 cells among 5 billion erythrocytes, 10 million leukocytes, 200–500 platelets in 1 ml of peripheral blood, which is equivalent to finding a needle in a haystack [112–114]. The difficulty in isolating CTC is due to their significant heterogeneity and non-identified phenotypic profile. There is also a lack of information on the most valid markers for cells with the highest metastatic potential, the detection and study of which is diagnostically and prognostically significant [116, 117].

A wide range of methodological approaches is used to identify CTC. Enrichment strategies can be based on both biological properties (expression of membrane markers) and physical characteristics (size, density, electric charge) and are usually combined with identification methods based on the detection of membrane markers (e.g., immunofluorescence, immunohistochemistry, FISH, etc.) or expression of specific genes, which are identified by real-time PCR or quantitative PCR.

Isolation of CTC can be based on their both positive selection among normal blood cells and negative selection with leukocyte depletion. However, the use of *ex vivo* technologies does not allow imitating the entire metastatic cascade, the components of which are CTC. These methods are more suitable for studying the CTC molecular biological characteristics and screening of targeted drugs [118–120].

The murine models, which are used to study CTC in the metastatic cascade, are divided into several types or groups. The first group includes models of spontaneous metastasis [121, 122]. These models are based on orthotopic transplantation of tumor cells (e.g., transplantation of prostate cancer cells into the prostate gland of male mice) followed by monitoring of disease progression over time. The unquestionable advantage of this methodological approach is the ability to model all stages of the tumor process from the growth of the primary tumor to the development of metastases.

The second group combines animal models based on intravenous injection of tumor cells [123–125]. The advantage of these models is their shorter duration, because there is no stage of development of the primary tumor. Despite the fact that tumor cells introduced in this way are potentially able to spread to all tissues and organs, in reality they form a foci of tumor growth where they first enter the capillary bed. Therefore, the disadvantages of this approach are the lack of ability to predictively model metastasis in a particular organ. In addition, the absence of the primary tumor stage makes the reproduction of the pathophysiology of the process incomplete.

Both described groups of methods for modeling the metastatic process use syngeneic tumor cells. The third group consists of genetic engineering models (GEMM), based on the manipulation of the expression of proto-oncogenes or oncosuppressor genes, and includes transgenic models and models based on gene knockout [126, 127]. These models allow us to

investigate the role of genes associated with the formation of CTC and their ability to acquire DTC status and initiate the recurrence of the tumor process. However, genetic manipulations in such models affect all cells, such as a target organ or tissue, and thus do not replicate the natural course of events during the sporadic development of cancer that occurs due to the accumulation of genetic changes in a single cell.

The most eye-catching from the point of view of interpretation of pathophysiology of metastatic cancer are the models based on xenotransplantation of tumor cells, i.e., on introduction of human tumor cells to immunodeficient (immunocompromised) mice (PDX) [128–130]. Such models of metastatic tumor growth are created by orthotopic or subcutaneous transplantation of fresh surgically removed samples of human tumor tissue, rather than cultured tumor cells. This is the only type of model that allows personalized study of the metastatic cascade.

In spite of the undoubted advantages of this methodological approach, it has a number of disadvantages as well. Firstly, the creation of immunodeficiency in animals deprives the opportunity to study the participation of the immune system in the studied processes by experimenter and thus excludes from the study an important element of the pathophysiology of the metastatic cascade. Furthermore, such models do not allow the investigations of immunotherapeutic approaches in the treatment of metastatic disease.

Secondly, there is a significant variability in the engraftment of xenogeneic grafts, which depends on the type of tumor, the degree of its differentiation, etc. Thirdly, it is not always possible to obtain fresh tissue material for transplantation. Finally, in these models, achieving a detectable amount of CTC in the circulation sometimes takes a considerable period of time. Despite such significant limitations, xenotransplantation technology is widely used to study the biology of the metastatic cascade in breast cancer, melanoma, lung and prostate cancer, etc. The use of xenotransplantation of the enriched population of CTC obtained from peripheral blood samples from patients is an approach to improving this technology [131, 132]. However, there is also an obstacle to this improvement. The point is that for many cancers, isolation of CTC from the blood is a significant problem because of their extremely small number.

Nowadays, the solution to the problem of modeling the metastatic cascade for the study of the biology of CTC and DTC is a unification of all these methodological approaches and the combined efforts of specialists in various fields of biology and medicine.

Applications of the CTC in clinical strategies

Assessment and prediction of the disease course are of paramount tasks in oncology, as they allow stratify patients in order to develop an optimal treatment protocol and prevention of recurrence and metastasis. This problem requires the use of non-invasive methods, as invasive procedures, such as fine-needle aspiration biopsy, are traumatic, not representative of the disease as a whole and pose a risk of dissemination of the malignant neoplasm.

The appearance of liquid biopsy has opened up new perspectives for diagnosing and predicting recurrence and metastasis of cancer. Liquid biopsy — the analysis of tumors using biomarkers circulating in fluids such as blood — attracts considerable attention of specialists, despite the fact that this methodological approach has not entered the arsenal of standard tools in clinical oncology yet. The method of liquid biopsy analyzes various components of the tumor, which are released into the blood and other biological fluids, such as circulating nucleic acids (circulating tumor DNA (ctDNA), cell-free RNA (cfRNA)), tumor exosomes and CTC [133].

cfRNA includes mRNA and miRNA [134, 135]. Sequencing of cfRNA, which is found in the serum and plasma of cancer patients, especially miRNA, allows to obtain unique genetic information about the tumor. For example, circulating levels of miR-375 are a diagnostic marker for several types of cancer, including liver cancer, colorectal cancer and lung cancer [136].

ctDNA includes nuclear and mitochondrial DNA. Nucleic acids are released into the biological fluids including blood as a result of apoptosis or necrosis of tumor cells. High levels of free nucleic acids and the presence of specific mutations can be used as reliable biomarkers to determine the development and progression of the disease. In different types of tumors, ctDNA is characterized by specific changes in integrity and methylation, some changes in microsatellites and mutations. The main part of cell-free DNA (cfDNA), which is found in blood plasma, is the DNA of normal cells. ctDNA is only a small fraction of it. However, in terms of quantitative indicators,

this biomarker exceeds the indicators of CTC, which has a clear advantage.

Like CTC, ctDNA can characterize the stage of a tumor and even its metastatic potential, leading to a lengthy debate about the comparative characteristics of these two types of liquid biopsy. Nevertheless, the detection and analysis of CTC in liquid biopsy samples still has a number of advantages. In particular, the quantitative characteristics of ctDNA are insufficiently diagnostically and prognostically relevant, because the level of this circulating nucleic acid increases, for example, during pregnancy or during the physiological activation of hematopoiesis [137]. In addition, the ctDNA study does not make it possible to assess the sensitivity of the tumor to drugs, immunotherapy, etc.

The quantitative indicators of CTC in the blood correlate with the overall survival and disease free survival in many types of tumors [138]. For some tumors (stomach, lung, breast cancers, etc.), the number of CTC increases with an enlargement of the tumor size and with the development of distant metastases [139]. Diagnostic and prognostic significance of liquid biopsies with the determination of CTC is enhanced by its complementary proteomic analysis of isolated cells.

Determining the phenotypic characteristics of CTC allows to assess their metastatic potential and the risk of disease recurrence. For example, the presence of HER2-positive CTC in breast cancer biopsy specimens indicates a high risk of distant metastases and reduced overall survival [140]. The most promising phenotypic characteristics of the CTC in terms of their diagnostic and prognostic significance are markers of different stages of EMT and signs of "stemness" of these cells. In particular, the presence of transcription factors associated with EMT, such as Twist, Snail, ZEB-1, etc., as well as the detection of the so-called hybrid phenotype of CTC (cytokeratin + / vimentin + / CD45-) characterizes them as EMT-CTC and is a marker of their high metastatic potential [141]. Newly recognized markers of cell stemness and EMT along with well documented phenotypic characteristics might comprise a good set for cancer theranostics [142].

The expression of EMT-CTC markers of CTC increases the prognostic value of liquid biopsy with their detection [143] and predicts the risk of metastasis. The expression of certain phenotypic markers of CTC allows characterize the sensitivity of the tumor to chemo- and immunotherapeutic agents as well. For example, the expression level of PD-L1 is a prognostic marker of response to immunotherapy with PDl/PD-L1 pathway inhibitors [144, 145].

Despite significant advances in the development of liquid biopsy techniques in CTC analysis to predict metastasis and recurrence of oncopathology, there are some reports of the ineffectiveness of this methodological approach for some cancers. For instance, Chen et al. report the lack of prognostic value in assessing the quantitative and phenotypic characteristics of CTC for predicting the course and metastasis of hepatocellular carcinoma [146]. Yet, one of the reasons for the negative result may be the imperfect pre-analytical procedures used by this study group, as Sun et al. report that the quantitative and phenotypic characteristics of CTC isolated from the tumor efferent vessels and postpulmonary peripheral vessels differ significantly. According to the authors of this publication, the quantitative characteristics of CTC in the hepatic vein and peripheral vessels can be used to predict the development of metastases of hepatocellular carcinoma in the liver and lungs, respectively [147].

It is possible that higher prognostic value can be achieved by a combination of different types of liquid biopsy. Furthermore, there are reports of new candidates for the role of biomarkers of metastasis in liquid biopsy specimens. Lin et al. and Lei et al. detected circulating tumor endothelial cells (CTEC) in liquid biopsy specimens, which the authors of those publications believe are the result of an endothelial-mesenchymal transition (Endo-MT) process. Both research groups emphasize that aneuploid CD31+ CTEC, along with CD31- CTC, constitute a unique pair of circulating cell biomarkers for predicting tumor metastasis [148].

From the point of view of the clinical perspective, new treatment strategies focused on the mechanisms of formation and residence of CTC deserve some attention. For example, an anticoagulant therapy used in cancer patients and animal models of tumor growth may reduce the risk of tumor metastasis by minimizing CTM arrest in the PMN of the metastatic niche. Due to the fact that platelets promote the circulation and homing of CTM, experimental studies show the effectiveness of therapeutic strategies aimed at inhibiting the interactions of these structures. In addition, animal models have shown the effectiveness of genetically modified and functionalized platelets to control MRD [53].

A new step towards the development of a methodology for the clinical use of CTC

biology is the development of a photoacoustic method for detecting the minimum number of these cells in patients with melanoma with the possibility of their further elimination using laser pulses [149].

Immunotherapeutic approaches are promising from the point of view of development of treatment modalities targeting CTC. As it was mentioned earlier, the cells of the immune system in the microenvironment of the primary tumor contribute to the formation of CTC and their EMT, as well as they are a part of CTM and contribute to their viability both in the circulatory system and in the metastatic niche. An additional argument in favor of the development of targeted immunotherapy to combat CTC is the fact that they are able to avoid immune surveillance. Tumor growth models have shown the effectiveness of several immunotherapeutic approaches against CTC. The first is the use of PD-1/PD-L1 signaling cascade inhibitors. Blockade of these signaling pathways makes CTC sensitive to cytotoxic effects of tumor-specific CD8 + T lymphocytes [150]. Still, it should be noted that not all tumor cells, including CTC, are characterized by overexpression of PD-L1, so the impact on this checkpoint in this case may not be effective enough. An attractive candidate for the role of a target for immunotherapy targeting CTC is CD47 is one of the so called “do not eat me” signals, which is overexpressed on the surface of majority tumor cells and prevents their phagocytosis by macrophages [151]. Lian et al. ombined in their study the blockade of both ligands, which resulted in a profound inhibition of metastasis of breast cancer in mice [152].

The next immunotherapeutic approach involves the use of monoclonal antibodies to specific and functionally important CTC membrane receptors. For example, antibodies against CD44 inhibit the adhesion of CTC and CTM in the metastatic niche to the ECM [153], whereas antibodies against EpCAM perform the functions of opsonins and make CTC sensitive to both macrophage phagocytosis and antibody-dependent cellular cytotoxicity (ADCC) mediated by natural killers [154]. The use of leukocytes functionalized with E-selectin or TRAIL prevents the adhesion of CTC and CTM to vascular endothelium in PMN and is also considered as a promising immunotherapeutic approach for the prevention of metastasis, directed against CTC [155].

These and other innovative approaches give a hope that the theranostic potential of CTC is much greater than what we know today.

Conclusions

Summing up recent advances on the biology of CTC and the prospects for their use in cancer theranostics, it should be noted that significant progress in this area of science, even more convincingly proves the attractiveness of these cells as targets for cancer therapy, including cancer relapse and its metastasis from the standpoint of precision and personalized medicine.

Endowed with numerous mutations and aberrant gene expression, migration plasticity and properties of stem cells, the capacity to avoid immune surveillance, having an immunosuppressive effect and maintaining long-term latency without losing all these properties, CTC embody all the pathological changes that distinguish malignant cell from normal cell. For this reason, probably, the traditional antiproliferative therapy concedes individualized therapy targeted at these cells, which is believed is the future of oncology. For the purpose of embodiment an individualized therapy in reality, it is still necessary to solve a very difficult task — to accept a challenge entitled “catch me if you can” ran by CTC.

The authors thank Yehor Pashkevych for technical support in figure design.

The literature review was supported by the project funded by the Ministry of Education and Science of Ukraine (State Registration No.0119U100168).

REFERENCES

1. *Bettio M., Carvalho R. N., Dimitrova N., Dyba T., Flego M., Giusti F., Martos C., Neamtiu L., Nicholson N., Randi G., Nicholl C.* European Commission, Joint Research Centre (JRC), Ispra, Italy. *EMJ Oncol*. 2019, 7 (1), 48–49. Abstract No AR05. https://www.emjreviews.com/oncology/abstract/measuring-the-cancer-burden-in-europe-the-european-cancer-information-system-ecis/
2. *Siegel R. L., Miller K. D., Jemal A.* Cancer statistics, 2020. *CA: A Cancer Journal for Clinicians*. 2020, 70 (1), 7–30. https://doi.org/10.3322/caac.21590
3. *Galmarini C. M.* Lessons from Hippocrates: Time to Change the Cancer Paradigm. *International Journal of Chronic Diseases*. 2020, V. 2020, P. 4715426. https://doi.org/10.1155/2020/4715426
4. *LeDran H. F.* Mémoire avec un précis de plusieurs observations sur le cancer. *Memories de l'academie royale de chirurgie*. 1757, V. 3, P. 1–54.
5. *Récamier J. C.* Recherchessurletraitement du cancer sur la compression methodique simple ou combinee et sur l'histoire generale de la meme maladie, 2nd ed.1829. *Gabon, Paris*.
6. *Thiersch K.* Der Epithelial krebs, namentlich der Hand. 1865. *Engelmann, Leipzig*.
7. *Langenbeck B.* On the development of cancer in the veins, and the transmission ofcancer from man to the lower animals. *Edinb. Med. Surg. J.* 1841, 55 (147), 251–253.
8. *Virchow R.* Cellular pathologie. *Nutr. Rev.* 1858, P. 23–25.
9. *Ashworth T. R.* A case of cancer in which cells similar to those in the tumors wereseen in the blood after death. *Aust. Med. J.* 1869, V. 14, P. 146–149.
10. *Engel H. C.* Cancer cells in the blood; a five to nine year follow up study. *Ann. Surg*. 1959, 149 (4), 457–461. https://doi.org/10.1097/00000658-195904000-00001
11. *Pantel K., Schlimok G., Braun S., Kutter D., Lindemann F., Schalle, G., Funke I., Izbicki J. R., Riethmüller G.* Differential expression of proliferation-associated molecules in individual micrometastatic carcinoma cells. *J. Natl. Cancer Inst.* 1993, 85 (17), 1419–1424. https://doi.org/10.1093/jnci/85.17.1419
12. *Pantel K., Izbicki J., Passlick B., Angstwurm M., Häussinger K., Thetter O., Riethmüller G.* Frequency and prognostic significance of isolated tumour cells in bone marrow of patients with non-small-cell lung cancer without overt metastases. *Lancet*. 1996, 347 (9002), 649–653. https://doi.org/10.1016/s0140-6736(96)91203-9
13. *Nowell P. C.* The clonal evolution of tumor cell populations. *Science*. 1976, 194(4260), 23–28. https://doi.org/10.1126/science.959840
14. *Folkman J.* Tumor angiogenesis: therapeutic implications. *N. Engl. J. Med.* 1971, 285 (21), 1182–1186. https://doi.org/10.1056/NEJM197111182852108
15. *Folkman J., Watson K., Ingber D., Hanahan D.* Induction of angiogenesis during the transition from hyperplasia to neoplasia. *Nature*. 1989, 339 (6219), 58–61. https://doi.org/10.1038/339058a0
16. *Liotta L. A., Steeg P. S., Stetler-Stevenson W. G.* Cancer metastasis and angiogenesis: an imbalance of positive and negative regulation. *Cell*. 1991, 64 (2), 327–336. https://doi.org/10.1016/0092-8674(91)90642-c
17. *Liotta L. A., Kleinerman J., Saidel G. M.* Quantitative relationships of intravascular tumor cells, tumor vessels, and pulmonary metastases following tumor implantation. *Cancer Res.* 1974, 34 (5), 997–1004.
18. *Prasetyanti P. R., Medema J. P.* Intra-tumor heterogeneity from a cancer stem cell perspective. *Mol. Cancer*. 2017, 16 (1), 41. https://doi.org/10.1186/s12943-017-0600-4
19. *Albini A., Bruno A., Gallo C., Pajardi G., Noonan D. M., Dallaglio K.* Cancer stem cells and the tumor microenvironment: interplay in tumor heterogeneity. *Connect. Tissue Res.* 2015, 56 (5), 414–425. https://doi.org/10.3109/03008207.2015.1066780
20. *Fouad Y. A., Aanei C.* Revisiting the hallmarks of cancer. *Am. J. Cancer Res.* 2017, 7 (5), 1016–1036.
21. *Greenburg G., Hay E. D.* Epithelia suspended in collagen gels can lose polarity and express characteristics of migrating mesenchymal cells. *J. Cell Biol*. 1982, 95 (1), 333–339. https://doi.org/10.1083/jcb.95.1.333
22. *Jalal S., Shi S., Acharya V., Huang R. Y., Viasnoff V., Bershadsky A. D., Tee Y. H.* Actin cytoskeleton self-organization in single epithelial cells and fibroblasts under isotropic confinement. *J. Cell Sci.* 2019, 132 (5), jcs220780. https://doi.org/10.1242/jcs.220780
23. *Karamanou K., Franchi M., Vynios D., Brézillon S.* Epithelial-to-mesenchymal transition and invadopodia markers in breast cancer: Lumican a key regulator. *Semin. Cancer Biol.* 2020, V. 62, P. 125–133. https://doi.org/10.1016/j.semcancer.2019.08.003
24. *Liao T. T., Yang M. H.* Hybrid Epithelial/Mesenchymal State in Cancer Metastasis: Clinical Significance and Regulatory Mechanisms. *Cells*. 2020, 9 (3), 623. https://doi.org/10.3390/cells9030623
25. *Nersesian S., Williams R., Newsted D., Shah K., Young S., Evans P. A., Allingham J. S., Craig A. W.* Effects of Modulating Actin Dynamics on HER2 Cancer Cell Motility and Metastasis. *Sci Rep.* 2018, 8 (1), 17243. https://doi.org/10.1038/s41598-018-35284-9

26. *Chaffer C. L., San Juan B. P., Lim E., Weinberg R. A.* EMT, cell plasticity and metastasis. *Cancer Metastasis Rev.* 2016, 35 (4), 645–654. https://doi.org/10.1007/s10555-016-9648-7
27. *Peixoto P., Etcheverry A., Aubry M., Missey A., Lachat C., Perrard J., Hendrick E., Delage-Mourroux R., Mosser J., Borg C., Feugeas J. P., Herfs M., Boyer-Guittaut M., Hervouet E.* EMT is associated with an epigenetic signature of ECM remodeling genes. *Cell Death Dis.* 2019, 10 (3), 205. https://doi.org/10.1038/s41419-019-1397-4
28. *Ridley A. J.* Rho GTPase signalling in cell migration. *Curr. Opin. Cell Biol.* 2015, V. 36, P. 103–112. https://doi.org/10.1016/j.ceb.2015.08.005
29. *Kazanietz M. G., Caloca M. J.* The Rac GTPase in Cancer: From Old Concepts to New Paradigms. *Cancer Res.* 2017, 77 (20), 5445–5451. https://doi.org/10.1158/0008-5472.CAN-17-1456
30. *Gonzalez D. M., Medici D.* Signaling mechanisms of the epithelial-mesenchymal transition. *Sci. Signaling*. 2014, 7 (344), re8. https://doi.org/10.1126/scisignal.2005189
31. *Nieszporek A., Skrzypek K., Adamek G., Majka M.* Molecular mechanisms of epithelial to mesenchymal transition in tumor metastasis. *Acta Biochim. Pol.* 2019, 66 (4), 509–520. https://doi.org/10.18388/abp.2019_2899
32. *Ribatti D., Tamma R., Annese T.* Epithelial-Mesenchymal Transition in Cancer: A Historical Overview. *Transl. Oncol.* 2020, 13 (6), 100773. https://doi.org/10.1016/j.tranon.2020.100773
33. *Jolly M. K., Ware K. E., Gilja S., Somarelli J. A., Levine H.* EMT and MET: necessary or permissive for metastasis? *Mol. Oncol.* 2017, 11 (7), 755–769. https://doi.org/10.1002/1878-0261.12083
34. *Pastushenko I., Brisebarre A., Sifrim A., Fioramonti M., Revenco T., Boumahdi S., Van Keymeulen A., Brown D., Moers V., Lemaire S., DeClercq S., Minguijón E., Balsat C., Sokolow Y., Dubois C., De Cock F., Scozzaro S., Sopena F., Lanas A., D'Haene N., Blanpain C.* Identification of the tumour transition states occurring during EMT. *Nature*. 2018, 556 (7702), 463–468. https://doi.org/10.1038/s41586-018-0040-3
35. *Derynck R., Weinberg R. A.* EMT and Cancer: More Than Meets the Eye. *Dev. Cell.* 2019, 49 (3), 313–316. https://doi.org/10.1016/j.devcel.2019.04.026
36. *Claudia Tanja Mierke.* Physics of Cancer, Volume 1: Interplay between tumor biology, inflammation and cell mechanics. Published October 2018. *Copyright © IOP Publishing Ltd*. 2018. CHAPTER 1. Initiation of a neoplasm or tumor. https://doi.org/10.1088/978-0-7503-1753-5ch1
37. *Kim D. H., Xing T., Yang Z., Dudek R., Lu Q., Chen Y. H.* Epithelial Mesenchymal Transition in Embryonic Development, Tissue Repair and Cancer: A Comprehensive Overview. *J. Clin. Med.* 2017, 7 (1), 1. https://doi.org/10.3390/jcm7010001
38. *Faheem M. M., Seligson N. D., Ahmad S. M., Rasool R. U., Gandhi S. G., Bhagat M., Goswami A.* Convergence of therapy-induced senescence (TIS) and EMT in multistep carcinogenesis: current opinions and emerging perspectives. *Cell Death. Discov.* 2020, V. 6, P. 51. https://doi.org/10.1038/s41420-020-0286-z
39. *Jordan N. V., Johnson G. L., Abell A. N.* Tracking the intermediate stages of epithelial-mesenchymal transition in epithelial stem cells and cancer. *Cell Cycle*. 2011, 10 (17), 2865–2873. https://doi.org/10.4161/cc.10.17.17188
40. *Cao Z., Livas T., Kyprianou N.* Anoikis and EMT: Lethal "Liaisons" during Cancer Progression. *Crit. Rev. Oncog.* 2016, 21 (3–4), 155–168. https://doi.org/10.1615/CritRevOncog.2016016955
41. *Wei C., Yang C., Wang S., Shi D., Zhang C., Lin X., Liu Q., Dou R., Xiong B.* Crosstalk between cancer cells and tumor associated macrophages is required for mesenchymal circulating tumor cell-mediated colorectal cancer metastasis. *Mol. Cancer.* 2019, 18 (1), 64. https://doi.org/10.1186/s12943-019-0976-4
42. *Yang C., Dou R., Wei C., Liu K., Shi D., Zhang C., Liu Q., Wang S., Xiong B.* Tumor-derived exosomal microRNA-106b-5p activates EMT-cancer cell and M2-subtype TAM interaction to facilitate CRC metastasis. *Mol. Ther.* 2021, 29 (6), 2088–2107. https://doi.org/10.1016/j.ymthe.2021.02.006
43. *Cortés M., Sanchez-Moral L., de Barrios O., Fernández-Aceñero M. J., Martínez-Campanario M. C., Esteve-Codina A., Darling D. S., Győrffy B., Lawrence T., Dean D. C., Postigo A.* Tumor-associated macrophages (TAMs) depend on ZEB1 for their cancer-promoting roles. *EMBO J.* 2017, 36 (22), 3336–3355. https://doi.org/10.15252/embj.201797345
44. *Xu R., Won J. Y., Kim C. H., Kim D. E., Yim H.* Roles of the Phosphorylation of Transcriptional Factors in Epithelial-Mesenchymal Transition. *J. Oncol.* 2019, V. 2019, P. 5810465. https://doi.org/10.1155/2019/5810465
45. *Alidadiani N., Ghaderi S., Dilaver N., Bakhshamin S., Bayat M.* Epithelial mesenchymal transition Transcription Factor (TF): The structure, function and microRNA feedback loop. *Gene.* 2018, V. 674, P. 115–120. https://doi.org/10.1016/j.gene.2018.06.049
46. *Mohammed S. I., Torres-Luquis O., Walls E., Lloyd F.* Lymph-circulating tumor cells show

distinct properties to blood-circulating tumor cells and are efficient metastatic precursors. *Mol. Oncol.* 2019, 13 (6), 1400–1418. https://doi.org/10.1002/1878-0261.12494
47. *Kolostova K., Pospisilova E., Pavlickova V., Bartos R., Sames M., Pawlak I., Bobek V.* Next generation sequencing of glioblastoma circulating tumor cells: non-invasive solution for disease monitoring. *Am. J. Transl. Res.* 2021, 13 (5), 4489–4499.
48. *Kowalik A., Kowalewska M., Góźdź S.* Current approaches for avoiding the limitations of circulating tumor cells detection methods-implications for diagnosis and treatment of patients with solid tumors. *Transl. Res.* 2017, V. 185, P. 58–84.e15. https://doi.org/10.1016/j.trsl.2017.04.002
49. *Christou N., Meyer J., Popeskou S., David V., Toso C., Buchs N., Liot E., Robert J., Ris F., Mathonnet M.* Circulating Tumour Cells, Circulating Tumour DNA and Circulating Tumour miRNA in Blood Assays in the Different Steps of Colorectal Cancer Management, a Review of the Evidence in 2019. *Biomed. Res. Int.* 2019, V. 2019, P. 5953036. https://doi.org/10.1155/2019/5953036
50. *Millner L. M., Linder M. W., Valdes R. Jr.* Circulating tumor cells: a review of present methods and the need to identify heterogeneous phenotypes. *Ann. Clin. Lab. Sci.* 2013, 43 (3), 295–304.
51. *Plaks V., Kong N., Werb Z.* The cancer stem cell niche: how essential is the niche in regulating stemness of tumor cells? *Cell Stem. Cell.* 2015, 16 (3), 225–238. https://doi.org/10.1016/j.stem.2015.02.015
52. *Agnoletto C., Corrà F., Minotti L., Baldassari F., Crudele F., Cook W. J. J., Di Leva G., d'Adamo A. P., Gasparini P., Volinia S.* Heterogeneity in Circulating Tumor Cells: The Relevance of the Stem-Cell Subset. *Cancers (Basel).* 2019, 11 (4), 483. https://doi.org/10.3390/cancers11040483
53. *Wang W. C., Zhang X. F., Peng J., Li X. F., Wang A. L., Bie Y. Q., Shi L. H., Lin M. B., Zhang X. F.* Survival Mechanisms and Influence Factors of Circulating Tumor Cells. *Biomed. Res. Int.* 2018, V. 2018, P. 6304701. https://doi.org/10.1155/2018/6304701
54. *Krog B. L., Henry M. D.* Biomechanics of the Circulating Tumor Cell Microenvironment. *Adv. Exp. Med. Biol.* 2018, V. 1092, P. 209–233. https://doi.org/10.1007/978-3-319-95294-9_11
55. *Sprouse M. L., Welte T., Boral D., Liu H. N., Yin W., Vishnoi M., Goswami-Sewell D., Li L., Pei G., Jia P., Glitza-Oliva I. C., Marchetti D.* PMN-MDSCs Enhance CTC Metastatic Properties through Reciprocal Interactions via ROS/Notch/Nodal Signaling. *Int. J. Mol. Sci.* 2019, 20 (8), 1916. https://doi.org/10.3390/ijms20081916
56. *Choi H. Y., Yang G. M., Dayem A. A., Saha S. K., Kim K., Yoo Y., Hong K., Kim J. H., Yee C., Lee K. M., Cho S. G.* Hydrodynamic shear stress promotes epithelial-mesenchymal transition by downregulating ERK and GSK3β activities. *Breast Cancer Res.* 2019, 21 (1), 6. https://doi.org/10.1186/s13058-018-1071-2
57. *Dianat-Moghadam H., Azizi M., Eslami-S Z., Cortés-Hernández L. E., Heidarifard M., Nouri M., Alix-Panabières C.* The Role of Circulating Tumor Cells in the Metastatic Cascade: Biology, Technical Challenges, and Clinical Relevance. *Cancers (Basel).* 2020, 12 (4), 86. https://doi.org/10.3390/cancers12040867
58. *Alexandrova A. Y., Chikina A. S., Svitkina T. M.* Actin cytoskeleton in mesenchymal-to-amoeboid transition of cancer cells. *Int. Rev. Cell. Mol. Biol.* 2020, V. 356, P. 197–256. https://doi.org/10.1016/bs.ircmb.2020.06.002
59. *Wu J. S., Jiang J., Chen B. J., Wang K., Tang Y. L., Liang X. H.* Plasticity of cancer cell invasion: Patterns and mechanisms. *Transl. oncol.* 2021, 14 (1), 100899. https://doi.org/10.1016/j.tranon.2020.100899
60. *Chen L., Bode A. M., Dong Z.* Circulating Tumor Cells: Moving Biological Insights into Detection. *Theranostics.* 2017, 7 (10), 2606–2619. https://doi.org/10.7150/thno.18588
61. *Jones B. C., Kelley L. C., Loskutov Y. V., Marinak K. M., Kozyreva V. K., Smolkin M. B., Pugacheva E. N.* Dual Targeting of Mesenchymal and Amoeboid Motility Hinders Metastatic Behavior. *Mol. Cancer Res.* 2017, 15 (6), 670–682. https://doi.org/10.1158/1541-7786.MCR-16-0411
62. *Yu M.* Metastasis Stemming from Circulating Tumor Cell Clusters. *Trends Cell Biol.* 2019, 29 (4), 275–276. https://doi.org/10.1016/j.tcb.2019.02.001
63. *Giuliano M., Shaikh A., Lo H. C., Arpino G., De Placido S., Zhang X. H., Cristofanilli M., Schiff R., Trivedi M. V.* Perspective on Circulating Tumor Cell Clusters: Why It Takes a Village to Metastasize. *Cancer Res.* 2018, 78 (4), 845–852. https://doi.org/10.1158/0008-5472.CAN-17-2748
64. *Aktary Z., Alaee M., Pasdar M.* Beyond cell-cell adhesion: Plakoglobin and the regulation of tumorigenesis and metastasis. *Oncotarget.* 2017, 8 (19), 32270–32291. https://doi.org/10.18632/oncotarget.15650
65. *Lim S. B., Yeo T., Lee W. D., Bhagat A. A. S., Tan S. J., Tan D. S. W., Lim W. T., Lim C. T.* Addressing cellular heterogeneity in tumor and circulation for refined prognostication. *Proc. Natl. Acad. Sci. USA.* 2019, 116 (36), 17957–17962. https://doi.org/10.3390/ijms21072653
66. *Amintas S., Bedel A., Moreau-Gaudry F., Boutin J., Buscail L., Merlio J. P., Vendrely V., Da-*

bernat S., Buscail E. Circulating Tumor Cell Clusters: United We Stand Divided We Fall. *Int. J. Mol. Sci.* 2020, 21 (7), 2653. https://doi.org/10.3390/ijms21072653
67. *Castro-Giner F., Aceto N.* Tracking cancer progression: from circulating tumor cells to metastasis. *Genome Med.* 2020, 12 (1), 31. https://doi.org/10.1186/s13073-020-00728-3
68. *Mentis A. A., Grivas P. D., Dardiotis E., Romas N. A., Papavassiliou A. G.* Circulating tumor cells as Trojan Horse for understanding, preventing, and treating cancer: a critical appraisal. *Cell Mol. Life Sci.* 2020, 77 (18), 3671–3690. https://doi.org/10.1007/s00018-020-03529-4
69. *Micalizzi D. S., Maheswaran S., Haber D. A.* A conduit to metastasis: circulating tumor cell biology. *Genes. Dev.* 2017, 31 (18), 1827–1840. https://doi.org/10.1101/gad.305805.117
70. *Anvari S., Osei E., Maftoon N.* Interactions of platelets with circulating tumor cells contribute to cancer metastasis. *Sci. Rep.* 2021, 11 (1), 15477. https://doi.org/10.1038/s41598-021-94735-y
71. *Jiang X., Wong K. H. K., Khankhel A. H., Zeinali M., Reategui E., Phillips M. J., Luo X., Aceto N., Fachin F., Hoang A. N., Kim W., Jensen A. E.,. Sequist L. V., Maheswaran S., Haber D. A., Stott S. L., Toner M.* Microfluidic isolation of platelet-covered circulating tumor cells. *Lab. Chip.* 2017, 17 (20), 3498–3503. https://doi.org/10.1039/c7lc00654c
72. *YangL.,ShiP.,ZhaoG.,XuJ.,PengW.,ZhangJ., Zhang G., Wang X., Dong Z., Chen F., Cui H.* Targeting cancer stem cell pathways for cancer therapy. *Signal Transduct. Target. Ther.* 2020, 5 (1), 8. https://doi.org/10.1038/s41392-020-0110-5
73. *Gkountela S., Castro-Giner F., Szczerba B. M., Vetter M., Landin J., Scherrer R., Krol I., Scheidmann M. C., Beisel C., Stirnimann C. U., Kurzeder C., Heinzelmann-Schwarz V., Rochlitz C., Weber W. P., Aceto N.* Circulating Tumor Cell Clustering Shapes DNA Methylation to Enable Metastasis Seeding. *Cell.* 2019, 176 (1–2), 98–112.e14. https://doi.org/10.1016/j.cell.2018.11.046
74. *Lei M. M. L., Lee T. K. W.* Cancer Stem Cells: Emerging Key Players in Immune Evasion of Cancers. *Front. Cell Dev. Biol.* 2021, V. 9, P. 692940. https://doi.org/10.3389/fcell.2021.692940
75. *Nicolini A., Rossi G., Ferrari P., Carpi A.* Minimal residual disease in advanced or metastatic solid cancers: The G0-G1 state and immunotherapy are key to unwinding cancer complexity. *Semin. Cancer Biol.* 2020, S1044-579X(20)30075-4. https://doi.org/10.1016/j.semcancer.2020.03.009
76. *Tjensvoll K., Nordgård O., Skjæveland M., Oltedal S., Janssen E. A. M., Gilje B.* Detection of disseminated tumor cells in bone marrow predict late recurrences in operable breast cancer patients. *BMC Cancer.* 2019, 19 (1), 1131. https://doi.org/10.1186/s12885-019-6268-y
77. *Risson E., Nobre A. R., Maguer-Satta V., Aguirre-Ghiso J. A.* The current paradigm and challenges ahead for the dormancy of disseminated tumor cells. *Nat. Cancer.* 2020, 1 (7), 672–680. https://doi.org/10.1038/s43018-020-0088-5
78. *Marconato L., Facchinetti A., Zanardello C., Rossi E., Vidotto R., Capello K., Melchiotti E., Laganga P., Zamarchi R., Vascellari M.* Detection and Prognostic Relevance of Circulating and Disseminated Tumour Cell in Dogs with Metastatic Mammary Carcinoma: A Pilot Study. *Cancers (Basel).* 2019, 11 (2), 163. https://doi.org/10.3390/cancers11020163
79. *O'Sullivan B., Brierley J., Byrd D., Bosman F., KehoeS.,KossaryC.,PiñerosM.,VanEyckenE., Weir H. K., Gospodarowicz M.* The TNM classification of malignant tumours-towards common understanding and reasonable expectations. *Lancet Oncol.* 2017, 18 (7), 849–851. https://doi.org/10.1016/S1470-2045(17)30438-2
80. *Aguirre-Ghiso J., Sosa M.* Emerging Topics on Disseminated Cancer Cell Dormancy and the Paradigm of Metastasis. *Ann. Rev. Cancer Biol.* 2018, V. 2, P. 377–393. https://doi.org/10.1146/annurev-cancerbio-030617-050446
81. *Kilickap S., Aktas B. Y., Ozisik Y. Y.* (2019) Bone Marrow Micrometastases and Circulating Tumor Cells. In: Aydiner A., Igci A., Soran A. (eds). *Breast Disease. Springer, Cham.* https://doi.org/10.1007/978-3-030-04606-4_13
82. *Piranlioglu R., Lee E., Ouzounova M., Bollag R. J., Vinyard A. H., Arbab A. S., Marasco D., Guzel M., Cowell J. K., Thangaraju M., Chadli A., Hassan K. A., Wicha M. S., Celis E., Korkaya H.* Primary tumor-induced immunity eradicates disseminated tumor cells in syngeneic mouse model. *Nat. Commun.* 2019, 10 (1), 1430. https://doi.org/10.1038/s41467-019-09015-1
83. *Marcuzzi E., Angioni R., Molon B., Calì B.* Chemokines and Chemokine Receptors: Orchestrating Tumor Metastasization. *Int. J. Mol. Sci.* 2019, 20 (1), 96. https://doi.org/10.3390/ijms20010096
84. *Rafii S., Butler J. M., Ding B. S.* Angiocrine functions of organ-specific endothelial cells. *Nature.* 2016, 529 (7586), 316–325. https://doi.org/10.1038/nature17040
85. *Rycaj K., Li H., Zhou J., Chen X., Tang D. G.* Cellular determinants and microenvironmental regulation of prostate cancer metastasis. *Semin. Cancer Biol.* 2017, V. 44,

P. 83–97. https://doi.org/10.1016/j.semcancer.2017.03.009
86. *Dasgupta A., Lim A. R., Ghajar C. M.* Circulating and disseminated tumor cells: harbingers or initiators of metastasis? *Mol. Oncol*. 2017, 11 (1), 40–61. https://doi.org/10.1002/1878-0261.12022
87. *Zhang W., Bado I., Wang H., Lo H. C., Zhang X. H.* Bone Metastasis: Find Your Niche and Fit in. *Trends in Cancer*. 2019, 5 (2), 95–110. https://doi.org/10.1016/j.trecan.2018.12.004
88. *Sowder M. E., Johnson R. W.* Bone as a Preferential Site for Metastasis. *JBMR Plus*. 2019, 3 (3), e10126. https://doi.org/10.1002/jbm4.10126
89. *Esposito M., Guise T., Kang Y.* The Biology of Bone Metastasis. *Cold Spring Harb. Perspect. Med*. 2018, 8 (6), a031252. https://doi.org/10.1101/cshperspect.a031252
90. *Haider M. T., Smit D. J., Taipaleenmäki H.* The Endosteal Niche in Breast Cancer Bone Metastasis. *Front. Oncol*. 2020, V. 10, P. 335. https://doi.org/10.3389/fonc.2020.00335
91. *Liu C., Zhao Q., Yu X.* Bone Marrow Adipocytes, Adipocytokines, and Breast Cancer Cells: Novel Implications in Bone Metastasis of Breast Cancer. *Front. Oncol*. 2020, V. 10, P. 561595. https://doi.org/10.3389/fonc.2020.561595
92. *Carvalho R., Paredes J., Ribeiro A. S.* Impact of breast cancer cells´ secretome on the brain metastatic niche remodeling. *Semin. Cancer Biol*. 2020, V. 60, P. 294–301. https://doi.org/10.1016/j.semcancer.2019.10.011
93. *Seano G.* Targeting the perivascular niche in brain tumors. *Curr. Opin. Oncol*. 2018, 30 (1), 54–60. https://doi.org/10.1097/CCO.0000000000000417
94. *Maru Y.* The lung metastatic niche. *J. Mol. Med. (Berl)*. 2015, 93 (11), 1185–1192. https://doi.org/10.1007/s00109-015-1355-2
95. *Sharma S. K., Chintala N. K., Vadrevu S. K., Patel J., Karbowniczek M., Markiewski M. M.* Pulmonary alveolar macrophages contribute to the premetastatic niche by suppressing antitumor T cell responses in the lungs. *J. Immunol*. 2015, 194 (11), 5529–5538. https://doi.org/10.4049/jimmunol.1403215
96. *Kai F., Drain A. P., Weaver V. M.* The Extracellular Matrix Modulates the Metastatic Journey. *Dev. Cell*. 2019, 49 (3), 332–346. https://doi.org/10.1016/j.devcel.2019.03.026
97. *Lee Y. C., Kurtova A. V., Xiao J., Nikolos F., Hayashi K., Tramel Z., Jain A., Chen F., Chokshi M., Lee C., Bao G., Zhang X., Shen J., Mo Q., Jung S. Y., Rowley D., Chan K. S.* Collagen-rich airway smooth muscle cells are a metastatic niche for tumor colonization in the lung. *Nat. Commun*. 2019, 10 (1), 2131. https://doi.org/10.1038/s41467-019-09878-4
98. *Zhuyan J., Chen M., Zhu T., Bao X., Zhen T., Xing K., Wang Q., Zhu S.* Critical steps to tumor metastasis: alterations of tumor microenvironment and extracellular matrix in the formation of pre-metastatic and metastatic niche. *Cell Biosci*. 2020, V. 10, P. 89. https://doi.org/10.1186/s13578-020-00453-9
99. *Ren G., Esposito M., Kang Y.* Bone metastasis and the metastatic niche. *J. Mol. Med. (Berl)*. 2015, 93 (11), 1203–1212. https://doi.org/10.1007/s00109-015-1329-4
100. *Melzer C., von der Ohe J., Hass R.* Breast Carcinoma: From Initial Tumor Cell Detachment to Settlement at Secondary Sites. *Biomed. Res. Int*. 2017, V. 2017, P. 8534371. https://doi.org/10.1155/2017/8534371
101. *Manjili M. H.* Tumor Dormancy and Relapse: From a Natural Byproduct of Evolution to a Disease State. *Cancer Res*. 2017, 77 (10), 2564–2569. https://doi.org/10.1158/0008-5472.CAN-17-0068
102. *Meléndez-Rodríguez F., Urrutia A. A., Lorendeau D., Rinaldi G., Roche O., Böğürcü-Seidel N., Ortega Muelas M., Mesa-Ciller C., Turiel G., Bouthelier A., Hernansanz-Agustín P., Elorza A., Escasany E., Li Q., Torres-Capelli M., Tello D., Fuertes E., Fraga E., Martínez-Ruiz A., Pérez B., Aragonés J.* HIF1α Suppresses Tumor Cell Proliferation through Inhibition of Aspartate Biosynthesis. *Cell Rep*. 2019, 26 (9), 2257–2265.e4. https://doi.org/10.1016/j.celrep.2019.01.106
103. *Vinay D. S., Ryan E. P., Pawelec G., Talib W. H., Stagg J., Elkord E., Lichtor T., Decker W. K., Whelan R. L., Kumara H., Signori E., Honoki K., Georgakilas A. G., Amin A., Helferich W. G., Boosani C. S., Guha G., Ciriolo M. R., Chen S., Mohammed S. I., Kwon B. S.* Immune evasion in cancer: Mechanistic basis and therapeutic strategies. *Semin. Cancer Biol*. 2015, 35 (l), S185–S198. https://doi.org/10.1016/j.semcancer.2015.03.004
104. *Pein M., Oskarsson T.* Microenvironment in metastasis: roadblocks and supportive niches. *Am. J. Physiol. Cell Physiol*. 2015, 309 (10), C627–C638. https://doi.org/10.1152/ajpcell.00145.2015
105. *Pascual G., Avgustinova A., Mejetta S., Martín M., Castellanos A., Attolini C. S., Berenguer A., Prats N., Toll A., Hueto J. A., Bescós C., Di Croce L., Benitah S. A.* Targeting metastasis-initiating cells through the fatty acid receptor CD36. *Nature*. 2017, 541 (7635), 41–45. https://doi.org/10.1038/nature20791
106. *Phan T. G., Croucher P. I.* The dormant cancer cell life cycle. *Nature Rev. Cancer*. 2020, 20 (7), 398–411. https://doi.org/10.1038/s41568-020-0263-0
107. *Masucci M. T., Minopoli M., Del Vecchio S., Carriero M. V.* The Emerging Role of Neu-

trophil Extracellular Traps (NETs) in Tumor Progression and Metastasis. *Front. Immunol.* 2020, V. 11, P. 1749. https://doi.org/10.3389/fimmu.2020.01749
108. *Tayoun T., Faugeroux V., Oulhen M., Aberlenc A., Pawlikowska P., Farace F.* CTC-Derived Models: A Window into the Seeding Capacity of Circulating Tumor Cells (CTCs). *Cells*. 2019, 8 (10), 1145. https://doi.org/10.3390/cells8101145
109. *Kitz J., Lowes L. E., Goodale D., Allan A. L.* Circulating Tumor Cell Analysis in Preclinical Mouse Models of Metastasis. *Diagnostics (Basel)*. 2018, 8 (2), 30. https://doi.org/10.3390/diagnostics8020030
110. *Sobral-Filho R. G., DeVorkin L., Macpherson S., Jirasek A., Lum J. J., Brolo A. G.* Ex Vivo Detection of Circulating Tumor Cells from Whole Blood by Direct Nanoparticle Visualization. *ACS Nano.* 2018, 12 (2), 1902–1909. https://doi.org/10.1021/acsnano.7b08813
111. *Qiao Y., Li J., Shi C., Wang W., Qu X., Xiong M., Sun Y., Li D., Zhao X., Zhang D.* Prognostic value of circulating tumor cells in the peripheral blood of patients with esophageal squamous cell carcinoma. *OncoTargets and Therapy*. 2017, V. 10, P. 1363–1373. https://doi.org/10.2147/OTT.S129004
112. *Shen Z., Wu A., Chen X.* Current detection technologies for circulating tumor cells. *Chemical Society Reviews.* 2017, 46 (8), 2038–2056. https://doi.org/10.1039/c6cs00803h
113. *Van der Toom E. E., Verdone J. E., Gorin M. A., Pienta K. J.* Technical challenges in the isolation and analysis of circulating tumor cells. *Oncotarget*. 2016, 7 (38), 62754–62766. https://doi.org/10.18632/oncotarget.11191
114. *Li S., Plouffe B. D., Belov A. M., Ray S., Wang X., Murthy S. K., Karger B. L., Ivanov A. R.* An Integrated Platform for Isolation, Processing, and Mass Spectrometry-based Proteomic Profiling of Rare Cells in Whole Blood. *MCP*. 2015, 14 (6), 1672–1683. https://doi.org/10.1074/mcp.M114.045724
115. *Keller L., Pantel K.* Unravelling tumour heterogeneity by single-cell profiling of circulating tumour cells. *Nat. Rev. Cancer*. 2019, 19 (10), 553–567. https://doi.org/10.1038/s41568-019-0180-2
116. *Campos-Carrillo A., Weitzel J. N., Sahoo P., Rockne R., Mokhnatkin J. V., Murtaza M., Gray S. W., Goetz L., Goel A., Schork N., Slavin T. P.* Circulating tumor DNA as an early cancer detection tool. *Pharmacology & Therapeutics*. 2020, V. 207, P. 107458. https://doi.org/10.1016/j.pharmthera.2019.107458
117. *Kelley S. O., Pantel K. A.* New Era in Liquid Biopsy: From Genotype to Phenotype. *Clin. Chem.* 2020, 66 (1), 89–96. https://doi.org/10.1373/clinchem.2019.303339
118. *Ferreira M. M., Ramani V. C., Jeffrey S. S.* Circulating tumor cell technologies. *Mol. Oncol.* 2016, 10 (3), 374–394. https://doi.org/10.1016/j.molonc.2016.01.007
119. *Cho H., Kim J., Song H., Sohn K. Y., Jeon M., Han K. H.* Microfluidic technologies for circulating tumor cell isolation. *The Analyst.* 2018, 143 (13), 2936–2970. https://doi.org/10.1039/c7an01979c
120. *Sharma S., Zhuang R., Long M., Pavlovic M., Kang Y., Ilyas A., Asghar W.* Circulating tumor cell isolation, culture, and downstream molecular analysis. *Biotechnology Advances.* 2018, 36 (4), 1063–1078. https://doi.org/10.1016/j.biotechadv.2018.03.007
121. *Guerin M. V., Finisguerra V., Van den Eynde B. J., Bercovici N., Trautmann A.* Preclinical murine tumor models: a structural and functional perspective. *eLife*. 2020, V. 9, e50740. https://doi.org/10.7554/eLife.50740
122. *Kerbel R. S.* A Decade of Experience in Developing Preclinical Models of Advanced- or Early-Stage Spontaneous Metastasis to Study Antiangiogenic Drugs, Metronomic Chemotherapy, and the Tumor Microenvironment. *Cancer J.* 2015, 21 (4), 274–283. https://doi.org/10.1097/PPO.0000000000000134
123. *Welch D. R.* Technical considerations for studying cancer metastasis *in vivo*. *Clin. Exp. Metastasis*. 1997, 15 (3), 272–306. https://doi.org/10.1023/a:1018477516367
124. *Goodale D., Phay C., Postenka C. O., Keeney M., Allan A. L.* Characterization of tumor cell dissemination patterns in preclinical models of cancer metastasis using flow cytometry and laser scanning cytometry. *Cytometry A.* 2009, 75 (4), 344–355. https://doi.org/10.1002/cyto.a.20657
125. *Allan A. L., Vantyghem S. A., Tuck A. B., Chambers A. F., Chin-Yee I. H., Keeney M.* Detection and quantification of circulating tumor cells in mouse models of human breast cancer using immunomagnetic enrichment and multiparameter flow cytometry. *Cytometry A.* 2005, 65 (1), 4–14. https://doi.org/10.1002/cyto.a.20132
126. *Kersten K., de Visser K. E., van Miltenburg M. H., Jonkers J.* Genetically engineered mouse models in oncology research and cancer medicine. *EMBO Mol. Med*. 2017, 9 (2), 137–153. https://doi.org/10.15252/emmm.201606857
127. *Olive K. P., Politi K.* Translational therapeutics in genetically engineered mouse models of cancer. *Cold Spring Harb. Pro-*

toc. 2014, 2014 (2), 131–143. https://doi.org/10.1101/pdb.top069997
128. *Hashizume R., Gupta N.* Patient-derived Tumor Models for Diffuse Intrinsic Pontine Gliomas. *Curr. Neuropharmacol.* 2017, 15 (1), 98–103. https://doi.org/10.2174/1570159x14666160523144117
129. *Rebecca V. W., Somasundaram R., Herlyn M.* Pre-clinical modeling of cutaneous melanoma. *Nat. Commun.* 2020, 11 (1), 2858. https://doi.org/10.1038/s41467-020-15546-9
130. *Lee T. W., Lai A., Harms J. K., Singleton D. C., Dickson B. D., Macann A., Hay M. P., Jamieson S.* Patient-Derived Xenograft and Organoid Models for Precision Medicine Targeting of the Tumour Microenvironment in Head and Neck Cancer. *Cancers.* 2020, 12 (12), 3743. https://doi.org/10.3390/cancers12123743
131. *Lallo A., Schenk M. W., Frese K. K., Blackhall F., Dive C.* Circulating tumor cells and CDX models as a tool for preclinical drug development. *Transl. Lung Cancer Res*. 2017, 6 (4), 397–408. https://doi.org/10.21037/tlcr.2017.08.01
132. *Tellez-Gabriel M., Cochonneau D., Cadé M., Jubellin C., Heymann M. F., Heymann D.* Circulating Tumor Cell-Derived Pre-Clinical Models for Personalized Medicine. *Cancers*. 2018, 11 (1), 19. https://doi.org/10.3390/cancers11010019
133. *Alimirzaie S., Bagherzadeh M., Akbari M. R.* Liquid biopsy in breast cancer: A comprehensive review. *Clin. Genet.* 2019, 95 (6), 643–660. https://doi.org/10.1111/cge.13514
134. *Schwarzenbach H., Hoon D. S., Pantel K.* Cell-free nucleic acids as biomarkers in cancer patients. *Nat. Rev. Cancer.* 2011, 11 (6), 426–437. https://doi.org/10.1038/nrc3066
135. *Schwarzenbach H., Nishida N., Calin G. A., Pantel K.* Clinical relevance of circulating cell-free microRNAs in cancer. *Nat. Rev. Clin. Ooncol.* 2014, 11 (3), 145–156. https://doi.org/10.1038/nrclinonc.2014.5
136. *Pardini B., Sabo A. A., Birolo G., Calin G. A.* Noncoding RNAs in Extracellular Fluids as Cancer Biomarkers: The New Frontier of Liquid Biopsies. *Cancers.* 2019, 11 (8), 1170. https://doi.org/10.3390/cancers11081170
137. *Eslami-S Z., Cortés-Hernández L. E., Cayrefourcq L., Alix-Panabières C.* The Different Facets of Liquid Biopsy: A Kaleidoscopic View. *Cold Spring Harb. Perspect. Med.* 2020, 10 (6), a037333. https://doi.org/10.1101/cshperspect.a037333
138. *Fici P.* Cell-Free DNA in the Liquid Biopsy Context: Role and Differences Between ctDNA and CTC Marker in Cancer Management. *Methods Mol. Biol.* 2019, V. 1909, P. 47–73. https://doi.org/10.1007/978-1-4939-8973-7_4
139. *Maly V., Maly O., Kolostova K., Bobek V.* Circulating Tumor Cells in Diagnosis and Treatment of Lung Cancer. *In Vivo.* 2019, 33 (4), 1027–1037. https://doi.org/10.21873/invivo.11571
140. *Liang D. H., Hall C., Lucci A.* Circulating Tumor Cells in Breast Cancer. *Recent results in cancer research. Fortschritte der Krebsforschung. Progres dans les recherches sur le cancer.* 2020, V. 215, P. 127–145. https://doi.org/10.1007/978-3-030-26439-0_7
141. *Cortés-Hernández L. E., Eslami-S Z., Alix-Panabières C.* Circulating tumor cell as the functional aspect of liquid biopsy to understand the metastatic cascade in solid cancer. *Mol. Aspects Med*. 2020, V. 72, P. 100816. https://doi.org/10.1016/j.mam.2019.07.008
142. *Mushtaq M., Kovalevska L., Darekar S., Abramsson A., Zetterberg H., Kashuba V., Klein G., Arsenian-Henriksson M., Kashuba E.* Cell stemness is maintained upon concurrent expression of RB and the mitochondrial ribosomal protein S18-2. *Proc. Natl. Acad. Sci. USA.* 2020, 117 (27). https://doi.org/10.1073/pnas.1922535117
143. *Liu T., Xu H., Huang M., Ma W., Saxena D., Lustig R. A., Alonso-Basanta M., Zhang Z., O'Rourke D. M., Zhang L., Gong Y., Kao G. D., Dorsey J. F., Fan Y.* Circulating Glioma Cells Exhibit Stem Cell-like Properties. *Cancer Res.* 2018, 78 (23), 6632–6642. https://doi.org/10.1158/0008-5472.CAN-18-0650
144. *Okabe T., Togo S., Fujimoto Y., Watanabe J., Sumiyoshi I., Orimo A., Takahashi K.* Mesenchymal Characteristics and Predictive Biomarkers on Circulating Tumor Cells for Therapeutic Strategy. *Cancers*. 2020, 12 (12), 3588. https://doi.org/10.3390/cancers12123588
145. *Guan X., Ma F., Li C., Wu S., Hu S., Huang J., Sun X., Wang J., Luo Y., Cai R., Fan Y., Li Q., Chen S., Zhang P., Li Q., Xu B.* The prognostic and therapeutic implications of circulating tumor cell phenotype detection based on epithelial-mesenchymal transition markers in the first-line chemotherapy of HER2-negative metastatic breast cancer. *Cancer Commun. (Lond).* 2019, 39 (1), 1. https://doi.org/10.1186/s40880-018-0346-4
146. *Chen Y., Li S., Li W., Yang R., Zhang X., Ye Y., Yu J., Ye L., Tang W.* Circulating tumor cells undergoing EMT are poorly correlated with clinical stages or predictive of recurrence in hepatocellular carcinoma. *Sci. Rep.* 2019, 9 (1), 7084. https://doi.org/10.1038/s41598-019-43572-1
147. *Sun Y. F., Guo W., Xu Y., Shi Y. H., Gong Z. J., Ji Y., Du M., Zhang X., Hu B., Huang A., Chen G. G., Lai P., Cao Y., Qiu S. J., Zhou J., Yang X. R., Fan J.* Circulating Tumor Cells

from Different Vascular Sites Exhibit Spatial Heterogeneity in Epithelial and Mesenchymal Composition and Distinct Clinical Significance in Hepatocellular Carcinoma. *Clin. Cancer Res.* 2018, 24 (3), 547–559. https://doi.org/10.1158/1078-0432.CCR-17-1063

148. *Lin P. P.* Aneuploid Circulating Tumor-Derived Endothelial Cell (CTEC): A Novel Versatile Player in Tumor Neovascularization and Cancer Metastasis. *Cells.* 2020, 9 (6), 1539. https://doi.org/10.3390/cells9061539
149. *Galanzha E. I., Menyaev Y. A., Yadem A. C., Sarimollaoglu M., Juratli M. A., Nedosekin D. A., Foster S. R., Jamshidi-Parsian A., Siegel E. R., Makhoul I., Hutchins L. F., Suen J. Y., Zharov V. P. In vivo* liquid biopsy using Cytophone platform for photoacoustic detection of circulating tumor cells in patients with melanoma. *Sci. Transl. Med.* 2019, 11 (496), eaat5857. https://doi.org/10.1126/scitranslmed.aat5857
150. *Han Y., Liu D., Li L.* PD-1/PD-L1 pathway: current researches in cancer. *Am. J. Cancer Res.* 2020, 10 (3), 727–742.
151. *Zhang W., Huang Q., Xiao W., Zhao Y., Pi J., Xu H., Zhao H., Xu J., Evans C. E., Jin H.* Advances in Anti-Tumor Treatments Targeting the CD47/SIRPα Axis. *Front. Immunol.* 2020, V. 11, P. 18. https://doi.org/10.3389/fimmu.2020.00018
152. *Lian S., Xie R., Ye Y., Lu Y., Cheng Y., Xie X., Li S., Jia L.* Dual blockage of both PD-L1 and CD47 enhances immunotherapy against circulating tumor cells. *Sci. Rep.* 2019, 9 (1), 4532. https://doi.org/10.1038/s41598-019-40241-1
153. *Chen C., Zhao S., Karnad A., Freeman J. W.* The biology and role of CD44 in cancer progression: therapeutic implications. *J. Hematol. Oncol.* 2018, 11 (1), 64. https://doi.org/10.1186/s13045-018-0605-5
154. *Leone K., Poggiana C., Zamarchi R.* The Interplay between Circulating Tumor Cells and the Immune System: From Immune Escape to Cancer Immunotherapy. *Diagnostics (Basel).* 2018, 8 (3), 59. https://doi.org/10.3390/diagnostics8030059
155. *Zhong X., Zhang H., Zhu Y., Liang Y., Yuan Z., Li J., Li J., Li X., Jia Y., He T., Zhu J., Sun Y., Jiang W., Zhang H., Wang C., Ke Z.* Circulating tumor cells in cancer patients: developments and clinical applications for immunotherapy. *Mol. Cancer.* 2020, 19 (1), 15. https://doi.org/10.1186/s12943-020-1141-9

ЦИРКУЛЮВАЛЬНІ ПУХЛИННІ КЛІТИНИ: НА ЧОМУ МИ ЗУПИНИЛИСЯ?

І. Кривошлик, Л. Сківка

ННЦ «Інститут біології та медицини»
Київського національного університету
імені Тараса Шевченка

E-mail: skivkalarysa964@gmail.com

Метастазування та рецидив раку є основними причинами смертності у хворих на онкологічну патологію. Пухлинні клітини, які відокремлюються від первинної або вторинної пухлини і поширюються у кров, називають циркулювальними пухлинними клітинами (ЦПК). Вони характеризують мінімальну залишкову хворобу і є ключовими рушіями поширення пухлини у прилеглі тканини та віддалені органи. Використання ЦПК для діагностики і лікування онкологічної патології у клінічній практиці потребує глибокого розуміння їхньої біології, а також ролі в уникненні пухлиною імунного нагляду, стійкості до хіміо- та імунотерапії та феномену метастатичного спокою.

ЦИРКУЛИРУЮЩИЕ ОПУХОЛЕВЫЕ КЛЕТКИ: НА ЧЕМ МЫ ОСТАНОВИЛИСЬ?

И. Кривошлык, Л. Скивка

УНЦ «Институт биологии и медицины»
Киевского национального университета
имени Тараса Шевченко

E-mail: skivkalarysa964@gmail.com

Метастазирование и рецидив рака являются основными причинами смертности у больных с онкологической патологией. Опухолевые клетки, которые отделяются от первичной или вторичной опухоли и распространяются в кровь, называются циркулирующими опухолевыми клетками (ЦОК). Эти клетки характеризуют минимальную остаточную болезнь и являются ключевыми двигателями распространения опухоли в окружающие ткани и отдаленные органы. Использование ЦОК для диагностики и лечения онкологической патологии в клинической практике требует глубокого понимания их биологии, а также роли в ускользании опухоли от иммунного ответа, устойчивости к химио- и иммунотерапии и феномена метастатического покоя.

Мета. Огляд сучасних знань щодо біології ЦПК, а також перспектив їх використання для діагностики та спрямованого лікування метастатичної хвороби.

Методи. Комплексний огляд літератури із застосуванням баз даних MEDLINE, Biological Abstracts та EMBASE.

Результати. В огляді узагальнено і проаналізовано історичні відомості та сучасні дані щодо біології CTC, основних етапів їхнього життєвого циклу, ролі у метастатичному каскаді, клінічних перспектив їх використання як маркерів для діагностики та прогнозування перебігу захворювання, а також мішеней для лікування раку.

Висновки. Значний прогрес у галузі біології ЦПК та їх застосування у тераностиці раку переконливо доводить деєвість цих клітин як мішеней для прогнозу і лікування метастатичної хвороби. Ефективному використанню рідкої біопсії з кількісною та фенотиповою характеристикою ЦПК перешкоджає недосконаліть методології взяття біологічного матеріалу і відсутність надійних маркерів для оцінювання метастатичного потенціалу ЦПК різного походження. Різноманіття механізмів міграції та інвазії пухлинних клітин потребує розроблення комплексних терапевтичних підходів для антиметастатичної терапії щодо ЦПК. Зусилля, орієнтовані на вирішення цих основних питань, можуть сприяти розробленню нових ефективних стратегій лікування раку.

Ключові слова: циркулювальні пухлинні клітини, циркулювальні пухлинні мікроемболи, метастазування, епітелійно-мезенхімний перехід, мінімальна залишкова хвороба.

Цель. Обзор современных знаний по биологии ЦОК, а также перспектив их использования для диагностики и направленного лечения метастатической болезни.

Методы. Комплексный обзор литературы с использованием баз данных MEDLINE, Biological Abstracts и EMBASE.

Результаты. В обзоре обобщены и проанализированы исторические сведения и современные данные, касающиеся биологии ЦОК, основных этапов их жизненного цикла, роли в метастатическом каскаде, клинических перспектив их использования в качестве маркеров для диагностики и прогнозирования течения заболевания, а также мишеней для лечения рака.

Выводы. Значительный прогресс в области биологии ЦОК и их использования в тераностике рака убедительно доказывает действенность этих клеток в качестве мишеней для прогноза и лечения метастатического заболевания. Эффективному использованию жидкой биопсии с количественной и фенотипической характеристикой ЦОК препятствуют несовершенство методологии взятия биологического материала и отсутствие надежных маркеров для оценки метастатического потенциала ЦОК различного происхождения. Многообразие механизмов миграции и инвазии опухолевых клеток требует разработки комплексных терапевтических подходов для антиметастатической терапии, нацеленной на ЦОК. Усилия, направленные на решение этих основных вопросов, могут способствовать разработке новых эффективных стратегий лечения рака.

Ключевые слова: циркулирующие опухолевые клетки; циркулирующие опухолевые микроэмболы; метастазирование; эпителиально-мезенхимальный переход; минимальная остаточная болезнь.

UDC 615.37: 578.824.11 https://doi.org/10.15407.biotech14.04.028

BIOTECHNOLOGICAL RESEARCH IN THE CREATION AND PRODUCTION OF ANTIRABIC VACCINES

KRASNOPOLSKY Yu. M., PYLYPENKO D. M.

National Technical University "Kharkiv Polytechnic Institute", Ukraine

E-mail: yuriykrasnopolsky@gmail.com

Received 14.06.2021
Revised 01.07.2021
Accepted 31.08.2021

Rabies is a neurological disease of a viral nature, leading to death. Rabies virus is an RNA virus that invades the central nervous system, leading to neuronal dysfunction. Timely vaccination can prevent the diseases development.

Aim. The article is devoted to immunobiotechnological research aimed at creating antirabic vaccines.

Results. The history of the antirabic vaccines creation from the first inactivated vaccines obtained from nervous tissue to the cultivation of the virus on animal cell cultures is considered. The article presents commercially available anti-rabies vaccines: their composition, the used rabies virus strains, cell cultures, the methods of inactivation and purification. The technology of producing an anti-rabies vaccine based on a Pitman Moore virus strain and a chicken fibroblast cell culture is presented. The advantages of different vaccine types are considered: live attenuated, peptide, liposomal, RNA vaccines, vaccines based on viral vectors, transgenic plants and reverse genetics methods.

Conclusions. The development of biotechnology, immunology and virology makes it possible to improve constantly vaccine preparations, including those against rabies, increasing their effectiveness and safety.

Key words: immunobiotechnology; viral vaccines; antirabic vaccine; RNA virus; rabies virus.

Rabies (R) is one of the oldest neurological diseases caused by the rabies virus — *Rabdovirus* (RV). The virus belongs to the genus *Lyssavirus*, the *Rhabdoviridae* family. RV is a neurotropic, RNA negative single-stranded virus. RV causes a lethal encephalitis in mammals known as R, which causes 60,000 deaths worldwide annually, leading to death with the development of clinical symptoms. In Ukraine, 20894 people were vaccinated in 2019, 1938 of them were with a confirmed R diagnosis [1]. The virus enters the peripheral area after exposure and subsequently spreads to the central nervous system, causing neuronal dysfunction, which is the main cause of death in R [2].

All Rhabdoviruses have 2 main structural components: the helical nucleoprotein nucleus (RNP) and the surrounding envelope. The RV genome encodes five proteins: nucleoprotein (N), phosphoprotein (P), matrix protein (M), glycoprotein (G), polymerase (L). G forms about 400 spines densely located on the viral surface. Protein M is associated with both envelope and RNP and may be the central protein of the RV assembly (Fig. 1).

RV enters the nervous system by binding to nerve receptors such as acetylcholine, nerve cell adhesion, nerve growth factor receptors. The RV is then transported to the central nervous system by axonal (retrograde) transport, possibly by binding to cytoplasmic dynein. In axons, RV carries out retrograde transport by means of movement on the cytoskeleton tubes surface — they move from the plus-ends to the minus-ends (Fig. 2).

G, the only protein exposed on the surface of virions, is the main viral component responsible for the induction of host antibodies. G serves as an important vaccine immunogen (Vac) against R. Various constructs expressing protein-G are being developed using paramyxoviruses and adenovirus vectors that can induce sustained humoral immunity in the RV response [4].

Immunobiotechnology, in particular, vaccinology, enables to prevent the disease R with the help of vaccination, provided that it is carried out in a timely and correct manner.

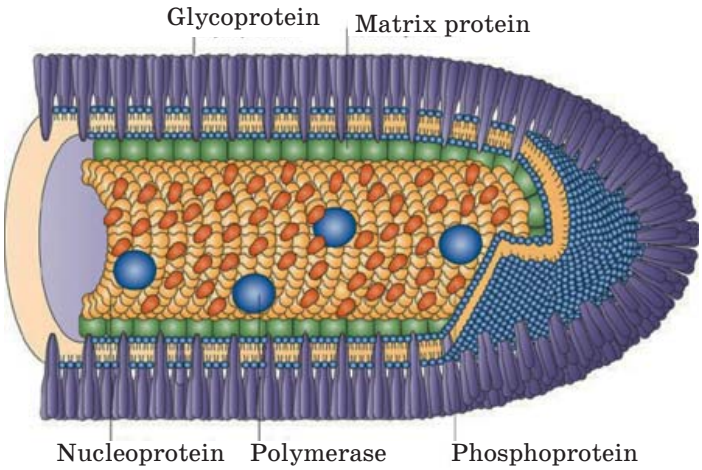

Fig. 1. **Schematic structure of the RV virion [3]**

Since the time of Louis Pasteur (1822–1895), Vacs for human versus R are made from inactivated RV. Since 1880, L. Pasteur began the experimentations aimed at artificially reducing the virulence of infectious agents and obtaining attenuated strains. He obtained weakened pathogen strains of chicken cholera and anthrax. L. Pasteur used the principles and methods of attenuation upon Vac against R receipt and practical use. Having received the so-called fixed RV (fixeRV) with a standard virulence degree, Pasteur injected RV suboccipitally into rabbits, causing them to become infected. Then the spinal cord of the animals was subjected to drying at different times, which caused RV attenuation and a decrease in the number of living RV particles. This research led to the creation of the anti-rabies Vac (antiRab-Vac). L. Pasteur applied his discoveries well beyond the animals, but to humans: a boy was brought to him from Alsace, who was bitten by a mad dog. Pasteur began a course of 13 injections of emulsified rabbit spinal cord material three days after the child was bitten. 90 passages were used by L. Pasteur for the first Vac with Virus Fixe. Vac against RV developed by L. Pasteur was obtained from neural tissue, and RV was inactivated by drying. However, this Vac posed a danger according to the possibility of RV activation and the development of allergic reactions due to the presence of myelin in the nervous tissue. For the first time, vaccination against R was carried out using the brain Vac, registered by L. Pasteur in 1885. Later, the safety of Vac was increased by phenol inactivation of RV (1911). However, after use, serious side effects were still observed, including several cases of paralysis and death. The main factor is hypersensitivity to myelin. Subsequently, it has been found that the amount of myelin in Vac could be reduced by using neonatal mice with lower myelin levels in the brain [6].

In Ukraine, until the early 80s, a lyophilized antiRab-Vac of the Fermi type, made from the brain of infected with Virus Fixe sheep, was used. The homogenized brain in a 0.9% NaCl solution containing 1.0% of phenol was inactivated for 8 days at a temperature of 20–22 °C. Sucrose is added to Vac and the mixture is lyophilized. Serious side effects associated with hypersensitivity to myelin were observed with Vac application. In addition, it is necessary to take into account the presence of various immunochemically active lipids in the brain Fermi Vac [7], which can lead to the appearance of anti-lipid antibodies [8]. It should be noted that the brain tissue contains gangliosides (Gan), which can serve as receptors for binding to RV. The study of Gan isolated from the cattle brain (GT1 and GD1a) in *in vitro* and *in vivo* experiments showed antiviral activity when infected with RV in animals at the early stages of infection. The survival value in comparison with the control (death of 100% of animals) ranged from 20 to 60% (virus activity was 50–100 LD_{50}), depending on the concentration of Gan [9].

As it can be seen from the above data, antiRab-Vac was originally obtained from neural tissue. Currently antiRab-Vacs are mainly Vacs based on cell cultures and avian embryos. In subsequent years, the specialists were faced with the task of creating antiRab-Vac production on biological substrates free from nervous tissue. Vacs began to be obtained on the basis of cell cultures of avian embryos: duck (embrio duck — ED), and later chick

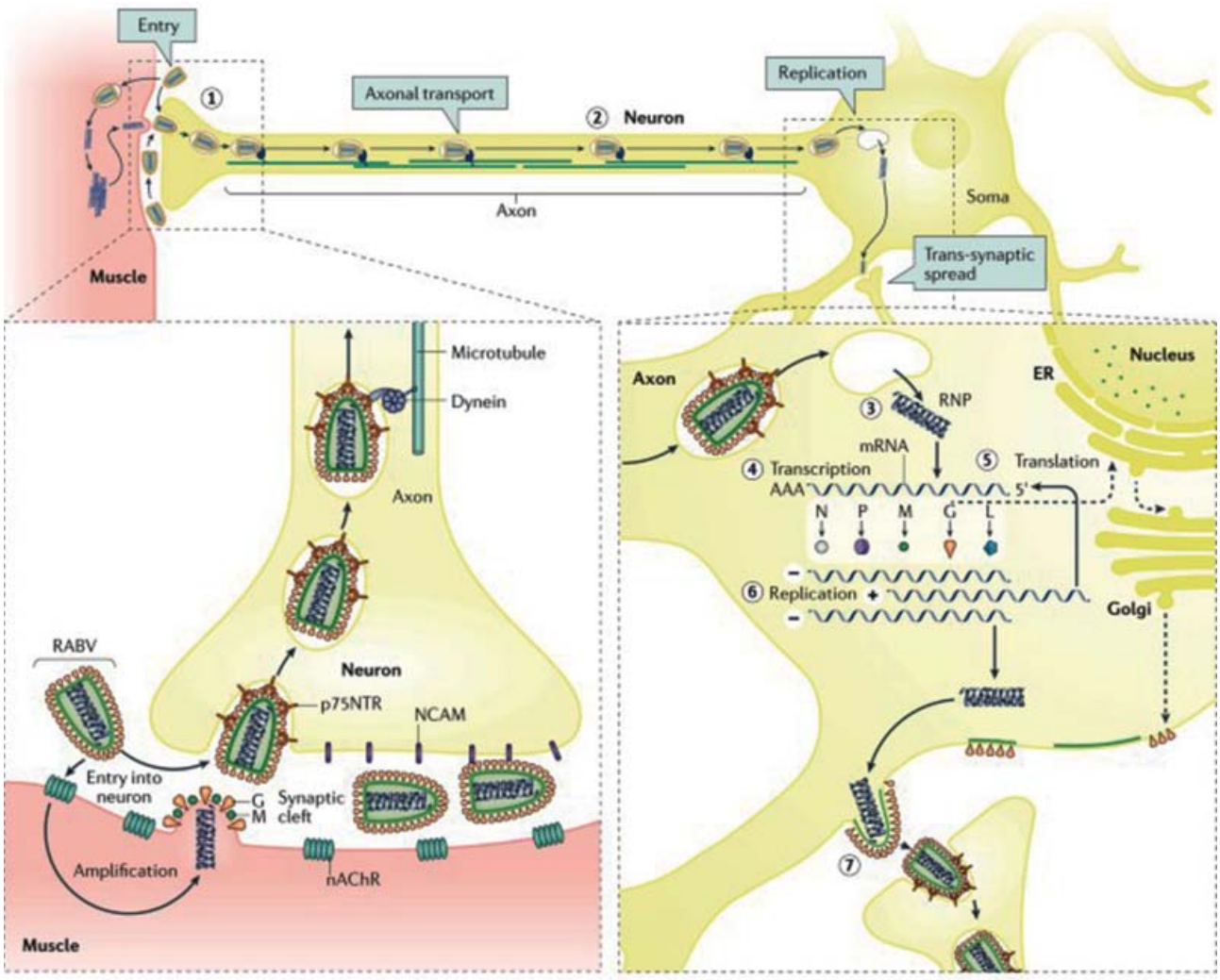

Fig. 2. **Diagram of RV penetration into the nervous system [5]:**
1 — receptor-mediated RV endocytosis on the presynaptic membrane; *2* — retrograde axonal RV transport toward the neuron body; *3* — the ribonucleoprotein release from the endocytic vesicle; *4* — viral mRNA transcription; *5* — viral proteins translation; *6* — full-length RNA genomes replication; *7* — viral particles assembly and release from a cell

(embrio chick — EC) for RV cultivation. Cell culture-based Vacs contain RV that multiply in cell substrates. In the process of developing Vacs containing inactivated RV, it was proposed to use other cells: primary culture of hamster kidney cells, human diploid cells (HDC), Vero cells, etc. [10]. Simultaneously with these studies, the possibility of various RV strains application was studied (Table 1). Human studies of Vacs containing the RV Flury low egg passage (Flury-LEP) strain have shown no side effects. However, these Vacs were characterized by insufficient immunogenicity. The use of the RV Flury high egg passage (Flury-HEP) strain increased the Vacs immunogenicity compared to the Flury-LEP-based preparation, but was slightly lower than the brain vaccine. Vac with inactivated Flury virus grown on ED was more effective, but its immunogenicity was lower than the brain vaccines.

Further studies were carried out using a culture of human fetal fibroblasts, which were HDCs with a limited lifespan. It was soon shown that fetal fibroblasts were susceptible to human viruses and free of latent viruses [11]. By the early 1960s, the highly immunogenic HDC line was used for RV propagation. HDC Vacs were first licensed in Europe in 1976 and in the USA in 1980 and are still in use today. In 1985, a purified concentrated Vac against rabies was obtained on Vero cells, which has a high immunogenicity comparable to Vac on HDC [12–15].

Currently, the requirements for AntiRab-Vacs developed by WHO are presented in a series of technical reports published in different

years, in which the requirements for AntiRab-Vacs are constantly increasing [16–18]. The reports provide the basic requirements for the production and control of AntiRab-Vacs for humans. The document describes in detail the cell cultures and requirements for them, considers the RVs allowed for use to obtain AntiRab-Vacs and for their control. The used standards and the main provisions of the production technology are described: cultivation, purification, and inactivation (β-propiolactone, formalin, etc.), adjuvants (aluminum hydroxide), requirements for the vaccine at different production stages.

Over the past period, antiRab-Vacs obtained by growing RVs on ED have been developed. However, these Vacs are less immunogenic than Vac from brain tissue. For ED drugs, 14 to 23 daily vaccinations are recommended, but sometimes even such high doses do not protect against Rab after intense contact with the source of infection. Another disadvantage of these Vacs is that the Vacs also contained myelin proteins, which caused adverse reactions, and as a result, the drug was forbidden by the WHO.

Subsequently, antiRab-Vac was obtained in cell and tissue culture. Vacs prepared in cell culture were not only safer compared to the vaccines based on brain tissue due to the neurotropic tissue absence, but also more effective.

Then AntiRab-Vacs were obtained: purified duck embryonic vaccine (PDEV); HDC-based one; purified EC cells-based Vac; purified VERO cells-based AntiRab-Vac; adsorbed AntiRab-Vac (RVA) obtained from hamster kidney primary cell culture.

The technological process leading to the development of the above Vacs included: Pitman Moore RV strain adaptation to stable cell lines such as VERO cells (Abhayrab and Verorab); HDC MRC-5. HDC-based Vac is considered the gold standard drug.

Currently, various RV strains and cell cultures are used to obtain AntiRab-Vacs (Table 1).

Currently, Vacs obtained from various RV strains using cell cultures of various origin are used for the prevention of Rab in humans (Table 2).

Currently, antiRab-Vacs such as Rabavert and Rabipur, represented by inactivated RVs, are widely used. Since inactivated Vacs cannot induce strong immunity to provide long-term protection against RV infection, recipients must receive multiple vaccinations over time, which requires new technological approaches to create Vacs. Rabipur (Table 2) was the first purified Vac obtained from chick embryo cells was licensed in Germany in 1984 and then in 60 more countries. The immunogenicity of Vac Rabipur has been confirmed in numerous clinical trials [19].

Rabipur is produced using the Flury-LEP RV strain grown on a primary fibroblast culture of chicken embryo cells. Virus in Vac is inactivated with β-propiolactone and purified by continuous density gradient centrifugation. As a result, a highly concentrated preparation stabilized with polygenin is obtained, followed by lyophilization. Rabipur is produced in Marburg, Germany and Ankleshwar, India.

Below it is a technological scheme of AntiRab-Vac obtained through the use of RV Pitman Moore and a cell culture of chicken fibroblasts [20]:

1 — preparation of ED and EC according to the classical scheme (9–11 days, at a temperature of 35–37 °C and humidity of 70–90%, trypsinization and centrifugation);

2 — infection of the primary culture of ED RV fibroblasts — 7 passages (adaptation), after which the resulting strain was cultured on the EC fibroblast culture — 4 passages, the selected embryos were trypsinized, centrifuged and the cells were suspended in the growth medium to a final concentration of 1.7×10^6 cells/ml;

3 — the suspension of trypsinized cells was filtered through a nylon filter and centrifuged (1000–1500 rpm, 15 min, at 2–4 °C). The cell sediment was suspended in fresh growth medium,

Table 1. **Cell cultures and RV strains used to obtain AntiRab-Vacs for humans**

Cell culture type	RV strains
HDC — human diploid cell culture	Flury-LEP — 40–50 passages
Primary canine kidney cell culture	Flury-HEP — 227–330 passages
Vero — kidney epithelium cells of the green African monkey	Pitman moore
	Vnukovo 32
BNK 21 — neonatal hamster kidney culture	Paris Pasteur
Chicken embryo primary culture	Rabbit fix
Hamster kidney primary cell culture	Street –Alabama Duffering
Chicken embryo primary cell culture	Challenge Virus Standart (CVS) 111

Table 2. **Characteristics of inactivated AntiRab-Vacs for humans**

Name of the vaccines	Strain	Cell culture	Purification type	Inactivator	Excipients per dose	Manufacturer
Rabipur, liof. > 2,5 ME	Flury LEP	Chicken embryo fibroblasts	Zonal ultracentrifugation in a sucrose density gradient	β-propiolactone	Sucrose — 75 mg, Hydrolyzed Gelatin — 10 mg (Polygelin)	Chiron Behring vaccines, India
Verorab, liof. > 2,5 ME	Wistar Rabies PM W 138-1503-34	Vero	Zonal ultracentrifugation in a sucrose density gradient	β-propiolactone	Maltose — 26.3 mg HSA — 2.5 mg	Sanofi Pasteur, France
Indirab, liof. > 2,5 ME	PM	Vero	Chromatography, ultrafiltration	β-propiolactone	Maltose — 25.0 mg HSA — 5 mg Merthiolate — 0,01%	Bharat Biotech, India
Kokav, liof. > 2.5 ME	Vnukovo 32	Syrian hamster kidney cells	Ultrafiltration	UV irradiation	HSA — 10 mg, sucrose — 75 mg, hydrolyzed gelatin — 10 mg (polygelin)	Scientific Production Association NPO Microgen, Russia
Imovax rabies, liof. > 2,5 ME	Wistar Rabies PM W 138-1503-3M	HDC	Ultrafiltration	β-propiolactone	HSA — 100 mg, neomycin — 150 mcg	Sanofi Pasteur, France
RabAvert, liof. > 2,5 ME	Fix virus, LEP Flury	Chicken fibroblasts	Zonal ultracentrifugation in a sucrose density gradient	β-propiolactone	HSA — 0.3 mg, Na-EDTA — 0.3 mg, sodium glutamine – 1 mg, hydrolyzed gelatin —– 12 mg (polygelin)	Glaxo Smith Kline, Belgium

Note: * PM – RV Pitman Moore strain; Vero —the kidneys epithelium cells of the green African monkey; Polygelin — a polymer of urea and polypeptides from denatured bovine gelatin; HSA — human serum albumin.

mixed and re-centrifuged under the same conditions. The cell suspension was stirred for 5–10 min at 35 ± 2 °C. The final cell concentration was adjusted with the growth medium to a concentration of $1.4–2.2\times10^6$ cells/ml;

4 — the cell suspension was inoculated with RV and incubated (90–120 min at 35 ± 2 °C) with stirring to adsorb the virus on the cells. An RV-infected cell suspension with a virus was incubated at a temperature of 34.5 ± 0.5 °C for 6 days;

5 — on the 4^{th}–5^{th} day of cultivation, the supernatant was taken (the 1^{st} harvest) and fresh growth medium was added. On the 7^{th}–8^{th} day the 2^{nd} harvest was taken. The harvests were stored at 2–8 °C;

6 — virus harvests were united, purified and concentrated using sucrose density gradient ultracentrifugation in a zonal centrifuge at 35,000 rpm. Corresponding bands containing live RV were selected at a sucrose concentration of 35–40%. During the monitoring period, the RV concentrate was stored at minus 60 °C (sterility, endotoxins, immunogenicity, etc. were monitored);

7 — the concentrate was thawed at 37 °C and cooled at 4 ± 2 °C, diluted with a stabilizing solution (sucrose, hydrolyzed gelatin, human serum albumin, sodium salts) to an antigen content of 8.5 IU/ml. The pH in Vac was adjusted to 8 ± 1 with 10% NaOH;

8 — β-propiolactone was added to the viral suspension to a final concentration of 0.025%. Incubation was carried out at 2–6 °C and constant stirring for at least 48 hours until complete RV inactivation;

9 — filling of primary packaging, lyophilization and sealing;

10 — Vac control.

Currently research is ongoing to create new forms of AntiRab-Vac. Research is carried out in a number of directions (Fig. 3):

Live attenuated Vacs — LAV. Unlike inactivated Vacs, LAVs mimic natural

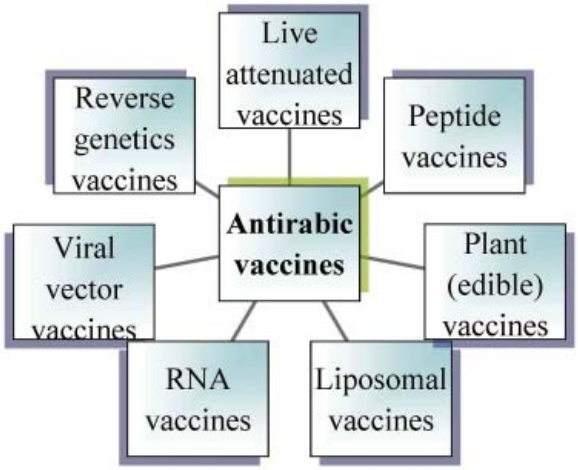

Fig. 3. **Types of vaccines against RV**

infection and often a single dose is sufficient to induce a sustained immune response. Until now, despite the wider use of LAV for oral vaccination against wild animals R (foxes, raccoons, etc.), LAV against domestic animals and humans R is still lacking. All LAVs used for wild animals are obtained as a result of repeated passage of SAD (street Alabama Dufferin) strains in cell culture, therefore, their possible return to virulence might become a practical limitation for their further development and usage for immunization of domestic animals, and especially for humans [21].

Peptide Vacs. There are known the works on the peptide Vacs creation against R. The effectiveness of the protein subunit, purified from the infected cells, G-protein for protection against R is studied. The G-protein of the R virus is the main protective antigen responsible for protective immunity against RV. In the study, the G-RV protein was introduced into a yeast cell and the resulting recombinant cell extracts containing the RV protein G protected guinea pigs from lethal RV infection when injected intramuscularly. However, these extracts did not protect mice infected with RV intracerebrally [22]. In general, Vacs based on RV protein subunits are low immunogenic and can cause limited immune responses.

AntiRab-Vacs of plant origin are the preparations based on transgenic plants, into the genome of which the corresponding fragment of the pathogenic microorganism genome has been inserted. In the literature, there are studies on the use of corn and tobacco for the RV G-protein expression for the production of "edible" Vac [23, 24]. Plant Vacs have not yet found application, despite the fact that the issue of creating such Vacs against RV and other infections has been studying for many years [25].

Liposomal (Ls) AntiRab-Vacs (LipoRV). LipoRV has been shown to promote the production of neutralizing antibodies to RV in BALBc mice. The Ls emulsion was prepared from hydrogenated soybean phosphatidylcholine and cholesterol. LipoRV consists of an Ls emulsion and an inactivated RV-Vac against RV. The immune response was compared between mice treated with LipoRV and inactivated AntiRab-Vac. In mice immunized with LipoRV, higher titers of the interleukin-2, interferon-gamma and the corresponding killer cells activity level were observed than in mice immunized with inactivated AntiRab-Vac. The authors' data also showed a higher survival value for mice that received 3 injections of LipoRV (56.2%) than 5 injections of inactivated AntiRab-Vac (40.6%) [26].

AntiRab-Vacs based on RNA. In the last decade, one of the strategies in the fight against infectious diseases has been RNA-Vac vaccination. Unlike DNA Vacs, which have a potential risk of integration with the host genome, RNA-based Vacs eliminate this danger. In addition, DNA-Vacs must be delivered to the nucleus and transcribed within the nucleus for antigen expression, which may not be effective in some cells. On the contrary, RNA-Vacs are directly translated into the cytoplasm, which not only eliminates the need for delivery to the nucleus, but leads to rapid antigen expression [27, 28]. RNA-based Vacs

are highly immunogenic and lead to consistent results [29, 30]. The impetus for the AntiRab-RNA-Vacs development could be the successful RNA-Vacs use for the COVID-19 prevention: RNA-Vacs of Pfaizer and Moderna firms. For example, Pfaizer Vac is a nucleoid-modified mRNA encoding a mutant form of the SARS-COV-2 spike protein, which is encapsulated in biodegradable lipid nanoparticles.

AntiRab-Vac based on viral vectors. Currently, a number of AntiRab-Vacs based on known viruses have been proposed: vesicular stomatitis, parainfluenza type 5, Newcastle disease, smallpox, human adenoviruses, etc. Genetically engineered vaccines based on these viral vectors make it possible to deliver into human or animal cells only genes encoding synthesis of the necessary antigens, which makes it possible not to use live pathogenic viruses when obtaining Vac. Recombinant Vacs are widely used today to control R in wild carnivores. A smallpox vaccine virus clone has been isolated, which forms the surface glycoprotein (G) RV. Vac containing recombinant cowpox virus carrying the gene for the basic glycoprotein (G) of the RV envelope has been obtained. Vac is often used orally to immunize foxes. Vac based on canine adenovirus has been created [31].

Vac against R obtained using reverse genetics method. Reverse genetics can reveal the function of genes. The researchers manipulate the genes sequence, changing or turning off a particular gene, and analyze what changes this leads to. This is the path of reverse genetics: from gene to trait, it has made it possible to create a new generation of AntiRab-Vacs [32, 33]. Reverse genetic methods offer an alternative solution for the development of safe and effective LAVs to prevent R, for example, the amino acid at position 333 of the glycoprotein (G) in several fixed RV strains is responsible for pathogenicity in adult mice. It was found that arginine at position 333 promotes the reversal of pathogenicity. In [21], a replicon was proposed as a live weakened AntiRab-Vac, in which the structural genes of Venezuelan equine encephalitis (VEEV) were replaced with the RV-G glycoprotein. Plasmid VEEV-RV-G was constructed using standard recombinant DNA techniques. The resulting glycoprotein sequence was amplified using an infectious clone as template and cloned into the VEEV replicon expression vector of alpha virus at AscI and PacI sites.

To further characterize VEEV-RV-G, the VEEV-RV-G particles were purified by ultracentrifugation and the protein composition of these particles was analyzed by SDS-PAGE. The RV-G protein was the only RV structural protein found in viral particles.

Bulky spherical particles of about 60–90 nm were observed on the surface of cells infected with VEEV-RV-G compared to the typical bullet-shaped RV particles. It has been shown that VEEV-RV-G can collect infectious viral particles that are very different from RV in both shape and size.

Glycoprotein-G (RV) provides efficient packaging of replicon chimeric RNA into infectious particles that can self-propagate in cell culture at high titers. VEEV-RV-G particles were highly attenuated in suckling mice and could induce strong humoral immune responses at relatively low doses. The mice were vaccinated with VEEV-RV-G intramuscularly, which protected the animals from lethal outcome in case of intracerebral infection with RV — CVS-24.

A number of studies and review materials are devoted to the creation, study and use of AntiRab-Vacs. The effectiveness of existing AntiRab-Vacs and the prospects for their development have been discussed in recent years [1, 19, 32, 34–36].

During the development and manufacture of Vacs, it is important to maintain the stability of the strains used. The development of molecular biology and biotechnology makes it possible to confirm the RV strains authenticity and their stability. The analysis of the Vnukovo-32 strain used to obtain AntiRab-Vac (cultured purified inactivated dry (KOKAV, Russia)) was performed. It was shown that the RNA structure of Vnukovo-312, CVS RV strains, which encodes a part of the G protein fragment, corresponds to a similar RNA fragment of RV. The 539 bp RNA structure of the RV strain, which encodes a fragment of protein G, is stable at all technology stages. The possibility of using restriction analysis to confirm the authenticity of the Vnukovo-32 RV strain at all stages of production, including the finished Vac form, has been shown [37].

Conclusions

Currently, inactivated viral Vacs are widely used for prevention of a number of infections. Some inactivated viral Vacs have been in use for decades and are generally well tolerated. Since viruses, when grown *in vitro*, usually enter the cell culture medium, they are separated from the infected cultures. The large viral particle size in comparison

with other macromolecules in the medium enables for easy particles separation using simple purification technologies based on separation of particles by size. The examples of such vaccines include polio virus, influenza virus, RV, and Japanese encephalitis virus. In an alternative approach used in the case of a killed viral vaccine (hepatitis A (HAV), Covid), the infected cells are lysed and the viral particles are purified. Viral particles are chemically inactivated, usually by treatment (β-propiolactone, formalin, radiation), and then the effect of the inactivated virus can be enhanced by adjuvants (for example, aluminum hydroxide or aluminum phosphate). It is possible to use Ls [25, 34] to enhance the immunogenicity of viral Vacs. Inactivated viral Vacs usually have high immunological activity, for example, 1 dose of hepatitis A vaccine provides protection in an amount of 50 ng. Thus, this classic strategy, characterized by an impeccable history of well-tolerated and effective vaccines creation, remains a very promising technology of choice for many viral Vacs, including AntiRab-Vacs.

Funding source. The work was performed within the research program "Comprehensive research and optimization of industrial and pharmaceutical biotechnologies" (State Registration No.0118U002336, 2018–2021). There is no conflict of interest.

REFERENCES

1. *Antonova L.O., Makovska I.F., Krupinina T.M.* The history of rabies control in Ukraine from the time of Pasteur to the present day. *Actual Infectology*. 2021, 9(1), 6–16. (In Russian). https://doi.org/10.22141/2312-413X.9.1.2021.228821
2. *Zhu S., Cuo C.* Rabies control and treanment: from prophylaxis strategies with curative potencial. *Viruses*. 2016, 8(11), 279–290.
3. *Schnell M.J., McGettigan J.P., Wirblich C., Papaneri A.* The cell biology of rabies virus: using stealth to reach the brain. *Nat. Rev. Microbiol.* 2010, 8(1), 51–61. https://doi.org/10.1038/nrmicro2260
4. *Wiktor T.J., Gyorgy E., Schlumberger D., Sokol F., Koprowski H.* Antigenic properties of rabies virus components. *J. Immunology*. 1973, 110, 269–276.
5. *Fooks A.R., Cliquet F., Finke S., Freuling C., Hemachudha T., Mani R.S., Müller T., Nadin-Davis S., Picard-Meyer E., Wilde H., Banyard A.C.* Rabies. *Nat. Rev. Dis. Primers.* 2017, 3, 17091. https://doi.org/10.1038/nrdp.2017.91
6. *Fuenzalida E., Palacios R., Borgano J.M.* Antirabies antibody response in man to vaccine made from infected sucking-mouse brains. *Bull. World Health Organ.* 1964, 30, 431–436.
7. *Holbets I. I. Krasnopolskyi Yu. M. Orlova H. L.* Vaccination of the anti-rabies vaccine in the warehouse and the role of lipids in the reactogenicity of the drug. *Pharm. J.* 1983, 2, 51–53. (In Ukrainian).
8. *Krasnopolskiy Yu.M., Golbets I.I., Sennikov G.A., Shvets V. I.* Immunochemistry of lipids. *Chem. Pharm. J.* 1981, 15(7), 13–25. (In Russian).
9. *Krasnopolskiy Yu.M., Shvets V.I.* Investigation of the effect of certain gangliosides on the resistance of mice to rabid virus. *Bull. Exp. Biol. Med.* 1987, CIV(12), 698–699. (In Russian).
10. *Zhu S., Li H., Wang C., Luo F., Guo.* Reverse genetics of rabies virus. New strateges to attenuate virus virulence for vaccine development. *J. Neurovirol.* 2015, 21, 335–345.
11. *Plotkin S. A.* Vaccine production in human diploid cell strains. *Am. J. Epidemiolog.* 1971, 94(3), 303–306. https://doi.org/10.1093/oxfordjournals.aje.a121323
12. *Giesen V., Gniel D., Malerczyk C.* 30 years of rabies vaccination with Rabipur: a summary of clinical data and global experience. *Expert Rev. Vaccines*. 2015, 14(3), 351–367. https://doi.org/10.1586/14760584.2015.1011134
13. *Wictor T. J., Koprowwski H.* Succesful immunization of primates with rabies vaccine preparazed in human diploid cell strain Wi38. *Proc. Soc. Exp. Biol. Med.* 1965, 118, 1069–1073. https://doi.org/10.3181/00379727-118-30048
14. *Plotkin S. A., Koprowski H.* Rabies vaccines. In Plotkin S. A., Orenstein W. A., Offit P. A. (Eds.) Vaccine. *Saunders / Elsevier.* 2008, 687–714.
15. Pharmacopoeial monograph 3.3.1.0025.15 Vaccine antirabies culture concentrated purified inactivated. *Pharmacopoeia of the Russian Federation.* (In Russian). Available at https://pharmacopoeia.ru/fs-3-3-1-0025-15-vaktsina-antirabicheskaya-kulturalnaya-kontsentrirovannaya-ochishhennaya-inaktivirovannaya/ (accessed14.06.2021).
16. WHO Expert Committee on Rabies. *World Health Organ. Series Tech. Rep.* Geneva. 1986, 709, 13–22. (In Russian).
17. WHO Recommendations for inactivated rabies vaccine for human use produced in cell

substrates and embryonated eggs. Annex 2. *World Health Organ. Tech. Rep. Ser.* 2007, 941, 83–132.
18. WHO Expert Consutation on rabies. *World Health Organ. Tech. Rep. Ser.* 2018, 931, 1–88.
19. *Abramova E. G., Nikiforov A. K., Movsesyants A. A., Zhulidov I. M.* Rabies and rabies immunobiological preparations: vaccinations pasteur to the contemporary biotechnology. *J. Microbiol. Epidemiol. Immunobiol.* 2019, 5, 83–94. (In Russian).
20. *Patel P. M., Patel P. R.* Adaptation of Pitman Moore strain of rabies virus to primery chick embryo fibroblast cell cultures. United States. *Patent US 8,361,776 B2.* Jan. 29, 2008.
21. *Zhang Y. N., Chen C., Deng C. L., Zhang C.-G., Li N., Wange Z., Zhao L., Zhang B.* A novel rabies vaccine based in infectious propagating particles derived from hybrid VEEV-Rabies replicon. *EBioMedicine*. 2019, 56, 102819.
22. *Klepfer S. R., Debouck C. Uffelman J., Jacobs P., Bollen A., Jones E.V.* Characterization of rabies glycoprotein expressed in yeust. *Arch. Virol*. 1993, 128(2), 269–286. https://doi.org/10.1007/BF01309439
23. *Ashzef S., Singh P. K., Yadav D. K.* High level expression of surface glucoprotein of rabies virus tobacco leaves and its immunoprotective activity in mice. *J. Biotechnology*. 2005, 119, 1–14.
24. *Loza-Rubio E., Rojas E., Gomeslet H., Olivera M. T. J., Gómez-Lim M.A.* Development of an edible rabies vaccine in miize using the vinukovo strain. *Dev. Biol*. 2008, 131, 477–482.
25. *Krasnopolskiy Yu. M., Borshchevskaya M. I.* Pharmaceutical biotechnology: Technology for the production of immunobiological drugs. Kharkiv: NTU "KhPI".2009, 351 p. (In Russian).
26. *Miao L., Yang V., Yan M., Li Y., Zhao J., Guo J., Zheng D.* Enhanced Immune response to Rabies viruses by the use of a liposome adjuvantin vaccines. *Virus Immunol*. 2017, 30(10), 727–733. https://doi.org/10.1089/vim.2017.0093
27. *Tam Y., Hope M.J., Weissman D., Pardi N.* Nucleside — modified RNA for inducing an adaptive immune response United States. *Patent WO 2016/176330 A1*. Non. 3, 2018.
28. *Jackson L. A., Anderson E. J., Rouphael N. G., Roberts P. C., Makhene M., Coler R. N., McCullough M.P., Chappell J.D., Denison M.R., Stevens L. J., Pruijssers A. J., McDermott A., Flach B., Doria-Rose N. A., Corbett K. S., Morabito K. M., O'Dell S., Schmidt S. D., Swanson P. A. 2nd, Padilla M., Mascola J. R., Neuzil K. M., Bennett H., Sun W., Peters E., Makowski M., Albert J., Cross K., Buchanan W., Pikaart-Tautges R., Ledgerwood J. E., Graham B. S., Beigel J. H.; mRNA-1273 Study Group.* An mRNA Vaccine against SARS-CoV-2 — Preliminary Report. *N. Engl. J. Med*. 2020, 383(20), 1920–1931. https://doi.org/10.1056/NEJMoa2022483
29. *Hassett K.J., Benenato K.E., Jacquinet E., Lee A., Woods A., Yuzhakov O., Himansu S., Deterling J., Geilich B.M., Ketova T., Mihai C., Lynn A., McFadyen I., Moore M.J., Senn J.J., Stanton M.G., Almarsson Ö., Ciaramella G., Brito L.A.* Optimization of lipid nanoparticles for intramuscular administration of mRNA vaccines. *Mol. Ther. Nucleic Acids*. 2019, 15, 1–11. https://doi.org/10.1016/j.omtn.2019.01.013
30. *Zhu S., Cuo C.* Rabies control and treanment: from prophylaxis strategies with curative potencial. *Viruses*. 2016, 8(11), 279–290. https://doi.org/10.3390/v8110279
31. *Zhu S., Li H., Wang C., Luo F., Guo C.* Reverse genetics of rabies virus. New strateges to attenuate virus virulence for vaccine development. *J. Neurovirol*. 2015, 21, 335–345. https://doi.org/10.1007/s13365-015-0350-2
32. *Garagulya G.I., Matkovska S.G., Garkavaya V.V.* Antirbic vaccines: retrospective review. *Probl. Zooengineering Vet. Med.* 2015, 30(22), 149–153. (In Russian).
33. *Takayama-Ito M., Inoue K., Shoji Y., Inoue S., Iijima T., Sakai T., Kurane I., Morimoto K.* A highly attenuated rabies virus HEP-Flury strain reverts to virulent by single amino acid substitution to arginine at position 333 in glycoprotein. *Virus Res*. 2006, 119(2), 208–215. https://doi.org/10.1016/j.virusres.2006.01.014
34. *Dietzschold B., Wang H.H., Rupprecht C.E., Celis E., Tollis M., Ertl H., Heber-Katz E., Koprowski H.* Induction of protective immunity against rabies by immunization with a rabies virus ribonucleoprotein. *PNAS*. 1987, 84(24), 9165–9169.
35. *Sedova E.S., Shmarov M.M.* New recombinant rabies vaccines. *BIOpreparations. Prevention, Diagnosis, Treatment*. 2016, 16(4), 219–228. (In Russian).
36. *Shishkov A.V., Lozovoy D.A., Borisov A.V., Mikhalishin D.V.* Testing of Ferarabivac anti-rabies live vaccine for wild carnivores for its immunogenicity and protectivity. *Veterinary Sci. Today*. 2020, 1(32), 31–37. (In Russian). https://doi.org/10.29326/2304-196X-2020-1-32-31-37
37. *Ignatyev G. M., Oksanich A. S., Antonova L. P., Samartseva T. G., Mosolova S. V., Mefed K. M., Gmyl L. V., Netesova N. A.* Molecular Genetic Testing of Stability and Identification of Vnukovo-32 Strain Used for Production of the Cultural Concentrated Purified Inactivated Dry Rabies Vaccine. *BIOpreparations. Prevention, Diagnosis, Treatment*. 2020, 20(2), 107–115. (In Russian). https://doi.org/10.30895/2221-996X-2020-20-2-107-115

БІОТЕХНОЛОГІЧНІ ДОСЛІДЖЕННЯ ПРИ СТВОРЕННІ ТА У ВИРОБНИЦТВІ АНТИРАБІЧНИХ ВАКЦИН

Ю. М. Краснопольський
Д. М. Пилипенко

Національний технічний університет «Харківський політехнічний інститут», Україна

E-mail: yuriykrasnopolsky@gmail.com

Сказ — неврологічне захворювання вірусного походження, що призводить до летальних наслідків. Вірус сказу є РНК-вірусом, який, проникаючи у центральну нервову систему, спричинює дисфункцію нейронів. Своєчасна вакцинація дає змогу запобігти розвиткові захворювання.

Мета. Статтю присвячено імунобіотехнологічним дослідженням, спрямованим на створення антирабічних вакцин.

Результати. Розглянуто історію створення таких вакцин – від перших інактивованих, отриманих з нервової тканини, до вирощування вірусу на культурах клітин тварин. Наведено дані про наявні на ринку антирабічні вакцини: їхній склад, використовувані штами вірусу сказу, культури клітин, способи інактивації та очищення вірусу. Описано технологію отримання антирабічної вакцини на основі штаму вірусу Pitman Moore і культури клітин курячих фібробластів. Розглянуто переваги різних видів вакцин: живих атенуйованих, пептидних, ліпосомальних, РНК-вакцин, вакцин, отриманих на основі вірусних векторів, трансгенних рослин і методів зворотної генетики.

Висновки. Розвиток біотехнології, імунології та вірусології дає змогу постійно вдосконалювати вакцинні препарати, зокрема й проти сказу, підвищуючи їхню ефективність і безпеку.

Ключові слова: імунобіотехнологія; вірусні вакцини; антирабічна вакцина; РНК-вірус; вірус сказу.

БИОТЕХНОЛОГИЧЕСКИЕ ИССЛЕДОВАНИЯ ПРИ СОЗДАНИИ И В ПРОИЗВОДСТВЕ АНТИРАБИЧЕСКИХ ВАКЦИН

Ю. М. Краснопольский
Д. М. Пилипенко

Национальный технический университет «Харьковский политехнический институт», Украина

E-mail: yuriykrasnopolsky@gmail.com

Бешенство — неврологическое заболевание вирусной природы, приводящее к летальному исходу. Вирус бешенства представляет собой РНК-вирус, который, проникая в центральную нервную систему, приводит к дисфункции нейронов. Своевременная вакцинация позволяет предотвратить развитие заболевания.

Цель. Статья посвящена иммунобиотехнологическим исследованиям, направленным на создание антирабических вакцин.

Результаты. Рассмотрена история создания антирабических вакцин – от первых инактивированных, полученных из нервной ткани, до выращивания вируса на культурах клеток животных. Приведены данные об имеющихся на рынке антирабических вакцинах: их составе, используемых штаммах вируса бешенства, культурах клеток, способах инактивации и очистки. Описана технология получения антирабической вакцины на основе штамма вируса Pitman Moore и культуры клеток куриных фибробластов. Рассмотрены преимущества разных видов вакцин: живых аттенуированных, пептидных, липосомальных, РНК-вакцин, вакцин, полученных на основе вирусных векторов, трансгенных растений и методов обратной генетики.

Выводы. Развитие биотехнологии, иммунологии и вирусологии позволяет постоянно совершенствовать вакцинные препараты, в том числе и против бешенства, повышая их эффективность и безопасность.

Ключевые слова: иммунобиотехнология; вирусные вакцины; антирабическая вакцина; РНК-вирус; вирус бешенства.

UDC 519.8.812.007 https://doi.org/10.15407.biotech14.04.038

MATHEMATICAL MODEL FOR THE INVESTIGATION OF HYPOXIC STATES IN THE HEART MUSCLE AT VIRAL DAMAGE

N. I. ARALOVA[1], *O. M. KLYUCHKO*[2], *V. I. MASHKIN*[1], *I. V. MASHKINA*[3], *PAWEŁ RADZIEJOWSKI*[4], *MARIA RADZIEJOWSKA*[4]

[1]V. M. Glushkov Institute of Cybernetics of National Academy of Sciences of Ukraine, Kyiv
[2]National Aviation University, Educational & Research Institute of Air Navigation, Kyiv, Ukraine
[3]Borys Grinchenko Kyiv University, Ukraine
[4]Czestochowa University of Technology, Poland

E-mail: aralova@ukr.net

Received 15.06.2021
Revised 29.07.2021
Accepted 31.08.2021

The main complications of organism damaged by SARS-CoV-2 virus are various cardiovascular system lesions. As a result, the secondary tissue hypoxia is developed and it is relevant to search the means for hypoxic state alleviation. Mathematical modeling of this process, followed by the imitation of hypoxic states development, and subsequent correction of hypoxia at this model may be one of the directions for investigations.

Aim. The purpose of this study was to construct mathematical models of functional respiratory and blood circulatory systems to simulate the partial occlusion of blood vessels during viral infection lesions and pharmacological correction of resulting hypoxic state.

Methods. Methods of mathematical modeling and dynamic programming were used. Transport and mass exchange of respiratory gases in organism, partial occlusion of blood vessels and influence of antihypoxant were described by the systems of ordinary nonlinear differential equations.

Results. Mathematical model of functional respiratory system was developed to simulate pharmacological correction of hypoxic states caused by the complications in courses of viral infection lesions. The model was based on the theory of functional systems by P. K. Anokhin and the assumption about the main function of respiratory system. The interactions and interrelations of individual functional systems in organism were assumed. Constituent parts of our model were the models of transport and mass exchange of respiratory gases in organism, self-organization of respiratory and blood circulatory systems, partial occlusion of blood vessels and the transport of pharmacological substance.

Conclusions. The series of computational experiments for averaged person organism demonstrated the possibility of tissue hypoxia compensation using pharmacological substance with vasodilating effect, and in the case of individual data array, it may be useful for the development of strategy and tactics for individual patient medical treatment.

Key words: functional respiratory system; transport and mass exchange of respiratory gases; hypoxic state; partial occlusion of blood vessels.

Review of some publications with cardiovascular complications of COVID-19 and necessity of mathematical modeling use. The series of cases of strange pneumonia were registered in China on December 2019. New strain of coronavirus SARS-CoV-2, which was the causative agent of acute respiratory disease — coronavirus disease 2019 (COVID-19) have been identified in course of the subsequent studies. The epidemic turned into pandemic during brief period of time. Currently, there are quite a lot of publications with the attempts to trace and systematize current information about coronavirus

infection SARS-CoV-2 since the beginning of the epidemic. Out of the domestic authors, we should like to mention the review of S. V. Komisarenko [1] first of all; it includes up-to-date data on etiology, epidemiology, pathogenesis, clinical manifestations, and principles of diagnosis and treatment of new type of coronavirus infection, including the ideas about COVID-19 influence on cardiovascular system.

The reports about various cardiovascular complications of COVID-19 appeared in scientific literature quite quickly [2, 3]. Some types of cardiovascular system damages have been described already in literature [4]: acute myocardial damage, heart rhythm disturbances, myocarditis, the onset and/or aggravation of heart failure, pulmonary embolism [5–8]. High mortality rates: 10.5% among the patients with cardiovascular diseases (CVD), and 6.0% — with arterial hypertension [6, 7] were registered among the patients with COVID-19 and concomitant cardiovascular diseases in the studied reviews. In general, the potential mechanisms of SARS-CoV-2 influences on cardiovascular system were summarized according to [2–8], and demonstrated on Fig. 1.

The mechanisms causing the damage of cardiovascular system under the influence of SARS-CoV-2 have not been fully established. But in [9] the factor of the patients' age was mentioned as the first one in the list, as well as aggravation of the courses of many chronic diseases (including cardiovascular diseases) with SARS-CoV-2 background.

Since the information on the mechanisms of COVID-19 action was limited still, the analysis of the data from previous studies about the outbreaks of viral pneumonia and acute respiratory syndrome in the Middle East, as well as seasonal influenza, will help to understand better the mechanisms of coronavirus action on cardiovascular system, as it was emphasized in [10]. Understanding of SARS-CoV-2 cardiovascular effects is seen as quite important for the development of ways to provide timely comprehensive medical care during such lesions. Coronavirus influence on humans, and potential mechanisms of this infection effects on cardiovascular system based on the analysis of the large number of publications and clinical studies were described in [10] (Fig. 1).

Direct damaging effect of SARS-CoV-2 on cardiomyocytes was proved in [11]. In addition, the severe courses of COVID-19 (pneumonia, ARDS — acute respiratory distress syndrome) were accompanied by significant disorders in gases exchange, which caused hypoxemia. Oxygen delivery to tissues decreased during hypoxemia. Thus, the energy supply of

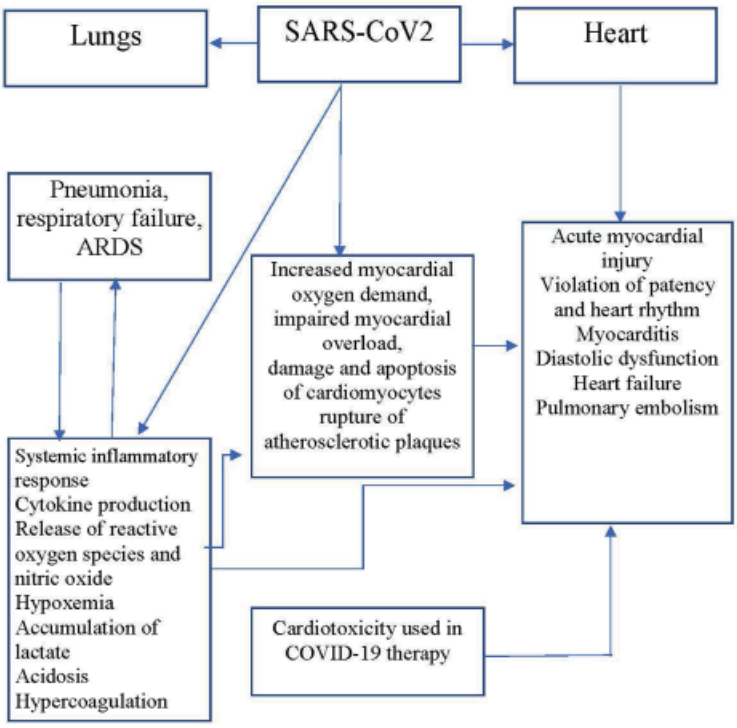

Fig. 1. **Potential mechanisms of SARS-CoV-2 effects on cardiovascular system [2–8]**

cellular metabolism decreased and anaerobic fermentation increased causing intracellular acidosis and reactive oxygen species release, which, consequently, destroyed phospholipid layer of cell membranes with the damage and apoptosis of cardiomyocytes [4].

Lactate accumulation and hypoxia caused by respiratory failure leaded to the formation of diastolic dysfunction, insufficient myocardial perfusion, accompanied by hypercoagulation, which can cause the development of acute myocardial infarction [12].

In general, the scheme of cardiovascular system involvement into described phenomena basing on [5, 9, 12–20] was represented on Fig. 2 [10].

Coronavirus infection influence on cardiovascular system was described in [21], in order to clear up and develop the algorithm for correct medical care provision for the people with cardiovascular diseases. This study was based on already known data on epidemiological characteristics of SARS and MERS [6, 7, 22–24], and studies of cardiovascular system damages in cases of pre-existing diseases and studied viral pathology.

The potential impact of COVID-19 on cardiovascular system was observed in [25]. The statistics of complications during COVID-19 from [19, 26, 27] were suggested; in particular, it was noted that in study with 75 patients hospitalized with COVID-19, the acute myocardial infarction caused 2 of 5 deaths. Also, an analysis of [22, 23, 28–30] had demonstrated the presence of large percentage of cardiovascular pathologies in patients with COVID-19; but these patients had not such pathologies before. It was concluded that until specific medical preparations against SARS-CoV-2 become available, the treatment of COVID-19 will be limited mainly by supportive therapy and treatment of complications [25].

An analysis of literature sources from Pub Med database was carried out in [31] using the keywords COVID-19 and SARS-CoV-2. The aim of the work was to collect and systematize contemporary information accumulated recently on pathophysiological mechanisms of SARS-CoV-2 effects on cardiovascular system, and the main acute cardiovascular complications of COVID-19. The sources [7, 29, 30, 32–57] with the description of pathophysiological mechanisms of the influence of SARS-CoV-2 on cardiovascular system were analyzed in [31]. The author concluded that in many cases SARS-CoV-2 caused various cardiovascular complications through the acute inflammatory damage of myocytes, provoking ventricular dysfunction, coagulopathy. Hypoxemia lead to insufficient

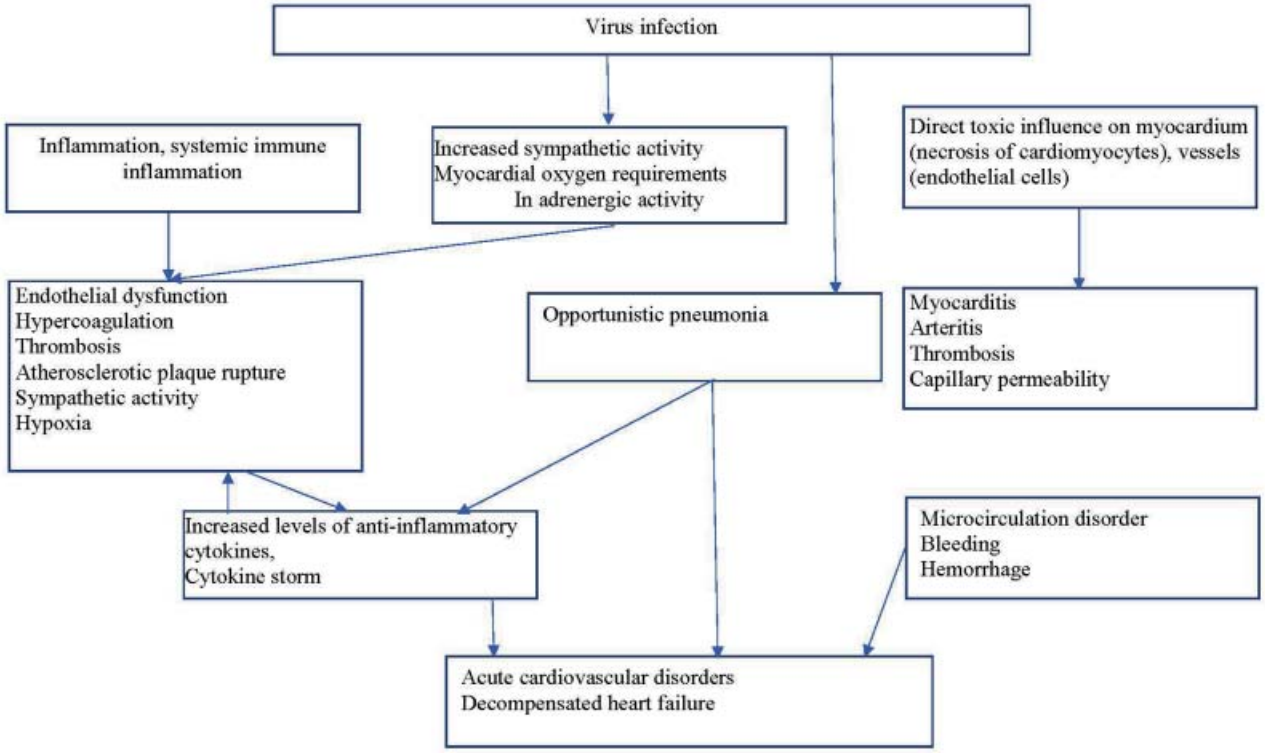

Fig. 2. **Influence of coronavirus infection (COVID -19) on cardiovascular system [10]**

oxygen supply to the myocardium [53], with the decrease of cardiac output and circulating blood volume; the sympathetic nervous system was activated to maintain circulatory homeostasis and perfusion of vitally important organs; all this leaded to even greater imbalance between the oxygen demand of the heart and oxygen delivery, as a result of which the heart muscle was damaged [54]. Other systemic factors lead to myocardial damage were acid-base imbalance, respiratory and metabolic acidosis, and electrolyte imbalance [55].

The publications from Pub Med, Google Scholar E-library databases for 2020 devoted to SARS-CoV-2 influences on cardiovascular system were analyzed in [58]. According to some authors [6, 7, 19, 30, 59–72], the spreading of concomitant cardiovascular diseases in patients with identified COVID-19 and the mechanisms of COVID-19 influence on cardiovascular system were analyzed [7, 30, 64, 73–75].

Summarizing the above, one has to note that all this evidenced not only about the need of symptomatic treatment, which was quite obvious, but also that it was desirable to have at least some ideas or approaches of possibility of patient's state alleviation. Therefore, for such cases it seems appropriate to apply mathematical modeling, which allows simulating such disturbances in organism. So, the aim of this work was the development of mathematical model of partial vascular occlusion and simulation of antihypoxant influence.

Mathematical model. The mathematical model of controlled part of respiratory system [76–78] was represented by the system of ordinary differential equations, which described the dynamics of oxygen tension at all stages of its path in the organism; and in brief form it was [79–80]:

$$\frac{dp_iO_2}{d\tau} = \phi(p_iO_2, p_iCO_2, \eta_i, \dot{V}, Q, Q_{t_i}, G_{t_i}O_2, q_{t_i}O_2), \quad (1)$$

$$\frac{dp_iCO_2}{d\tau} = \psi(p_iO_2, p_iCO_2, \eta_i, \dot{V}, Q, Q_{t_i}, G_{t_i}CO_2, q_{t_i}CO_2), \quad (2)$$

where the functions φ and ψ were described in details in [76–78]; V – ventilation; η — degree of hemoglobin saturation with oxygen; Q — volumetric rate of systemic and Q_{t_i} — local blood flows; $q_{t_i}O_2$ — rate of oxygen consumption by the i-th tissue reservoir; $q_{t_i}O_2$— rate of carbon dioxide release in i-th tissue reservoir.

The flow rates $G_{t_i}O_2$ of oxygen from the blood to the tissue and carbon dioxide from the tissue to the blood were determined by the ratio

$$G_{t_i} = D_{t_i}S_{t_i}(p_{ct_i} - p_{t_i}), \quad (3)$$

where D_{t_i} are coefficients of gases permeability through the air-blood barrier, S_{t_i} is the surface area of gas exchange.

In case of partial occlusion of the artery, which is divided into arterial vessels of right and left sides, the equations of mathematical models of mass transfer and mass exchange of respiratory gases in the blood of tissue capillaries were presented in [78, 81]:

$$\frac{dp_{ct_i}O_2}{d\tau} = \frac{1}{V_{ct_i}(\alpha_1 + \gamma \cdot Hb\frac{\partial \eta_{ct_i}}{\partial p_{ct_i}O_2})}(\alpha_1 Q_{t_i}(p_aO_2 - p_{ct_i}O_2) +$$
$$+ \gamma \cdot Hb \cdot Q_{t_i}(\eta_a - \eta_{ct_i}) - G_{t_i}O_2), \quad (4)$$

$$\frac{dp_{t_i}O_2}{d\tau} = \frac{1}{V_{t_i}(\alpha_1 + \gamma_{Mb} \cdot Mb\frac{\partial \eta_{t_i}}{\partial p_{t_i}O_2})}(G_{t_i}O_2 - q_{t_i}O_2), \quad (5)$$

Description of changes in oxygen tensions in heart tissues in the model of respiratory gas transport in organism, in case of partial artery occlusion have the form [78, 81]:

$$\frac{dp_{ct_k}O_2}{d\tau} = \frac{1}{(V_{ct_k} - \int_{\tau_0}^{T}(Q_{t_k} - \tilde{Q}_{t_k})d\tau \cdot (\alpha + \gamma \cdot Hb\frac{\partial \eta_{ct_k}}{\partial p_{ct_k}O_2})} \times$$
$$\times(\alpha_1 \cdot \tilde{Q}_{t_k} \cdot p_{t_k}O_2 + \gamma \cdot Hb \cdot \tilde{Q}_{t_k} \cdot \eta_{ct_k} -$$
$$-G_{t_k}O_2 - \alpha_1 \cdot Q_{t_k} \cdot p_{ct_k}O_2 + \gamma_{Hb} \cdot Hb \cdot Q_{t_k} \cdot \eta_{ct_k}), \quad (6)$$

$$\frac{dp_{t_k}O_2}{d\tau} = \frac{1}{V_{t_k}(\alpha_1 + \gamma_{Mb} \cdot Mb_k\frac{\partial \eta_{t_k}}{\partial p_{t_k}O_2})}(G_{t_k}O_2 - q_{t_k}O_2), \quad (7)$$

where the index $k = r, l$ corresponded to the left or right side of the heart; α_1, α_2 — solubility of gases in blood plasma; Hb, BH — the concentration of hemoglobin and buffer bases in the blood; γ, γ_{BH} — Hüfner constants; V_v — the volume of venous fluid; z_j — the degree of blood saturation with oxygen or carbon dioxide; Q_{t_k} — volumetric rate of coronary blood flow determined by the model of functional respiratory system (FRS); Q_{t_k} its actual rate in case of pathological changes in the heart. It is clear that $\tilde{Q}_{t_k} < Q_{t_k}$, i. e. the

actual blood flow rate with partial vascular permeability is lower than for the organism of healthy person.

If we assume that coronary vessels of the left and right parts of the heart are not damaged, then, with partial occlusion of the artery, the oxygen stress gradients in absolute value will be greater than corresponding gradients in case of vessel damage and, depending on occlusion degree, hypoxia in the heart muscle will be less pronounced.

If the vessels of the left or right side of the heart were damaged, then hypoxia occurred, being caused by partial occlusion of one part of the heart muscle, in the other, the volumetric blood flow rate would be greater than necessary. This would lead to the increase in oxygen tension in this part, i.e. an asymmetry in oxygen tensions distribution in the heart muscle appeared. When the degree of damage of arterial vessels that supply the blood to left and right sides of the heart was different, hypoxia was developed in the tissues of both parts of the heart, which was caused by different degrees of vascular occlusion, and then the distribution of oxygen tension will also be asymmetric.

Using this model, it was possible to analyze the situations when complete occlusion of the capillary bed occurred in elementary part of the heart muscle. In the initial period, there will be a sharp depletion of oxygen reserves from the blood, a mismatch in its supply with the needs of the tissues that surround the capillary, then the oxygen tension in this tissue area will become critical and this part will not be able to take part in the pumping function of the heart. Thus, in case of coronary vessels damage, the distribution of oxygen in the heart muscle depends on the degree of capillary bed damage and its localization.

In order to alleviate the hypoxic state, a number of medical substance are used for today; and for the optimization of the choice of medical substance, we proposed to use mathematical models that will simulate the effect of this substance, on organism of individual person.

The equations for the changes in tensions of oxygen and pharmacological substance in the blood of arterial flows were as follows [78, 82]:

$$\frac{dp_aO_2}{d\tau} = \frac{1}{V_a(\alpha_1+\gamma\cdot Hb\frac{\partial\eta_a}{\partial p_aO_2})}[\alpha_1(Q-Q_{sh})p_{Lc}O_2 + \\ +\gamma\cdot Hb\cdot(Q-Q_{sh})(\eta_{Lc}-\eta_a)+ \\ +\alpha_1 Q_{sh}p_{\bar{v}}O_2]+\frac{1}{V_a(\alpha_1+\gamma\cdot Hb\frac{\partial\eta_a}{\partial p_aO_2})}+ \\ +[\gamma\cdot BH\cdot Q_{sh}\eta_{\bar{v}}-\alpha_1 Qp_aO_2-\gamma\cdot BH\cdot q\eta_a], \quad (8)$$

$$\frac{dc_{f_a}}{d\tau} = \frac{1}{V_a}((Q-Q_{sh})c_{f_{lc}}+Q_{sh}c_{f_{\bar{v}}}-Qc_{f_a}. \quad (9)$$

It should be taken into account that the levels of gases tensions and substance concentrations is formed as a result of instant mixing of flows coming from the blood of pulmonary capillaries and the blood mixed with gases and substance.

Arterial blood vessels are branched into microcirculatory networks of organs and tissues. The classical mathematical model of mass transfer and mass exchange of respiratory gases presented above, describes the dynamics of respiratory gases tensions in *m* tissue reservoirs, among which, as a rule, tissues of the brain, kidneys, liver, gastrointestinal tract, cardiac and skeletal muscles, bone and adipose tissues are distinguished.

Equations (6) and (7), which described the changes in respiratory gases tensions in the blood washing the tissue and in tissue fluid of the reservoir, were supplemented by following equations for the concentrations of pharmacological substance for the blood of tissue capillaries:

$$\frac{dc_{f_{ct_i}}}{d\tau} = \frac{1}{V_{ct_i}}(Q_{t_i}(c_{f_a}-c_{f_{ct_i}})-G_{f_{t_i}}), \quad (10)$$

and for tissue fluid we supplemented the equations (6)–(7) with the expression

$$\frac{dc_{f_{t_i}}}{d\tau} = \frac{G_{f_{t_i}}}{V_{t_i}}, \quad (11)$$

where

$$G_{f_{t_i}} = D_{f_{t_i}}S_{t_i}(c_{f_{ct_i}}-c_{f_{t_i}}). \quad (12)$$

During the development of mathematical model of transport and mass exchange of respiratory gases and pharmacological substance, it was assumed that the substance

did not participated in metabolic processes directly, but it was regulatory factor for hypoxia stabilizing and compensation.

Let's suppose that pharmacological substance *f* belongs to pharmacological group that promotes vasodilation of capillary walls. Its effect on smooth muscles leads to more free penetration of oxygen and carbon dioxide through the barriers separating blood and tissue fluid and, at the same time, to the decrease of the rate of oxygen utilization by smooth muscles of capillaries.

Therefore, the amount of gas flow through the membrane between blood and tissue fluid can be expressed by the ratio:

$$G_{j_{t_i}} = K(c_{f_{t_i}}) \cdot D_{j_{t_i}} \cdot S_{t_i}(p_{j_{ct_i}} - j_{t_i}), \qquad (13)$$

where $K(c_{f_{t_i}})$ — functional enhancer of diffusion process of respiratory gases into the tissue reservoir. According to [82], some experimental studies permit to suggest that $1 \le K(c_{f_{t_i}}) \le 2$ for most pharmacological substance of this type.

In the venous bed the blood from the organs and tissues was mixed and transported to the lungs for oxygenation. Therefore, the equations for oxygen transport in mixed venous blood

$$\frac{dp_{\bar{v}}O_2}{d\tau} = \frac{1}{V_{\bar{v}}(\alpha_1 + \gamma \cdot Hb \frac{\partial \eta_{\bar{v}}}{\partial p_{\bar{v}}O_2})} \times$$

$$\times [\alpha_1 (\sum_{t_i} Q_{t_i} \cdot p_{ct}O_2 - Q \cdot p_{\bar{v}}O_2) -$$

$$-\gamma \cdot Hb \cdot Q \cdot \eta_{\bar{v}}], \qquad (14)$$

have to be supplemented by the equation for concentration of pharmacological substance:

$$\frac{dc_{f_v}}{d\tau} = \frac{1}{V_{\bar{v}}} (\sum_{t_i} Q_{t_i} c_{f_{t_i}} + c_{f_a} Q_{f_{t_i}} - Q c_{f_v}). \qquad (15)$$

Differential equations and algebraic relations (1–15) describe fully the transport and mass exchange of respiratory gases and pharmacological substance in selected structure of respiratory system of respiratory cycle. The described mathematical model makes it possible to predict oxygen, carbon dioxide and nitrogen regimes of organism under the disturbing influences in forms of inhalation, oral, intramuscular and intravenous administration of pharmacological preparation.

In our model it was assumed that intravenous influence of antihypoxant was the most effective. In this case, the dynamics of substance *f* in mixed venous blood was:

$$\alpha_f V_v \frac{dc_{f_v}}{d\tau} = \sum_{t_i} \alpha_f Q_{t_i} c_{f_{t_i}} + d_f Q_{f_{t_i}} - \alpha_f Q c_{f_v}, \qquad (16)$$

where ($c_{f_{t_i}}$ — concentration of pharmacological substance in the blood of tissue capillaries of the region; t_i, ($c_{f_{t_i}}$ –concentration of substance in tissue fluid of the region t_i.

It is assumed that the removal of antihypoxant *f* from the organism is carried out through the kidneys, and the change in substance *f* concentration in the renal tissue is determined by the equation:

$$\alpha_{f_i} V_{t_i} \frac{dc_{f_{t_i}}}{d\tau} = G_{f_{t_i}} - \alpha_{t_i} Q_f c_{t_i}, \qquad (17)$$

where Q_f is the filtration rate of the liquid. It was assumed that the volumetric filtration rate was 0.035 mg/s.

Pharmacological correction of tissue hypoxia in case of vascular patency lesions. Results of numerical experiment. Series of experiments was carried out on mathematical model of hypoxic states pharmacological correction. The scheme of software package was shown on Fig. 3.

The results of computer analysis of the effect of antihypoxant influence on the organism of averaged person have been demonstrated below. Injected dose was 10 mg, preparation administration was done by pulsed intramuscular injection. The used substance had the ability to dilate blood vessels. The data on organism functional state with basal metabolism and during hypoxia caused by diseases of cardiovascular system were demonstrated in Table 2 [78].

The dynamics of partial pressures and tensions of respiratory gases in the organism after the imitation of antihypoxant injection were presented in Table 2.

The data given in Table 2 indicated that through 20 hours after the injection of pharmacological substance a new round of tissue hypoxia development had started. Oxygen tensions in tissues began to fall, and carbon dioxide tensions began to increase. Let's note that current concentration of the preparation in arterial blood reached the norm, equal to half of the average concentration of the substance earlier — through 18.5 hours after the injection.

Table 1. **Indicators of partial pressures and tensions of respiratory gases in healthy organism and with vascular occlusion**

Functional state		Tensions of respiratory gases in parts of the structure of respiratory system in mmHg									
		alveoli	arteria	brain	heart	liver	kidney	skelet. muscles	skin	other tissues	veins
Healthy organism	O_2 CO_2	125 38.5	95.2 41.5	38.1 46.54	27.7 48.73	42.4 45.6	66.7 48.6	31.8 54.1	37.0 51.8	37.0 51.3	39.9 51.02
CAD patient	O_2 CO_2	128 37.1	95.6 41.9	35.8 47.6	24.6 48.8	40.0 47.3	51.1 49.2	25.3 55.3	35.7 53.1	36.7 53.1	37.8 52.0

Note. CAD — coronary artery disease, CAD patient — patient with CAD.

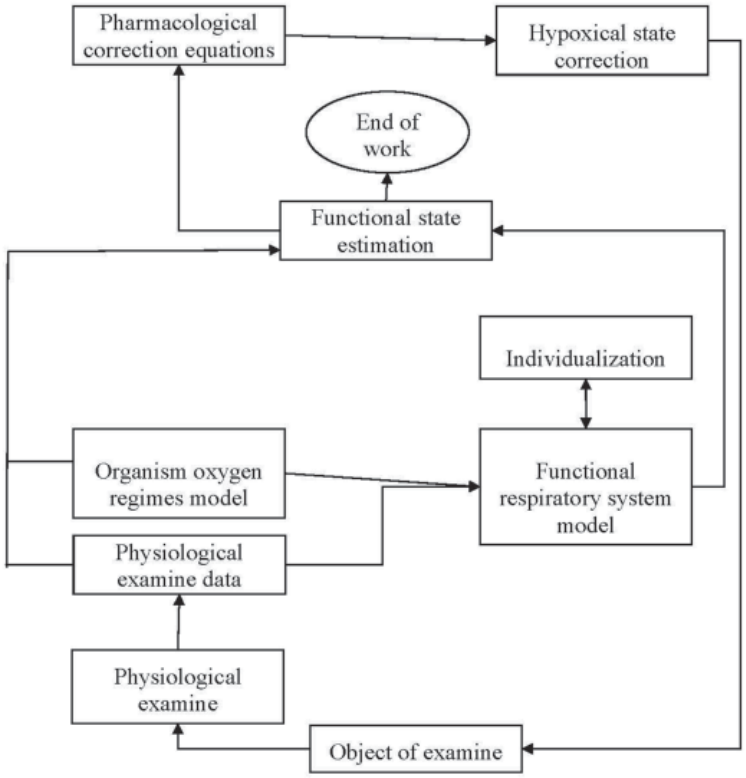

Fig. 3. **Scheme of the work of software package for simulation of pharmacological correction of hypoxic state at vascular occlusion**

In framework of our mathematical model we would like to emphasize that the results of computer analysis relate to the effect of pharmacological substance with only the characteristic we picked up for this model — the ability to dilate blood vessels, increasing the ability of respiratory gases to penetrate tissue reservoirs. As a rule, pharmacological substance s consist of several biologically active compounds. We hope that inclusion into pharmacological substance of substances that increase the oxygen capacity of the blood, in particular, increase the hemoglobin content in the blood, and will contribute to greater effectiveness of the substance for hypoxia compensation. However, the stimulation of erythropoiesis can contribute to an increase in hematocrit, higher density of red blood cells in circulating blood, and this can cause vascular thrombosis.

And in this case, for individual choice of the substance, the method of its influence and dosage, it is possible to use the algorithmic and software supply for mathematical model of respiratory gases transport in the organism in modification [79].

The iterative procedure for applying of proposed software package in this case will be as follows:

1. An instrumental examination of the patient is carried out. We get the data about

Table 2. **Indices of partial pressures and tensions of respiratory gases after antihypoxant injection**

Time after injection		Tensions of respiratory gases in parts of the structure of respiratory system in mmHg after the substance administration									
		alveoli	arte-ria	brain	heart	liver	kidney	skelet. muscles	skin	other tissues	veins
1 h	O_2 CO_2	125.6 36.2	95.0 41.2	36.5 47.3	25.1 47.8	40.8 46.9	52.0 48.7	26.5 54.8	35.8 52.8	36.5 53.0	38.0 52.3
5 h	O_2 CO_2	125.58 36.8	95.2 41.8	36.7 47.2	25.8 47.6	41.3 47.1	55.6 48.8	28.1 54.6	36.1 52.4	36.6 52.4	38.2 53.0
10 h	O_2 CO_2	125.2 37.3	95.1 41.3	37.1 46.4	25.9 47.95	41.6 45.7	60.1 48.6	29.6 54.2	36.3 51.9	36.6 51.9	38.5 51.0
15 h	O_2 CO_2	125.0 38.0	95.3 41.0	37.3 46.1	26.0 47.5	41.4 44.2	58.0 48.0	29.3 54.3	36.3 52.0	36.3 52.0	38.3 51.1
20 h	O_2 CO_2	125.1 37.8	95.2 40.9	37.1 46.8	25.6 48.1	40.65 46.2	56.3 48.2	28.75 54.5	36.0 52.2	36.1 52.2	37.9 53.0

lungs ventilation, composition of alveolar and exhaled air, frequency of respiration, blood pressure, frequency of heart construction, hemoglobin, blood acidity, and etc., which are the initial data for the model of organism oxygen regimes [78, 83, 84]

2. Basing on the data of instrumental examination, we calculate such indicators as minute volume of the respiration, minute volume of the blood, rate of oxygen consumption by the organism, the economy, intensity and efficiency of oxygen regimes of the organism, the data characterizing the hypoxic state.

3. The data of instrumental examination and the part of the data obtained in calculation of organism oxygen regimes were used as input ones for the operation of respiratory gas transport model described above. Thus, in such a way, the individualization of the model was carried out.

4. On individualized model we simulated the state of the rest of individual person. We obtained the values of the tensions of oxygen and carbon dioxide in the tissues of individual organs, which allow us to estimate the degree of tissue hypoxia.

5. Further we simulated the injection of pharmacological substance. Obtained data were analyzed and, thus, the optimal options for the use of specific preparation were selected.

We would like to note in addition that on Fig. 3 the immune response model was not subdivided separately, as it was done in [80]. This is due to the fact that we deal with already disturbed respiratory and blood circulatory systems and this is taken into account in given initial data. It was also inappropriate, from the point of view of the authors, to give any physiological interpretation of the data obtained in numerical experiment. It is clear that for the test task they can be erroneous. It is important that with the help of developed complex of information support, with the array of individual initial data, it is possible to simulate various doses of pharmacological substance and, thus, to objectify and optimize this process.

Conclusions

Thus, a complex mathematical model for simulating of cardiovascular system damage and correction of the resulting hypoxic state was suggested in present article. Our united model consists on the models of transport and mass exchange of respiratory gases, self-organization of respiratory and blood circulatory systems, partial vascular occlusion and pharmacological correction. On the developed software package, a series of computational experiments was carried out for the organism of averaged person, the imitation of antihypoxant injection — pharmacological influence with only characteristic — the ability to expand blood vessels, increasing the ability of respiratory gases to penetrate into tissue reservoirs. Naturally, since the test task was examined, it could be concluded that this approach could be used to alleviate the complicated course of the disease. For more specific conclusions the arrays with patient's individual data have to be used.

The review was prepared within the framework of the research work "To develop the mathematical models of mechanisms for interaction of body functional systems and the integration methods of their mathematical models to maintain the reliability and safety of human life in extreme conditions" (State Registration No. 0114U001052).

REFERENCES

1. *Komisarenko S. V.* World Coronavirus Crisis. *K. Publishing House LAT&K*. 2020, 120 p.
2. *Avula A., Nalleballe K., Narula N., Sapozhnikov S., Dandu V., Toom S., Glaser A., Elsayegh D.* COVID-19 presenting as stroke. Brain, Behavior, and Immunity. 2020, V. 87, P. 115–119. https://doi.org/10.1016/j.bbi.2020.04.077
3. *Leisman D. E., Deutschman C. S., Legrand M.* Facing COVID-19 in the ICU: vascular dysfunction, thrombosis, and dysregulated inflammation. *Intensive Care Med*. 2020, 46 (6), 1105–1108. https://doi.org/10.1007/s00134-020-06059-6
4. *Bazdyrev E. D.* Coronavirus disease: global problem of the 21 st century. *Comlex issues of Cardiovascular Diseases.* 2020, 9 (2), 6–16. https://doi.org/10.17802/2306-1278-2020-9-2-6-16 (In Russian).
5. *Longquan Li, Tian Huang, Yongqing Wang, Zhengping Wang, Yuan Liang, Taobi Huang, Huiyun Zhang, Weiming Sun, Yuping Wang.* COVID-19 patients' clinical characteristics, discharge rate, and fatality rate of metaanalysis, Volume 92, Issue 6. *Special Issue on New co ronavirus (2019-nCoV or SARS-CoV-2) and the outbreak of the respiratory illness (COVID-19):* Part-III, June 2020 Pages 577–583. https://doi.org/10.1002/jmv.25757
6. *Chaolin Huang, Yeming Wang, Xingwang Li, Lili Ren, Jianping Zhao, Yi Hu, Li Chang, Guohui Fan, Jiuyang Xu, Xiaoying Gu, Zhenshun Cheng, Ting Yu, Jiaan Xia, Yuan Wei, Wenjuan Wu, Xuelei Xie, Wen Yin, Hui Li, Min Liu, Yan Xiao, Hong Gao, Li Guo, Jungang Xie, Guangfa Wang, Rongmeng Jiang, Zhancheng Gao, Qi Jin, Jianwei Wang, Bin Cao.* Clinical features of patients infected with 2019 novel coronavirus in Wuhan, China Lancet. 2020, 395 (10223), 497–506. https://doi.org/10.1016/SO140-6736(20)30183-5. Lancet. 2020, 395 (10223), 496. https://doi.org/10.1016/S0140-6736(20)30252-X
7. *Dawei Wang, Bo Hu, Chang Hu, Fangfang Zhu, Xing Liu, Jing Zhang, Binbin Wang, Hui Xiang, Zhenshun Cheng, Yong Xiong, Yan Zhao, Yirong Li, Xinghuan Wang, Zhiyong Peng*. Clinical Characteristics of 138 Hospitalized Patients With 2019 Novel Coronavirus-Infected Pneumonia in Wuhan. *China. JAMA*. 2020, 323 (11), 1061–1069. https://doi.org/10.1001/jama.2020.1585
8. *Fei Zhou, Ting Yu, Ronghui D, Guohui Fan, Ying Liu, Zhibo Liu, Jie Xiang, Yeming Wang, Bin Song, Xiaoying Gu, Lulu Guan, Yuan Wei, Hui Li* Clinical course and risk factors for mortality of adult inpatients with COVID-19 in Wuhan, China: a retrospective cohort study *The Lancet*, 395(10229), 1054–1062 — March 2020 doi: 10.1016/S0140-6736(20)30566-3
9. *Driggin E., Mahesh M. V., Bikdeli B., Chuich T., Laracy J., Biondi-Zoccai G., Brown T. S., Der Nigoghossian C., Zidar D. A., Haythe J., Brodie D., Beckman J. A., Kirtane A. J., Stone G. W., Krumholz H. M., Parikh S. A.* Cardiovascular Considerations for Patients, Health Care Workers, and Health Systems During the COVID-19 Pandemic. *J. Am. Coll. Cardiol*. 2020, 75 (18), 2352–2371. https://doi.org/10.1016/j.jacc.2020.03.031
10. *Larina V. N., Golovko M. G., Larin V. G.* Possible effects of coronavurus infection (COVID-19) on the cardiovascular system. *Bulletin of RSMU*. 2020, V. 2, P. 5–12. (In Russian). https://doi.org/10.24075/brsmu.2020.020.
11. *Oudit Y., Kassiri Z., Jiang C., Liu P. P., Poutanen S. M., Penninger J. M., Butany J.* SARS-coronavirus modulation of myocardial ACE2 expression and inflammation in patients. *Eur. J. Clin. Invest.* 2009, 39 (7), 618–625. https://doi.org/10.1111/j.1365-2362.2009.02153.x
12. *Zhe Xu, Lei Shi, Yijin Wang, Jiyuan Zhang, Lei Huang, Chao Zhang, Shuhong Liu, Peng Zhao, Hongxia Liu, Li Zhu, Yanhong Tai, Changqing Bai, Tingting Gao, Jinwen Song, Peng Xia, Jinghui Dong, Jingmin Zhao, Fu-Sheng Wang.* Pathological findings of COVID-19 associated with acute respiratory distress syndrome. *Lancet Respir. Med.* 2020, 8 (4), 420–422. https://doi.org/10.1016/S2213-2600(20)30076-X
13. *Menachery V. D., Yount B. L., Debbink Jr.K., Agnihothram S., Gralinski L. E., Plante J. A., Graham R. L., Scobe T., Ge Xing-Yi, Donaldson E. F., Randell S. H., Lanzavecchia A., Marasco W. A., Shi Z-Li, Baric R. S.* A SARS-like cluster of circulating bat coronaviruses shows potential for human emergence. *Nature Med*. 2015, V. 21, P. 1508–1513. https://doi.org/10.1038/nm.3985
14. *Yushun Wan, Jian Shang, Graham R., Baric R. S., Fang Li.* Receptor Recognition by the Novel Coronavirus from Wuhan: an Analysis Based on Decade-Long Structural Studies of SARS Coronavirus. *J. Virol.* 2020, 94 (7), 1–9. https://doi.org/10.1128/jvi.00127-20
15. *Hong Peng Jia, Dwight C. Look, Lei Shi, Hickey M., Pewe L., Netland J., Farzan M., Wohlford-Lenane C., Perlman S., McCray P. B. Jr.* ACE2 Receptor Expression and Severe Acute Respiratory Syndrome Coronavirus Infection Depend on Differentiation of Human Airway Epithelia. *J. Virol.* 2005, 79 (23), 14614–14621. https://doi.org/10.1128/jvi.79.23.14614-14621.2005
16. *Sodhi C. P., Wohlford-Lenane C., Yamaguchi Y., Prindle T., Fulton W. B., Wang S.,*

McCray P. B. Jr., Chappell M., Hackam D. J., Jia H. Attenuation of pulmonary ACE2 activity impairs inactivation of des-Arg^9 bradykinin/BKB1R axis and facilitates LPS-induced neutrophil infiltration. *Am. J. Physiol. Lung Cell Mol. Physiol.* 2018, 314 (1), 17–31. https://doi.org/10.1152/ajplung.00498.2016

17. *Nanshan Chen, Min Zhou, Xuan Dong, Jieming Qu, Fengyun Gong, Yang Han, Yang Qiu, Jingli Wang, Ying Liu, Yuan Wei, Jia An Xia, Ting Yu, Xinxin Zhang, Li Zhang.* Epidemiological and clinical characteristics of 99 cases of 2019 novel coronavirus pneumonia in Wuhan, China: a descriptive study. *Lancet*. 2020, 395 (10223), 507–513. https://doi.org/10.1016/S0140-6736(20)30211-7
18. *Short K. R., Kroeze E. J. B. V., Fouchier R. A. M., Kuiken T.* Pathogenesis of influenza-induced acute respiratory distress syndrome. *Lancet Infect. Dis.* 2014, 14 (1), 57–69. https://doi.org/10.1016/S01473-3009(13)70286-X
19. *Wei-jie Guan, Zheng-yi Ni, Yu Hu, Wen-hua Liang, Chun-quan Ou, Jian-xing He, Lei Liu, Hong Shan, Chun-liang Lei, David S. C. Hui, Bin Du, Lan-juan Li, Guang Zeng, Kwok-Yung Yuen, Ru-chong Chen, Chun-li Tang, Tao Wang, Ping-yan Chen, Jie Xiang, Shi-yue Li, Jin-lin Wang, Zi-jing Liang, Yi-xiang Peng, Li Wei, Yong Liu, Ya-hua Hu, Peng Peng, Jian-ming Wang, Ji-yang Liu, Zhong Chen, Gang Li, Zhi-jian Zheng, Shao-qin Qiu, Jie Luo, Chang-jiang Ye, Shao-yong Zhu, Nan-shan Zhong.* Clinical Characteristics of Coronavirus Disease 2019 in China. *N Engl. J. Med.* 2020, V. 382, P. 1708–1720. https://doi.org/10.1056/NEJMoa2002032
20. *Xiaobo Yang, Yuan Yu, Jiqian Xu, Huaqing Shu, Jia'an Xia, Hong Liu, Yongran Wu, Lu Zhang, Zhui Yu, Minghao Fang, Ting Yu, Yaxin Wang, Shangwen Pan, Xiaojing Zou, Shiying Yuan, You Shang.* Clinical course and outcomes of critically ill patients with SARS-CoV-2 pneumonia in Wuhan, China: a single-centered, retrospective, observational study. *Lancet Respir. Med.* 2020. 2600 (20), 1–7. https://doi.org/10.1016/S2213-2600(20)30079-5
21. *Kopytsy M., Rodionova I., Tytarenko N., Hilova Y., Kutya I., Kobets A.* Features of the cardiovascular system lesion in patients with COVID-19. *ScienceRise: Med. Sci.* 2020, 3 (36), 4–12. https://doi.org/10.15587/2519-4798.2020.204011 (In Russian).
22. *Yu C.-M., Wong R. S.-M., Wu E. B., Kong S.-L., Wong J., Yip G. W.-K., Soo Y. O. Y., Chiu M. L. S., Chan Y.-S., Hui D., Lee N., Wu A., Leung C.-B., Sung J. J.-Y.* Cardiovascular complications of severe acute respiratory syndrome. *Postgrad. Med. J.* 2006, V. 82, P. 140–144. http://dx.doi.org/10.1136/pgmj.2005.037515
23. *Li S. S., Cheng C., Fu C., Chan Y., Lee M., Chan J. W., Yiu S.* Left Ventricular Performance in Patients With Severe Acute Respiratory Syndrome. *Circulation.* 2003, V. 108, P. 1798–1803. https://doi.org/10.1161/01.CIR.0000094737.21775.32
24. *Alhogbani T.* Acute myocarditis associated with novel Middle East respiratory syndrome coronavirus. *Ann. Saudi Med.* 2016, 36 (1), 78–80. https://doi.org/10.5144/0256-4947.2016.78
25. *Mikhaylovskaya T. V., Yakovleva N. D., Safronov M. A., Kharlamova Ya. L.* Porenyial. Effects of COVID-19 on the Cardiovascular System. *Physical and Reabilitation Medicine, Medical Reabilitation*. 2020, No 2, P. 133–139. https://doi.org/1036425/rehab34080 (In Russian).
26. *Madjid M., Safavi-Naein Payam., Solomon S. D., Vardeny O.* Potential Effects of Coronaviruses on the Cardiovascular System. A Review. *JAMA Cardiol.* 2020, 5 (7), 831–840. https://doi.org/10.1001/jamacardio.2020.1286
27. *Peiris J. S. M., Chu C. M., Cheng V. C. C., Chan K. S., Hung I. F. N., Poon L. L. M., Law K. I., Tang B. S. F., Hon T. Y. W., Chan C. S., Chan K. H., Ng J. S. C., Zheng B. J., Ng W. L., Lai R. W. M., Guan Y., Yuen K. Y.* Clinical progression and viral load in a community outbreak of coronavirus-associated SARS pneumonia: a prospective study. *Lancet*. 2003, 361 (9371), 1767–1772. https://doi.org/10.1016/S0140-6736(03)13412
28. *Pek Yoon Chong, Paul Chui, Ai E. Ling, Teri J. Franks, Dessmon Y. H. Tai, Yee Sin Leo, Gregory J. L. Kaw, Gervais Wansaicheong, Kwai Peng Chan, Lynette Lin Ean Oon, Eng Swee Teo, Kong Bing Tan, Noriko Nakajima, Tetsutaro Sata, William D. Travis.* Analysis of deaths during the severe acute respiratory syndrome (SARS) epidemic in Singapore: challenges in determining a SARS diagnosis. *Arch. Pathol. Lab. Med*. 2004, 128 (2), 195–204. https://doi.org/10.1043/1543-2165(2004)128<195:AODDTS>2.0.CO;2
29. *Zhe Xu, Lei Shi, Yijin Wang, Jiyuan Zhang, Lei Huang, Chao Zhang, Shuhong Liu, Peng Zhao, Hongxia Liu, Li Zhu, Yanhong Tai, Changqing Bai, Tingting Gao, Jinwen Song, Peng Xia, Jinghui Dong, Jingmin Zhao, Fu-Sheng Wang.* Pathological findings of COVID-19 associated with acute respiratory distress syndrome. *Lancet Respir. Med.* 2020, 8 (4), 420–422. https://doi.org/10.1016/S2213-2600(20)30076-X
30. *Shaobo Shi, Mu Qin, Bo Shen, Yuli Cai, Tao Liu, Fan Yang, Wei Gong, Xu Liu, Jinjun*

Liang, Qinyan Zhao, He Huang, Bo Yang, Congxin Huang. Association of Cardiac Injury With Mortality in Hospitalized Patients With COVID-19 in Wuhan, China. *JAMA Cardiol.* 2020, 5 (7), 802–810. https://doi.org/10.1001/jamacardio.2020.0950

31. *Kanorskii S. G.* COVID-19 and the heart: direct and indirect impact. *Kubanskiy Nauchniy Meditsinskiy Vestnik*. 2021, 28 (1), 16–31. (In Russian). https://doi.org/10.25207/1608-2228-2021-28-1-16-31.
32. *Hoffmann M., Kleine-Weber H., Schroeder S., Krüger N., Herrler T., Erichsen S., Schiergens T. S., Herrler G., Wu N-H., Nitsche A., Müller M. A., Drosten C., Pöhlmann S.* SARS-CoV-2 Cell Entry Depends on ACE2 and TMPRSS2 and Is Blocked by a Clinically Proven Protease Inhibitor. *Cell.* 2020, 181 (2), 271–280. https://doi.org/10.1016/j.cell.2020.02.052
33. *Li M. Y., Li L., Zhang Y., Wang X. S.* Expression of the SARS-CoV-2 cell receptor gene *ACE2* in a wide variety of human tissues. *Infect. Dis. Poverty*. 2020, V. 9, P. 45. https://doi.org/10.1186/s40249-020-00662-x
34. *Forrester S. J., Booz G. W., Sigmun*d *C. D., Coffman T. M., Kawai T., Rizzo V., Scalia R., Eguchi S*. Angiotensin II Signal Transduction: An Update on Mechanisms of Physiology and Pathophysiology. *Physiol. Rev.* 2018, 98 (3), 1627–1738. https://doi.org/10.1152/physrev.00038.2017
35. *Verdecchia P., Cavallini C., Spanevello A., Angeli F.* The pivotal link between ACE2 deficiency and SARS-CoV-2 infection. *Eur. J. Intern. Med*. 2020, V. 76, P. 14–20. https://doi.org/10.1016/j.ejim.2020.04.037
36. *South A. M., Diz D. I., Chappell M. C.* COVID-19, ACE2, and the cardiovascular consequences. *Heart and Circulatory Physiology*. https://doi.org/10.1152/ajpheart.00217.2020
37. *Jiu Chang Zhong, Ratnadeep Basu, Danny Guo, Fung L. Chow, Simon Byrns, Manfred Schuster, Hans Loibner, Xiu-hua Wang, Josef M. Penninger, Zamaneh Kassiri, Gavin Y. Oudit*. Angiotensin-Converting Enzyme 2 Suppresses Pathological Hypertrophy, Myocardial Fibrosis, and Cardiac Dysfunction 2010. *Circulation*. 2010, 122 (7), 717–728 https://doi.org/10.1161/CIRCULATIONAHA.110.955369
38. *Tanwar V., Adelstein J. M., Wold L. E.* Double trouble: combined cardiovascular effects of particulate matter exposure and coronavirus disease 2019. *Cardiovasc. Res.* 2021, 117 (1), 85–95. https://doi.org/10.1093/cvr/cvaa293
39. *Ye Q., Wang B., Mao J.* The pathogenesis and treatment of the "Cytokine Storm" in COVID-19. *J. Infect.* 2020, 80 (6), 607–613. https://doi.org/10.1016/j.jinf.2020.03.037
40. *Guang Chen, Di Wu, Wei Guo, Yong Cao, Da Huang, Hongwu Wang, Tao Wang, Xiaoyun Zhang, Huilong Chen, Haijing Yu, Xiaoping Zhang, Minxia Zhang, Shiji Wu, Jianxin Song, Tao Chen, Meifang Han, Shusheng Li, Xiaoping Luo, Jianping Zhao, Qin Ning.* Clinical and immunological features of severe and moderate coronavirus disease 2019. *J. Clin. Invest.* 2020, 130 (5), 2620–2629. https://doi.org/10.1172/JCI137244
41. *Mehta P., McAuley D. F., Brown M., Sanchez E., Tattersall R. S., Manson J. J. HLH Across Speciality Collaboration, UK*. COVID-19: consider cytokine storm syndromes and immunosuppression. *Lancet*. 2020, 395 (10229), 1033–1034. https://doi.org/10.1016/S0140-6736(20)30628-0
42. *Siddiqi H. K., Mehra M. R.* COVID-19 illness in native and immunosuppressed states: A clinical-therapeutic staging proposal. *J. Heart Lung Transplant*. 2020, 39 (5), 405–407. https://doi.org/10.1016/j.healun.2020.03.012
43. *Inciardi R. M., Lupi L., Zaccone G., Italia L., Raffo M., Tomasoni D., Cani D. S., Cerini M., Farina D., Gavazzi E., Maroldi R., Adamo M., Ammirati E., Sinagra G., Lombardi C. M., Metra M*. Cardiac Involvement in a Patient With Coronavirus Disease 2019 (COVID-19). *JAMA Cardiol.* 2020, 5 (7), 819–824. https://doi.org/10.1001/jamacardio.2020.1096
44. *Zeng J. H., Liu Y. X., Yuan J., Wang F. X., Wu W. B., Li J. X., Wang L. F., Gao H., Wang Y., Dong C. F., Li Y. J., Xie X. J., Feng C., Liu L.* First case of COVID-19 complicated with fulminant myocarditis: a case report and insights. *Infection*. 2020, 48 (5), 773–777. https://doi.org/10.1007/s15010-020-01424-5
45. *Liu K., Fang Y. Y., Deng Y., Liu W., Wang M. F., Ma J. P., Xiao W., Wang Y. N., Zhong M. H., Li C. H., Li G. C., Liu H. G.* Clinical characteristics of novel coronavirus cases in tertiary hospitals in Hubei Province. *Chin. Med. J. (Engl.)*. 2020, 133 (9), 1025–1031. https://doi.org/10.1097/CM9.0000000000000744
46. *Tavazzi G., Pellegrini C., Maurelli M., Belliato M., Sciutti F., Bottazz A., Sepe P. A., Resasco T., Camporotondo R., Bruno R., Baldanti F., Paolucci S., Pelenghi S., Iotti G. A., Mojoli F., Arbustini E*. Myocardial localization of coronavirus in COVID-19 cardiogenic shock. *Eur. J. Heart Failure*. 2020, 5 (22), 911–915. https://doi.org/10.1002/ejhf.1828
47. *Fox S. E., Li G., Akmatbekov A., Harbert J. L., Lameira F. S., Brown J. Q., Heide R. S. V.* Unexpected Features of Cardiac Pathology in COVID-19 Infection. *Circulation*. 2020, V. 142, P. 1123–

1125 https://doi.org/10.1161/CIRCULATIONAHA.120.049465
48. *Kogan E. A., Berezovskiy Yu. S., Blagova O. V., Kukleva A. D., Bogacheva G. A., Kurilina E. V., Kalinin D. V., Bagdasaryan T. R., Semeyonova L. A., Gretsov E. M., Ergeshov A. E., Fomin V. V.* Miocarditis in Patients with COVID-19 Confirmed by Immunohistochemical. *Kardiologiya*. 2020, 60 (7), 4–10. (In Russian). https://doi.org/10.18087/cardio.2020.7.n1209.
49. *Mehra M. R., Ruschitzka F.* COVID-19 Illness and Heart Failure: A Missing Link? *JACC Heart Fail*. 2020, 8 (6), 512–514. https://doi.org/10.1016/j.jchf.2020.03.004
50. *Aykut Cilli, Ozlem Cakin, Emine Aksoy, Feyza Kargin, Nalan Adiguzel, Zuhal Karakurt, Begum Ergan, Seda Mersin, Selen Bozkurt, Fatma Ciftci, Melike Cengiz.* Acute cardiac events in severe community-acquired pneumonia: A multicenter study. *A Clin. Respir. J*. 2018, 28 (7), 2212–2219. https://doi.org/10.1111/crj.12791
51. *Cowan L. T., Lutsey P. L., Pankow J. S., Matsushita K., Ishigami J., Lakshminarayan K.* Inpatient and Outpatient Infection as a Trigger of Cardiovascular Disease: The ARIC Study. *J. Amer. Heart Assoc.* 2018, V. 7, P. e 009683. https://doi.org/10.1161/JAHA.118.009683
52. *Babapoor-Farrokhran S., Gill D., Walker J., Rasekhi R. T., Bozorgnia B., Amanullah A.* Myocardial injury and COVID-19: Possible mechanisms. *Life Sci*. 2020, V. 253, P. 117723. https://doi.org/10.1016/j.lfs.2020.117723
53. *Florea V. G., Cohn J.* N The Autonomic Nervous System and Heart Failure. *Circulation Res.* 2014, V. 114, P. 1815–182. https://doi.org/10.1161/CIRCRESAHA.114.302589
54. *Xiong T. Y., Redwood S., Prendergast B., Chen M.* Coronaviruses and the cardiovascular system: acute and long-term implications. *Eur. Heart J*. 2020, 41 (19), 1798–1800. https://doi.org/10.1093/eurheartj/ehaa231
55. *Bansal M.* Cardiovascular disease and COVID-19. Diabetes & Metabolic Syndrome: *Clin. Res. Rev*. 2021, 15 (1), 477. https://doi.org/10.1016/j.dsx.2020.03.013
56. *Thygesen K., Alpert J. S., Jaffe A. S., Chaitman B. R., Bax J. J., Morrow D. A., White H. D.* Executive Group on behalf of the Joint European Society of Cardiology (ESC)/American College of Cardiology (ACC)/American Heart Association (AHA)/World Heart Federation (WHF) Task Force for the Universal Definition of Myocardial Infarction. Fourth Universal Definition of Myocardial Infarction (2018). *J. Am. Coll. Cardiol.* 2018, 72 (18), 2231–2264. https://doi.org/10.1016/j.jacc.2018.08.1038
57. *Chapman A. R., Shah A. S. V., Lee K. K., Anand A., Francis O., Adamson P., McAllister D. A., Strachan F. E., Newby D. E., Mills N. L.* Long-Term Outcomes in Patients With Type 2 Myocardial Infarction and Myocardial Injury. *Circulation*. 2018, 137 (12), 1236–1245. https://doi.org/10.1161/CIRCULATIONAHA.117.031806
58. *Polonskaya Y. V., Kashtanova E. V., Stakhneva E. M., Sadowski E. V., Ragino Yu. I.* COVID-19 and cardiovascular diseases. *Ateroscleroz*. 2020, 16 (2), 73–79. (In Russian). https://doi.org/10.15372/ATER20200207
59. *Arentz M., Yim E., Klaff Li., Lokhandwala S., Riedo F. X., Chong M., Lee M.* Characteristics and Outcomes of 21 Critically Ill Patients With COVID-19 in Washington State. *JAMA*. 2020, 323 (16), 1612–1614. https://doi.org/10.1001/jama.2020.4326
60. *Yang X., Yu Y., Xu J., Shu H., Xia J., Liu H., Wu Y., Zhang L., Yu Z., Fang M., Yu T., Wang Y., Pan S., Zou X., Yuan S., Shang Y.* Clinical course and outcomes of critically ill patients with SARS-CoV-2 pneumonia in Wuhan, China: a single-centered, retrospective, observational study. *Lancet Respir. Med*. 2020, 8 (5), 475–481. https://doi.org/10.1016/S2213-2600(20)30079-5
61. *Liu K., Fang Y. Y., Deng Y., Liu W., Wang M. F., Ma J. P., Xiao W., Wang Y. N., Zhong M. H., Li C. H., Li G. C., Liu H. G.* Clinical characteristics of novel coronavirus cases in tertiary hospitals in Hubei Province. *Chin. Med. J. (Engl.)*. 2020, 133 (9), 1025–1031. https://doi.org/10.1097/CM9.0000000000000744
62. *Zhang J. J., Dong X., Cao Y. Y., Yuan Y. D., Yang Y. B., Yan Y. Q., Akdis C. A., Gao Y. D.* Clinical characteristics of 140 patients infected with SARS-CoV-2 in Wuhan, China. *Allergy*. 2020, 75 (7), 1730–1741. https://doi.org/10.1111/all.14238
63. *Pingzheng Mo, Yuanyuan Xing, Yu Xiao, Liping Deng, Qiu Zhao, Hongling Wang, Yong Xiong, Zhenshun Cheng, Shicheng Gao, Ke Liang, Mingqi Luo, Tielong Chen, Shihui Song, Zhiyong Ma, Xiaoping Chen, Ruiying Zheng, Qian Cao, Fan Wang, Yongxi Zhang.* Clinical characteristics of refractory COVID-19 pneumonia in Wuhan, China. Clin. Infect. Dis. *ciaa270*. 2020. https://doi.org/10.1093/cid/ciaa270
64. *Guo T., Fan Y., Chen M., Wu X., Zhang L., He T., Wang H., Wan J., Wang X., Lu Z.* Cardiovascular Implications of Fatal Outcomes of Patients With Coronavirus Disease 2019 (COVID-19). *JAMA Cardiol*. 2020, 5 (7), 811–818. https://doi.org/10.1001/jamacardio.2020.1017

65. *Huang C., Wang Y., Li X., Ren L., Zhao J., Hu Y., Zhang L., Fan G., Xu J., Gu X., Cheng Z., Yu T., Xia J., Wei Y., Wu W., Xie X., Yin W., Li H., Liu M., Xiao Y., Gao H., Guo L., Xie J., Wang G., Jiang R., Gao Z., Jin Q., Wang J., Cao B.* Clinical features of patients infected with 2019 novel coronavirus in Wuhan, *China. Lancet.* 2020, 395 (10223), 497–506. https://doi.org/10.1016/S0140-6736(20)30183-5
66. *Tao Chen, Di Wu, Huilong Chen, Weiming Yan, Danlei Yang, Guang Chen, Ke Ma, Dong Xu, Haijing Yu, Hongwu Wang, Tao Wang, Wei Guo, Jia Chen, Chen Ding, Xiaoping Zhang, Jiaquan Huang, Meifang Han, Shusheng Li, Xiaoping Luo, Jianping Zhao, Qin Ning.* Clinical characteristics of 113 deceased patients with coronavirus disease 2019: retrospective study. *BMJ.* 2020, V. 368, P. m1295. https://doi.org/10.1136/bmj.m1295
67. *Wang L., He W., Yu X., Hu D., Bao M., Liu H., Zhou J., Jiang H.* Coronavirus disease 2019 in elderly patients: Characteristics and prognostic factors based on 4-week follow-up. *J. Infect.* 2020, 80 (6), 639–645. https://doi.org/10.1016/j.jinf.2020.03.019
68. *Lian J., Jin X., Hao S., Cai H., Zhang S., Zheng L., Jia H., Hu J., Gao J., Zhang Y., Zhang X., Yu G., Wang X., Gu J., Ye C., Jin C., Lu Y., Yu X., Yu X., Ren Y., Qiu ., Li L., Sheng J., Yang Y.* Analysis of Epidemiological and Clinical Features in Older Patients With Coronavirus Disease 2019 (COVID-19) Outside Wuhan. *Clin. Infect. Dis.* 2020, 71 (15), 740–747. https://doi.org/10.1093/cid/ciaa242
69. *Guan W. J., Liang W. H., Zhao Y., Liang H. R., Chen Z. S., Li Y. M., Liu X. Q., Chen R. C., Tang C. L., Wang T., Ou C. Q., Li L., Chen P. Y., Sang L., Wang W., Li J. F., Li C. C., Ou L. M., Cheng B., Xiong S., Ni Z. Y., Xiang J., Hu Y., Liu L., Shan H., Lei C. L., Peng Y. X., Wei L., Liu Y., Hu Y. H., Peng P., Wang J. M., Liu J. Y., Chen Z., Li G., Zheng Z. J., Qiu S. Q., Luo J., Ye C. J., Zhu S., Cheng L. L., Ye F., Li S. Y., Zheng J. P., Zhang N. F., Zhong N. S., He J. X.* China Medical Treatment Expert Group for COVID-19. Comorbidity and its impact on 1590 patients with COVID-19 in China: a nationwide analysis. *Eur. Respir. J.* 2020, 55 (5), 2000547. https://doi.org/10.1183/13993003.00547-2020
70. *Mancia G., Rea F., Ludergnani M., Apolone G., Corrao G.* Renin–Angiotensin–Aldosterone System Blockers and the Risk of Covid-19. *N Engl. J. Med.* 2020, V. 382, P. 2431–2440. https://doi.org/10.1056/NEJMoa2006923
71. *Mehra M. R., Desai S. S., Kuy S., Henry T. D., Patel A. N.* Cardiovascular Disease, Drug Therapy, and Mortality in Covid-19. *N Engl. J. Med.* 2020, 382 (25), e102. https://doi.org/10.1056/NEJMoa2007621
72. *Reynolds H. R., Adhikari S., Pulgarin C., Troxel A. B., Iturrate E., Johnson S. B., Hausvater A., Newman J. D., Berger J. S., Bangalore S., Katz S. D., Fishman G. I., Kunichoff D., Yu Chen, Ogedegbe G., Hochman J. S.* Renin–Angiotensin–Aldosterone System Inhibitors and Risk of Covid-19. *N Engl. J. Med.* 2020, V. 382, P. 2441–2448. https://doi.org/10.1056/NEJMoa2008975
73. *Klok F. A., Kruip M. J. H. A., van der Meer N. J. M., Arbous M. S., Gommers D. A. M. P. J., Kant K. M., Kaptein F. H. J., van Paassen J., Stals M. A. M., Huisman M. V., Endeman H.* Incidence of thrombotic complications in critically ill ICU patients with COVID-19. *Thromb. Res.* 2020, V. 191, P. 145–147. https://doi.org/10.1016/j.thromres.2020.04.013
74. *Varga Z., Flammer A. J., Steiger P., Haberecker M., Andermatt R., Zinkernagel A. S., Mehra M. R., Schuepbach R. A., Ruschitzka F., Moch H.* Endothelial cell infection and endotheliitis in COVID-19. *Lancet.* 2020, 395 (10234), 1417–1418. https://doi.org/10.1016/S0140-6736(20)30937-5
75. *Yafei Wang, Ying Zhou, Zhen Yang, Dongping Xia, Yi Hu, Shuang Geng.* Clinical Characteristics of Patients with Severe Pneumonia Caused by the SARS-CoV-2 in Wuhan, China. *Clinical Investigations.* 2020, V. 99, P. 649–657. https://pubmed.ncbi.nlm.nih.gov/32841948/. https://doi.org/10.1159/000507940
76. *Onopchuk Yu. N.* Homeostasis of functional respiratory system as a result of intersystem and system-medium informational interaction. *Bioecomedicine. Uniform information space. Ed. by V. I. Gritsenko. Kyiv.* 2001, P. 59–84. (In Russian).
77. *Onopchuk Yu. N.* Homeostasis of the functional circulatory system as a result of intersystem and system-medium informational interaction. *Bioecomedicine. Uniform information space. Ed. by V. I. Gritsenko. Kyiv.* 2001, P. 85–104. (In Russian).
78. *Aralova N. I.* Mathematical models of functional respiratory system for solving the applied problems in occupational medicine and sports. *Saarbrücken: LAP LAMBERT Academic Publishing GmbH&Co, KG.* 2019, 368 p. (In Russian). ISBN 978-613-4-97998-6
79. *Aralova N. I.* Information technologies of decision making support for rehabilitation of sportsmen engaged in combat sport. *J. Automation Information Sci.* 2016, V. 3, P. 160–170. https://doi.org/10.1615/JAutomatInfScien.v48.i 6.70, pages 68-78

80. *Aralova N. I.* Integrated mathematical model of self-organization of functional systems of the organism for imitation viral diseases. *J. Automation Information Sci.* 2020, V. 3, P. 127–137. https://doi.org/10.1615/JAutomatInfScien.v52.i3
81. *Beloshitsky P. V., Onopchuk Yu. N., Aralova N. I., Semchik T. A.* Mathematic modeling of hypoxic states at heart ischemia. *Physiol. J.* 2004, 50 (3), 139–143. (In Russian).
82. *Liashko N. I., Onopchuck G. Yu.* Pharmacological correction of organism state. Mathematical model and its analysis. *Computer Mathematic*. 2005, V. 1, P. 127–134. (In Russian).
83. *Aralova A. A., Aralova N. I., Kovalchuk-Khimyuk L. A., Onopchuk Yu. N.* Automated information system for athletes functional diagnostics. *Control systems and machines.* 2008, V. 3, P. 73–78. (In Russian).
84. *Aralova N. I., Shakhlina L. Ya.-G., Futornyi S. M., Kalytka S. V.* Information Technologies for Substantiation of the Optimal Course of Interval Hypoxic Training in Practice of Sports Training of Highly Qualified Sportswomen. *J. Automat. Inf. Sci.* https://doi.org/2020.1:130–142.10.1615/JAutomatInfScien.v52.i1.50 pages 41-55

МАТЕМАТИЧНА МОДЕЛЬ ДЛЯ ДОСЛІДЖЕННЯ ГІПОКСИЧНИХ СТАНІВ СЕРЦЕВОГО М'ЯЗА ЗА ВІРУСНОГО УРАЖЕННЯ

Н. І. Аралова[1], *О. М. Ключко*[2], *В. І. Машкін*[1], *І. В. Машкіна*[3], *Paweł Radziejowski*[4], *Maria Radziejowska*[4]

[1]Інститут кібернетики ім. В. М. Глушкова НАН України, Київ
[2]Національний авіаційний університет, Київ, Україна
[3]Київський університет імені Бориса Грінченка, Україна
[4]Czestochowa University of Technology, Poland

E-mail: aralova@ukr.net

У зв'язку з тим, що одним з основних ускладнень за вірусного ураження SARS-CoV-2 є різні патології серцево-судинної системи і, як наслідок, вторинна тканинна гіпоксія, актуальним є пошук засобів для полегшення гіпоксичного стану. Одним із напрямів може бути математичне моделювання цього процесу з наступною імітацією розвитку гіпоксичного стану і подальшої корекції гіпоксії.

Мета. Побудувати математичну модель функціональної системи дихання і кровообігу для імітації часткової оклюзії судин за ураження вірусною інфекцією і фармакологічної корекції спричиненого гіпоксичного стану.

Методи. Застосовували методи математичного моделювання та динамічного програмування. Транспортування та масообмін респіраторних газів в організмі, часткову оклюзію судин і введення антигіпоксантів записували системою звичайних нелінійних диференціальних рівнянь.

МАТЕМАТИЧЕСКАЯ МОДЕЛЬ ДЛЯ ИССЛЕДОВАНИЯ ГИПОКСИЧЕСКИХ СОСТОЯНИЙ В СЕРДЕЧНОЙ МЫШЦЕ ПРИ ВИРУСНОМ ПОРАЖЕНИИ

Н. И. Аралова[1], *Е. М. Ключко*[2], *В. И. Машкин*[1], *И. В. Машкина*[3], *Paweł Radziejowski*[4], *Maria Radziejowska*[4]

[1]Институт кибернетики им. В. М. Глушкова НАН Украины, Киев
[2]Национальный авиационный университет, Киев, Украина
[3]Киевский университет имени Бориса Гринченко, Украина
[4]Czestochowa University of Technology, Poland

E-mail: aralova@ukr.net

В связи с тем, что одним из основных осложнений при поражении организма вирусом SARS-CoV- 2 являются различные патологии сердечно-сосудистой системы и, как следствие, вторичная тканевая гипоксия, актуальным является поиск средств для облегчения гипоксического состояния. Одним из направлений может быть математическое моделирование этого процесса с последующей имитацией развития гипоксического состояния и последующей коррекции гипоксии.

Цель. Построить математическую модель функциональной системы дыхания и кровообращения для имитации частичной окклюзии сосудов при поражении вирусной инфекцией и фармакологической коррекции возникшего гипоксического состояния.

Методы. Применялись методы математического моделирования и динамического программирования. Транспортировка и массообмен респираторных газов в организме, частичная окклюзия сосудов и введение антигипоксанта записывали системой обыкновенных нелинейных дифференциальных уравнений.

Результати. Розроблено математичну модель функціональної системи дихання для імітації фармакологічної корекції гіпоксичного стану, спричиненого ускладненим перебігом вірусної інфекції. Модель ґрунтується на теорії функціональних систем П. К. Анохіна і припущенні щодо основної функції системи дихання Передбачається взаємовплив і взаємозв'язок окремих функціональних систем організму. Складовими частинами комплексної моделі є моделі транспортування і масообміну респіраторних газів в організмі, самоорганізації системи дихання і кровообігу, часткової оклюзії судин і транспортування фармакологічного препарату.

Висновки. Проведено серію обчислювальних експериментів для організму середньостатистичної людини, яка показала можливості компенсації тканинної гіпоксії за допомогою фармакологічного препарату із судинорозширювальною дією. Запропонована модель, у разі наявності масиву індивідуальних даних, може бути корисною для вироблення стратегії і тактики лікування конкретного хворого.

Ключові слова: функціональна система дихання; транспортування та масообмін дихальних газів; гіпоксичний стан; часткове закупорювання судин.

Результаты. Разработана математическая модель функциональной системы дыхания для имитации фармакологической коррекции гипоксического состояния, вызванного осложненным течением вирусной инфекции. Модель базируется на теории функциональных систем П. К. Анохина и предположении об основной функции системы дыхания. Предполагается взаимовлияние и взаимосвязь отдельных функциональных систем организма. Составными частями являются модели транспортировки и массообмена респираторных газов в организме, самоорганизации системы дыхания и кровообращения, частичной окклюзии сосудов и транспортировки фармакологического препарата.

Выводы. Проведенная серия вычислительных экспериментов для организма среднестатистического человека показала возможности компенсации тканевой гипоксии с помощью фармакологического препарата с сосудорасширяющим действием и, при наличии массива индивидуальных данных, модель может оказаться полезной для выработки стратегии и тактики лечения конкретного больного.

Ключевые слова: функциональная дыхательная система; транспортировка и массообмен дыхательных газов; гипоксическое состояние; частичная окклюзия кровеносных сосудов.

UDC 602.6:577.2.18:577.112:582.661.21 https://doi.org/10.15407.biotech14.04.053

TRANSIENT EXPRESSION OF REPORTER GENES IN CULTIVARS OF *Amaranthus caudatus* L.

O. M. Yaroshko
M. V. Kuchuk
Institute of Cell Biology and Genetic Engineering of the National Academy of Sciences of Ukraine, Kyiv

E-mail: 90tigeryaroshko90@gmail.com

Received 18.06.2021
Revised 14.08.2021
Accepted 31.08.2021

Local cultivars of *A. caudatus*: Helios and Karmin were used as plant material. Amaranth is a new pseudocereal introduced in Ukraine. The plant biomass of amaranth is used in medicine, food industry and cosmetology industry.

Aim. The purpose of the work was to identify the optimal conditions for the transient expression of reporter genes in *Amaranthus caudatus* cultivars.

Methods. Biochemical and microscopy methods were used in the following work. Seedlings and adult plants of different age were infiltrated with agrobacterial suspensions separately (genetic vector pCBV19 with a *uidA* gene and genetic vector pNMD2501 with a *gfp* gene in *Agrobacterium tumefaciens* GV3101 strain).

Results. Transient expression of the *uidA* and *gfp* genes was obtained in amaranth plants after conduction series of experiments. The most intensive transient expression of *gfp* and *uidA* genes was observed in seedlings infiltrated at the age of 1 day. The maximum fluorescence of the GFP protein was observed on 5^{th}–6^{th} days.

Conclusions. It was shown that the cultivar Helios was more susceptible to agrobacterial infection than the cultivar Karmin. The effectiveness of *Agrobacterium* mediated transformation was from 16% to 95% for the Helios cultivar and from 12% to 93% for the Karmin cultivar. The obtained results indicate that the studied amaranth cultivars can potentially be used for obtaining transient expression of target genes and synthesizing target proteins in their tissues in the future.

Key words: *Amaranthus*, *uidA*; *gfp*; *Agrobacterium;* transient expression.

The term “transient gene expression” refers to the expression of genes that are expressed shortly after the nucleic acid of bacteria has been introduced into eukaryotic cells. During transient expression, there is no integration of foreign genes into the nuclear genome of plants. In this way the genetic material that has been integrated into plant cells is not inherited by offsprings during the sexual reproduction of plants [2].

Transient gene expression in plant systems has several advantages over stable expression. Transient expression technology does not need the regeneration of transformed tissues or organs, nor does it influence the plant genome stability. This technology allows accelerating the experiments, so the functions of the target genes can be studied 4–10 days after the incorporation of foreign genes in the plant cells. Transient expression allows studying the gene functioning in non-sterile conditions [1, 2]. Transient expression also permits protein interactions to be studied [3, 4].

Transient gene expression can be achieved via several methods of delivering of genetic information. One of which these is agroinfiltration which allows infiltrating many plants at the short time period. Moreover, several genetic vectors (with different genes) can be used for the infiltration of a single plant [5, 6].

Genetic constructs used to obtain transient expression often carry a gene where the target gene is transcriptionally fused to a reporter gene (for example, the *green fluorescent* gene (*gfp*)).

Reporter genes are those genes that encode proteins, the presence of which can be quickly detected by the appearance of fluorescence or specific staining of transformed tissues when stained with a dye. In turn, reporter proteins encoded by reporter genes can help to detect the localization of target proteins in certain organs, tissues, or organelles of plant cells [2].

Mainly, *gfp* and *uidA* are used as reporter genes. The presence of the *gfp* gene is detected by the appearance of green fluorescence of transformed plant tissues under blue rays. The presence of the *uidA* gene is detected by staining plant tissues in blue color when they come into contact with a specific dye. Genetic vectors with these genes are often used in *Agrobacterium*-mediated transformation, when it is necessary to obtain a transient or stable gene expression [2].

The choice of a particular reporter gene for use in experiments should be based on data from the localization in the plant cell of the product encoded by the reporter gene. Thus, the GFP protein encoded by the *gfp* gene is an effective reporter protein in experiments where the localization of the target protein is in the nucleus [7, 8], cytoplasm [9, 10], plasma membrane [10], Golgi apparatus [11], endoplasmic reticulum [9, 11], tonoplasts [12], mitochondria [13] and chloroplasts [11], while reporter yellow fluorescent protein (YFP) and mCherry are used to assess the localization of target protein in peroxisomes [6, 14].

Representatives of the *Amaranthus* genus were the objects of our investigation. The choice is due to the wide use of amaranth plant raw materials in various industries: food industry; pharmaceuticals, agriculture. Improving the quality of amaranth using genetic engineering methods offers considerable potential.

Representatives of *Amaranthus* genus have unique amino acid composition and are rich in biologically active compounds (squalene and amarantin). Squalene has anticancer and wound healing properties. Amarantin has an antioxidant effect [16]. The properties of *Amaranthus* can be improved using biotechnological methods to produce biologically valuable substances (for example, squalene and amarantin).

The possibility of transient expression of the *gus* gene was shown in our previous work for adult *A. caudatus* plants [16, 48]. Yet, there has been no information about obtaining the transient expression of the *gfp* gene in representatives of the *Amaranthus* genus. We show here for the first time the results of the transient expression of the *gfp* gene for the *Amaranthus* genus.

Materials and Methods

The objects of the research were cultivars of *Amaranthus caudatus*: Helios and Karmin. The seeds were obtained from the M. M. Grishko Botanical Garden of the National Academy of Sciences of Ukraine.

Plants of different age: 1 day-old seedlings, 10 day-old seedlings, 2 month-old adult plants were used in the experiments. To obtain 1-day-old seedlings, seeds were soaked for one day in water under non-sterile conditions (22–26 °C, 14-hour light period, illumination — 3 000–4 500 lx). To obtain 10-day-old seedlings and 2-month-old plants, seeds were sown in the pots with soil and grown in a greenhouse under the conditions of 22–26 °C, 14-hour light period and illumination — 3 000–4 500 lx.

The aim of the experiments was as follows: to check and evaluate the functioning of the pCBV19 and pNMD2501 genetic vectors of *A. tumefaciens* in *A. caudatus* plant tissues after *Agrobacterium*-mediated transformation; to determine the optimal age of plants for infiltration and to identify the plant's organs and tissues in which the transient gene expression occurs the most intensively.

The vacuum infiltration method [15] and methods for detection of *uidA* [17] and *gfp* genes presence were used to obtain transient gene expression.

Plants of different ages (previously mentioned) were infiltrated with agrobacterial suspensions. The strains GV3101 of *A. tumefaciens* harboring pCBV19 [16] and pNMD2501 genetic vectors separately were used in the work (supplementary material Fig. 1). The genetic vector pNMD2501 was kindly donated by NOMAD Bioscience GmbH (Germany). Genetic vector pCBV19 carried *uidA* gene, genetic vector pNMD2501 carried g*fp* gene.

The steps of preparation of agrobacterial suspension were described in the author's previous article [16].

Plants were infiltrated in a flask with a medium containing the agrobacterial suspension for 5 min, at 22–24 °C in a vacuum chamber under pressure of 0.1 mPa.

Detection of the *uidA* gene (β-glucuronidase activity) was carried out by histochemical assay on the 5th day after infiltration in the presence of substrate, X-gluc (5-bromo-4-chloro-3-indolyl-β–D-glucuronide) [17].

The leaves of the infiltrated plants and control plants (negative control) which were

not infiltrated, were taken and incubated in a histochemical buffer (50 mM sodium phosphate, pH 7.0; 50 mM EDTA, pH 8.0; 0.5 mM $K_3Fe(CN)6$; 0.5 mM $K_4Fe(CN)6$; 0.1% Triton X-100; 1 mM X-gluc). The histochemical reaction was stopped after 24h of incubation at 37 °C in the dark, followed by five rinses in 70% ethanol. Leaves of stably transformed *Nicotiana tabacum* plants were used as positive control.

Next, the leaves of adult plants and whole seedlings were placed on microscope slides for observation (Zeiss axiophot fluorescent microscope®, Germany; microscope magnification ×100 and ×200). Beta-glucuronidase protein (GUS) activity was detected visually by the appearance of blue staining of plant tissues. Leaves of stably transformed *Nicotiana tabacum* were used as positive control.

The presence of the GFP protein was detected after 4 days in the seedlings (that were immersed in a suspension of *A. tumefaciens* with genetic vector pNMD2501) and was evaluated visually under light with a wavelength in the range of 365–400 nm (Black ray®, model B 100 AP the ultraviolet lamp.) and a microscope with an attachment with a special filter (Plan-Neofluar). The result was considered as positive by the appearance of green tissue fluorescence. The results were documented by photographing on digital media.

Data collection and statistical analysis

One hundred plants (young seedlings) and 30 plants (2-month-old adult) of each variety were used for each part of the experiment. Namely 100 seedlings of cv. Helios and 100 seedlings of cv. Karmin (1-day-old); 100 seedlings 10-day-old of each cultivar and 30 plants of each cultivar (2-month-old) were infiltrated with suspension of *A. tumefaciens* (harboring pCBV19 genetic vector).

For the experiment of *gfp* expression were used 100 seedlings of cv. Helios and 100 seedlings of cv. Karmin (1-day-old); 100 seedlings 10-day-old of each cultivar; 30 plants of each cultivar (2-month-old) which were infiltrated with suspension of *A. tumefaciens* (harboring pNMD2501 genetic vector). The same quantity of seedlings and adult plants of each variety as mentioned above (for the experiment of transient expression of *uidA* and *gfp* gene) were used as negative control (non-infiltrated with agrobacterial suspension).

The percentage of *uidA*-positive plants for each age group (as a percentage expressed the number of plants in which were detected the presence of *uidA*/*gfp* genes from the total quantity of plants, which were infiltrated) was calculated after obtaining the results. The standard error (SE) and the arithmetical mean (M) were calculated using the Excel program 2007 and the *t*-Student criterion was calculated in the program Statistica in order to determine the accuracy of the obtained results.

Results and Discussion

Transient expression of uidA gene

The histochemical reaction was performed after conducting a series of experiments with infiltration [17]. Large areas of plant tissues stained in blue color were identified. Such staining occurred in plant tissues where the GUS protein was bound with the specific X-gluc substrate. This may indicate that after infiltration, bacterial genes were incorporated into plant cells, DNA was correctly transcribed and a functional GUS reporter protein was synthesized in plant tissues.

The intensity of blue staining varied among the plant groups of different ages, as well as varied the surface areas that were colored in the plants of different ages. In young seedlings (in most of the seedlings which were infiltrated at the age of one day) all parts of the plant (root, hypocotyl and cotyledons) were stained (supplementary material Fig. 2). The percentage of positive gus-stained plants for the cultivar Helios was 95%, for the cultivar Karmin — 93%. The areas in which the reporter protein GUS was synthesized (in 10-day-old seedlings) were mainly along the midrib and occupied most of the surface area of the leaf blade (more than 80%) (Fig. 1, supplementary material Fig. 3). The percentage of gus-positive plants (which were infiltrated at the age 10 days) for the cultivar Helios was 61.26%, for the cultivar Karmin — 41.55%.

In plants that were infiltrated at the age of 2 months, small areas stained in blue color were revealed only in the region of the midrib. The percentage of gus-positive plants was for the cultivar Helios — 16% and for the cv. Karmin 12% (supplementary material Fig. 4). These results indicate that very young seedlings 1-day-old of both cultivars (Helios and Karmin) were the most susceptible to agrobacterial infection. In seedlings that were infiltrated at the age of 10 days and 2 months, the cv. Helios displayed a higher susceptibility to agrobacterial infection. Perhaps this is due to the peculiarities of the biochemical composition

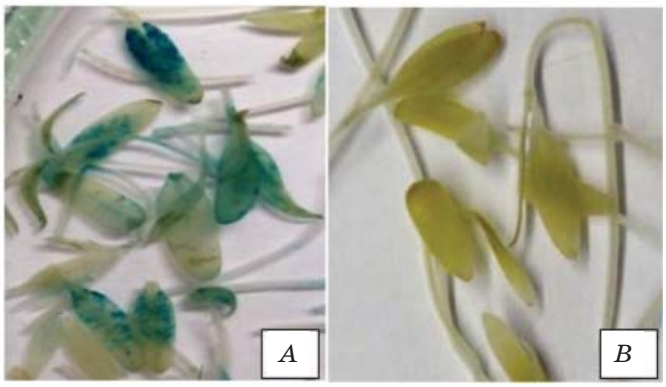

Fig. 1. **15-day-old seedlings of *A. caudatus* cv. Helios after the histochemical reaction:**
A — seedlings infiltrated with *A. tumefaciens* harboring genetic vector pCBV19;
B — non-infiltrated control seedlings

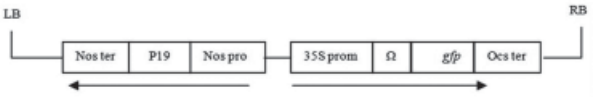

Supplementary material Fig. 1. **Schematic representation of the T-DNA site of the pNMD2501 genetic vector:**
LB — left border sequence; RB — right border sequence; Nos pro — nopaline synthase promoter; Nos ter — nopaline synthase terminator; 35S prom — promoter of cauliflower mosaic virus gene (CaMV); Ocs — octopine synthase terminator; Ω — regulatory sequence enhancer; gfp — green fluorescent protein gene; P19 — gene of protein P19 (suppressor of gene silencing)

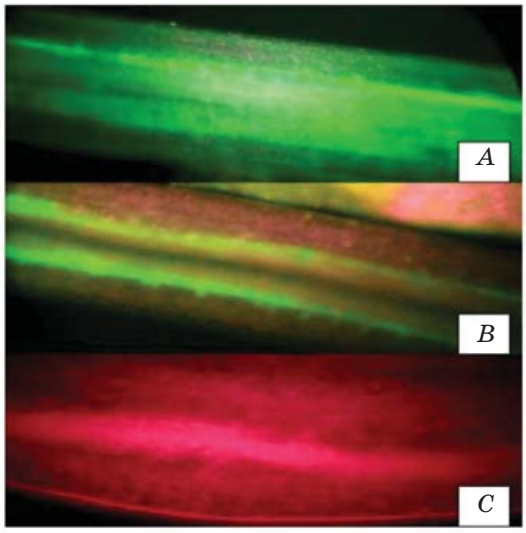

Fig. 2. **Hypocotyls of *A. caudatus* seedlings (15-day-old) which were infiltrated with *A. tumefaciens* harboring genetic vector pNMD2501 under UV light (*A*, *B*)** (magnifection ×200)
A — cv. Helios; *B* — cv. Karmin); *C* — hypocotyls of non-infiltrated control plant (cv. Helios) (magnifection ×200)

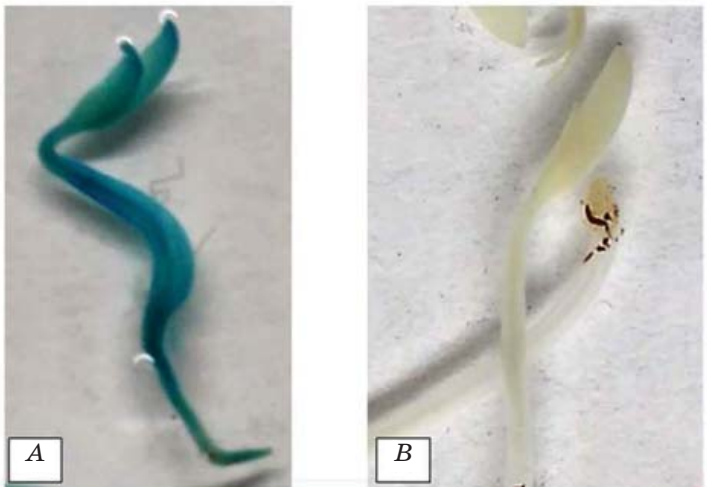

Supplementary material Fig. 2. **Seedlings of *A. caudatus* cv. Helios (6-day-old) after the histochemical reaction:**
A — seedlings infiltrated with *A. tumefaciens*, genetic vector pCBV19; *B* — non-infiltrated control seedlings of cv. Helios

of plants. The cultivar Karmin has a higher content of betacyanins than the cultivar Helios. Betacyanins can reduce the transformation efficiency of *Agrobacterium* [16].

Transient expression of gfp gene

The next stage of the work was the analysis of plants that were infiltrated *via A. tumefaciens* harboring genetic vector pNMD2501, carrying the *gfp* gene. The results of transient expression of the *gfp* gene were analyzed visually using an ultraviolet light and were considered as gfp-positive when green fluorescence of tissues appeared (Fig. 2–5).

In seedlings of both cultivars (which were infiltrated at the age of 10 days), green fluorescence was observed in hypocotyls and at the edges of leaf blades (Fig. 2, 3).

Microscopic examination revealed that the most intense transient expression of the *gfp* gene occurred in the vascular bundles of the hypocotyl and in the midrib of the leaf blade

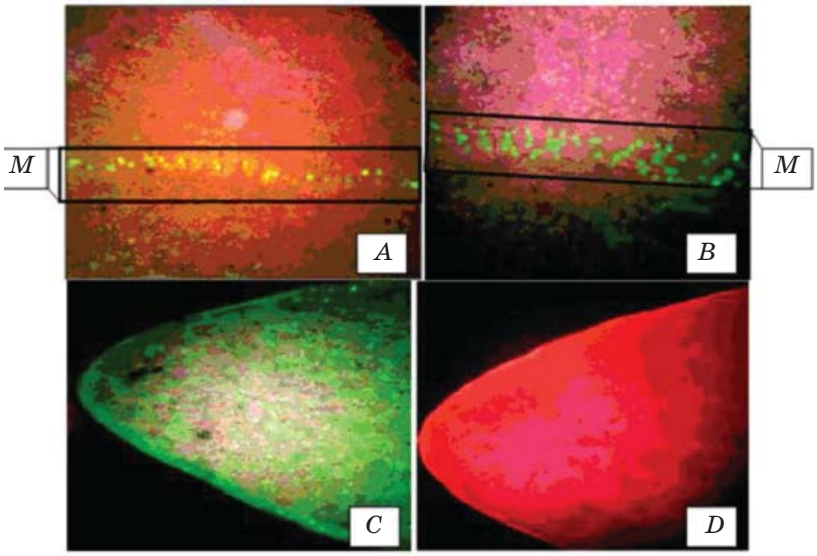

Fig. 3. **Cotyledonous leaves of *A. caudatus* seedlings (15-day old) which were infiltrated with *A. tumefaciens,* genetic vector pNMD2501 under UV light (*A*, *B*, *C*):**
A — cv. Helios (magnification ×100); *B* — cv. Karmin (magnification ×100); *C* — top of the cotyledonous leaf cv. Helios (magnification ×100); *D* — leaf of non-infiltrated control plant (cv. Helios); *M* — area of midrib

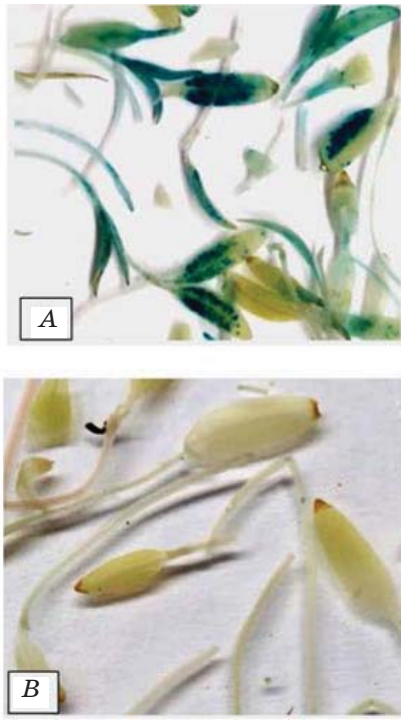

Supplementary material Fig. 3. **Seedlings of *A. caudatus* cv. Karmin (15-day-old) after the histochemical reaction:** *A* — seedlings infiltrated with *A. tumefaciens*, genetic vector pCBV19; *B* — non-infiltrated control seedlings)

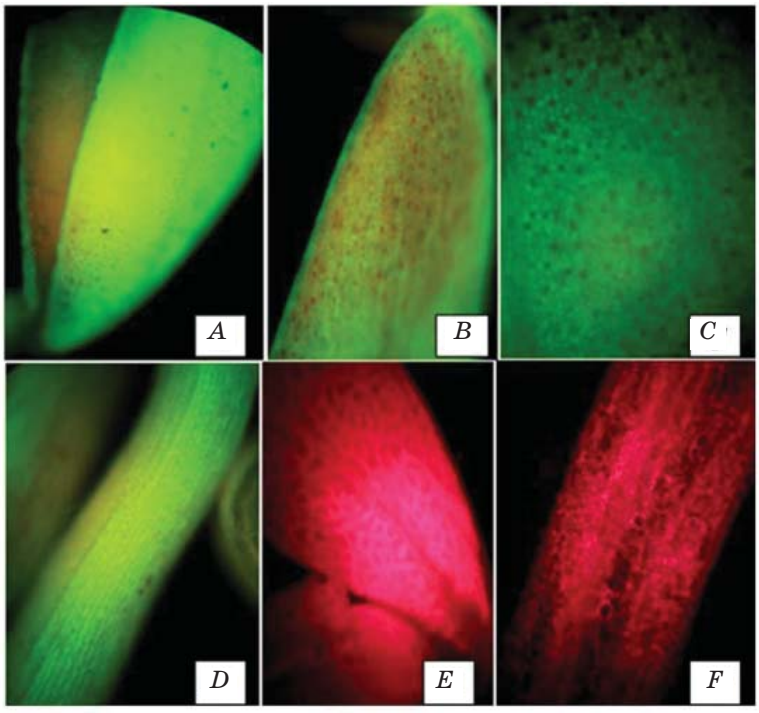

Fig. 4. **Seedlings of cv. Helios which were infiltrated with *A. tumefaciens* harboring genetic vector pNMD2501 (6-day old) under UV light (*A*, *B*, *C*, *D*):**
A — petiole and lower part of cotyledonous leaves (magnification ×100); *B* — top of the cotyledonous leaf (magnification ×100); *C* — hypocotyl (magnification ×200); *D* — hypocotyl (magnification ×100); *E* — cotyledonous leaves of non-infiltrated control plant (magnification ×100); *F* — hypocotyl of non-infiltrated control plant (magnification ×200)

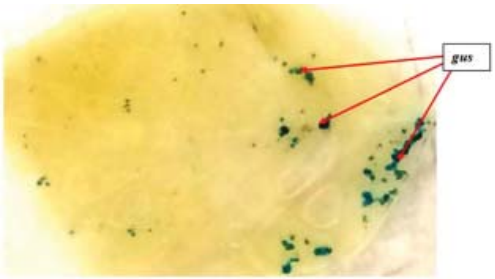

Supplementary material Fig. 4. **Leaf of *A. caudatus* variety Karmin (2-month-old) after the histochemical reaction (plant was infiltrated with *A. tumefaciens*, genetic vector pCBV19), gus —areas, where activity of β-glucuronidase was detected**

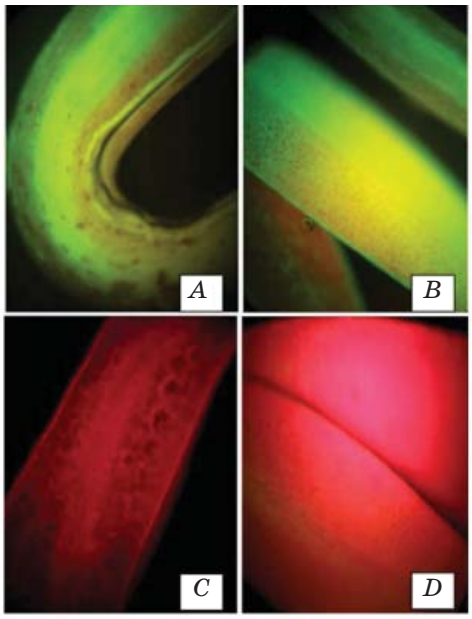

Fig. 5. **Seedlings of cv. Karmin which were infiltrated with *A. tumefaciens* harboring genetic vector pNMD2501 (6-day old) under UV light (*A*, *B*):**
A — hypocotyls (magnifection ×100);
B — hypocotyl and part of cotyledonous leaves (magnifection ×100); *C* — hypocotyl of non-infiltrated control plant (magnifection ×200); *D* — part of non-infiltrated control cotyledonous leaf (magnifection ×100)

(Fig. 3).

In seedlings, which were infiltrated at the age of 1 day (both cultivars), intensive green fluorescence was detected in all organs (root, hypocotyl, cotyledonous leaves) (Fig. 4, 5).

Microscopy of the seedlings which were infiltrated at the age of one day, revealed a very intense green glow in all tissues of the aforementioned seedling organs (Fig. 4, 5).

It should be noted that in plants that were infiltrated at the age of 2 months, only a points of green glow were visible on the leaf blades in the region of the central vein. So, we obtained transient expression of the *gus* and the *gfp* genes in all plants of all experimental groups.

Agrobacterial infiltration of the youngest seedlings (1 day-old) turned out to be more effective. Expression was more abundant in young plant tissues which intensively synthesized proteins. In plants that infiltrated at an older age, expression occurred mainly in vascular bundles and leaf midrib (seedlings infiltrated at the age of 10 days), or only in vascular bundles and leaf midrib (plants that infiltrated at the age of 2 months). It was found that amaranth cultivars have different susceptibility to agrobacterial infection. The cultivar Helios was more susceptible to agrobacterial infiltration (Fig. 6).

The number of plants in which were confirmed the expression of the *gus* gene was significantly or highly significantly different from those group of plants which were not infiltrated with *Agrobacterium*.

So far, transient gene expression has been obtained in the following plants: *Arabidopsis thaliana* [18, 19], *Capsicum annuum* [20, 21]; *Catharanthus roseus* [22, 23]; *Cucumis sativus* [24]; *Fragaria* × ananassa [12], *Fragaria vesca* [25], *Glycine max* [26], *Helianthus annuus* [27], *Juglans regia* [28, 29], *Lactuca sativa* [30], *Fagopyrum esculentum* [31], *Brasica napus* [32].

There is currently a great deal of experimental work on obtaining transient gene expression in *Nicotiana benthamiana* and review articles that mention the successful transient expression of various genes in *Nicotiana benthamiana* [33, 34].

According to the latest literature, the reporter *gfp* gene has been used in *Agrobacterium*-mediated transformation of the following plant species: *Fagopyrum esculentum* [31], *Setaria italic* [35], *Nicotiana tabacum* cv. Bright Yellow 2 [36], *Vigna unguiculata* [37], *A. hypohondriacus* and *A. hybridus* [38], *Oryza sativa* cv. Kitaake [39], *Setaria italica* [40], *Nicotiana benthamiana* [41], *Solanum lycopersicum* [41], *Solanum tuberosum* [41], *Physalis peruviana* [41].

The *uidA* reporter gene was used in *Agrobacterium*-mediated transformation of the

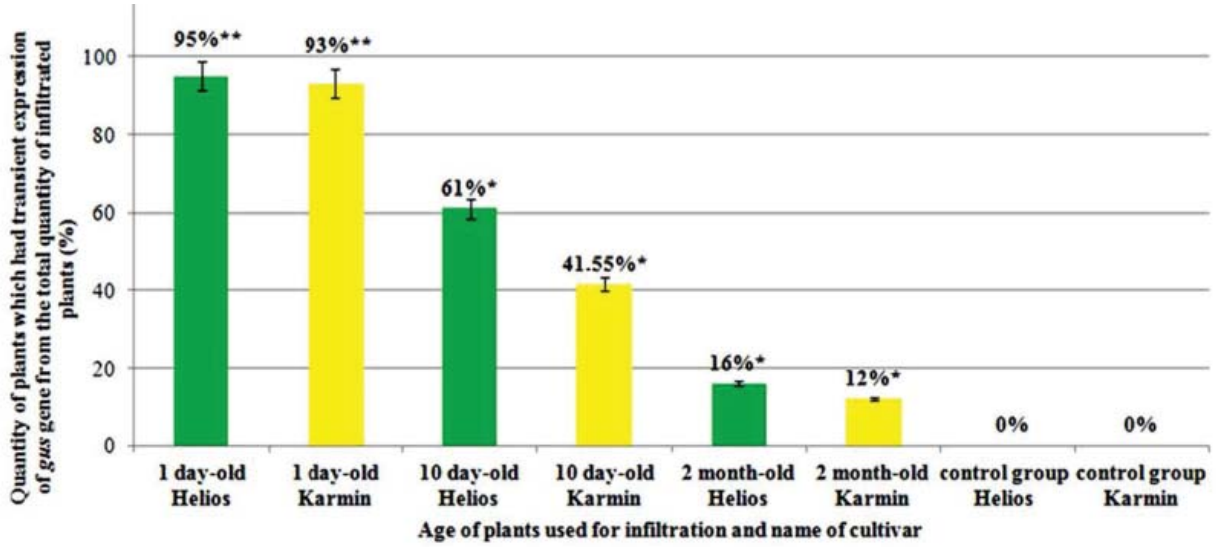

Fig. 6. **Effectiveness of vacuum infiltration of different age plants with agrobacterial suspension (*A. tumefaciens* harboring genetic vector pCBV19), expressed as a percentage:**
values showing significantly differences between the study groups and control groups are marked with asterisks * (* significant ($P < 0,05$); ** — highly significant ($P < 0,01$))

following plant species: *A. hypohondriacus* and *A. hybridus* [38], *Oryza sativa* cv. Kitaake [39], *Setaria italica* [40], *Cannabis sativa* [42].

There is only one report of transient gene expression in representatives of *A. hypochondriacus* and *A. hybridus* [38], indicating insufficient investigation in this sphere.

In our experiments, the most intensive fluorescence of the GFP protein was observed in seedlings infiltrated at the age of one day in all parts of plant. GFP fluorescence was observed also in the hypocotyls (areas of vascular bundles) and in cotyledon leaves (mainly point fluorescence in the area of midrib). In the leaves of 2-month-old plants fluorescence of GFP protein was observed with maximum fluorescence observed on 5^{th}–6^{th} days.

After infiltration of whole amaranth plants under vacuum with a suspension of *Agrobacterium tumefaciens* harboring the genetic vector pCBV19 and histochemical reaction, positive results of β-glucuronidase activity were obtained for two cultivars (Karmin and Helios) (blue areas). Gus-positive areas were located mainly in the middle and lateral veins. This may indicate that the most sensitive tissues to agrobacterial transformation and in which active protein synthesis occurs are the central and lateral veins [43, 44] (supplementary material Fig. 4).

It is known that when interpreting the results of the histochemical reaction, a number of problems may arise. For example, residues of live *Agrobacterium* suspension left on the surface of untransformed plant tissues can lead to false-positive results in standard histochemical analysis and thus may complicate the analysis of transformation results [16]. Usage of genetic vectors with intron increases the reliability of the histochemical analysis. An intron was presented in the pCBV19 genetic vector, to enable the histochemical reaction to take place only in plant tissues and this ruling out the possibility of a false positive result in the presence of agrobacterial contamination.

Chimeric genetic constructs have been used successfully in the *Agrobacterium*-mediated genetic transformation of several plants: *Spinacia oleracea* [45], *Momordica dioica* [46], *Spinacia oleracea* [47].

Our results of transient expression of the *uidA* gene after infiltration were not positive for all cultivars of *Amaranthus caudatus*. This may be due to differences in biochemical composition of the various cultivars, which in turn may affect susceptibility to *Agrobacterium* infection. In the leaves, β-glucuronidase activity was detected in the central vein. Our results of localization of the *gus* gene in plant tissues and organs during transient expression are similar to those obtained by Jun Jasic [44].

Conclusions

The optimal conditions for the transient expression of reporter genes in *Amaranthus caudatus* cultivars were determined. The most intensive transient expression of *gfp* and *gus*

genes was observed in seedlings which were infiltrated with agrobacterial suspensions at the age of one day. Maximum fluorescence of GFP protein was observed on 5^{th}–6^{th} days. It was shown that cultivar Helios was more susceptible to agrobacterial infection than the cultivar Karmin. The effectiveness of agrobacterial transformation was from 16% to 95% for the Helios cultivar and from 12% to 93% for the cultivar Karmin.

The obtained results indicate that the studied amaranth cultivars can potentially be used in the future for obtaining transient expression of target genes in their tissues and synthesis of target proteins in their tissues.

Funding sources

This research was conducted .within the general theme III-1-20 (State Registration number 0120U100849, from 2020).

REFERENCES

1. *Guidarelli M., Baraldi E.* Transient transformation meets gene function discovery: The strawberry fruit case. *Front. Plant Sci.* 2015, V. 6, P. 444. https://doi.org/10.3389/fpls.2015.00444
2. *Viacheslavova A. O., Berdychevets Y. N., Tiuryn A. A., Shymshylashvyly Kh. R., Mustafaev O., Holdenkova-Pavlova Y. V.* Expression of heterologous genes in plant systems: *New possibilities. Russ. J. Genet.* 2013, V. 48, P. 1067–1079.
3. *Cao J., Yao D., Lin F., Jiang M.* PEG-mediated transient gene expression and silencing system in maize mesophyll protoplasts: A valuable tool for signal transduction study in maize. *Acta Physiol. Plant.* 2014, V. 36, P. 1271–1281. https://doi.org/10.1007/s11738-014-1508-x
4. *Zhang Y., Su J., Duan S., Ao Y., Dai J., Liu J., Wang P., Li Y., Liu B., Feng D., Wang J., Wang H.* A highly efficient rice green tissue protoplast system for transient gene expression and studying light/chloroplast-related processes. *Plant Methods.* 2011, V. 7, P. 30. https://doi.org/10.1186/1746-4811-7-30
5. *Chen Q., Lai H.* Gene delivery into plant cells for recombinant protein production. *Biomed. Res. Int.* 2015, P. 932161.
6. *Shoji T.* Analysis of the intracellular localization of transiently expressed and fluorescently labeled copper-containing amine oxidases, diamine oxidase and N-methylputrescine oxidase in tobacco, using an *Agrobacterium* infiltration protocol. *Methods Mol. Biol.* 2018, V. 1694, P. 215–223.
7. *Sun X., Yu G., Li J., Liu J., Wang X., Zhu G., Zhang X., Pan H.* AcERF2, an ethylene-responsive factor of *Atriplex canescens*, positively modulates osmotic and disease resistance in *Arabidopsis thaliana*. *Plant Sci.* 2018, V. 274, P. 32–43. https://doi.org/10.1016/j.plantsci.2018.05.004
8. *Guo Y.-F., Shan W., Liang S.-M., Wu C.-J., Wei W., Chen J.-Y., Lu W.-J., Kuang J.-F.* MaBZR1/2 act as transcriptional repressors of ethylene biosynthetic genes in banana fruit. *Physiol. Plant.* 2019, V. 165, P. 555–568. https://doi.org/10.1111/ppl.12750
9. *Tyurin A.A., Kabardaeva K.V., Berestovoy M.A., Sidorchuk Yu. V., Fomenkov A. A., Nosov A. V., Goldenkova-Pavlova I. V.* Simple and reliable system for transient gene expression for the characteristic signal sequences and the estimation of the localization of target protein in plant cell. *Russ. J. Plant Physiol.* 2017, V. 64, P. 672–679. https://doi.org/10.1134/s1021443717040173
10. *Hua-Ying M., Wen-Ju W., Wei-Hua S., Ya-Chun S., Feng L., Cong-Na L., Ling W., Xu Z., Li-Ping X., You-Xiong Q.* Genome-wide identification, phylogeny, and expression analysis of Sec14-like PITP gene family in sugarcane. *Plant Cell Rep.* 2019, V. 38, P. 637–655. https://doi.org/10.1007/s00299-019-02394-1
11. *Olmedo P., Moreno A. A., Sanhueza D., Balic I., Silva-Sanzana C., Zepeda B., Verdonk J. C., Arriagada C., Meneses C., Campos-Vargas R.* A catechol oxidase AcPPO from cherimoya (Annona cherimola Mill.) is localized to the Golgi apparatus. *Plant Sci.* 2018, V. 266, P. 46–54. https://doi.org/10.1016/j.plantsci.2017.10.012
12. *Cheng J., Wen S., Xiao Sh., Lu B., Ma M., Bie Z.* Overexpression of the tonoplast sugar transporter CmTST2 in melon fruit increases sugar accumulation. *J. Exp. Bot.* 2018, V. 69, P. 511–523. https://doi.org/10.1093/jxb/erx440
13. *Wang B., Wang G., Shen F., Zhu S.* A glycine-rich RNA-binding protein, CsGR-RBP3, is involved in defense responses against cold stress in harvested cucumber (*Cucumis sativus* L.) fruit. *Front. Plant Sci.* 2018, V. 9, P. 540. https://doi.org/10.3389/fpls.2018.00540
14. *Wu B., Cao X., Liu H., Zhu C., Klee H., Zhang B., Chen K.* UDP-glucosyltransferase PpUGT85A2 controls volatile glycosylation in peach. *J. Exp. Bot.* 2019, V. 70, P. 925–936. https://doi.org/10.1093/jxb/ery419
15. *Martins P. K., Nakayama T. J., Ribeiro A. P., Dias B. A., Cunha B. D., Nepomuceno A. L., Harmon F. G., Kobayashi A. K., Molinari H. B. C. Setaria viridis* floral-dip: a

simple and rapid *Agrobacterium*-mediated transformation method. *Biotechnol. Rep.*. 2015, V. 6, P. 61–63. https://doi.org/10.1016/j.btre.2015.02.006
16. *Yaroshko O., Kuchuk M.* *Agrobacterium*-caused transformation of cultivars *Amaranthus caudatus* L. and hybrids of *A. caudatus* L. x *A. paniculatus* L. *Int. J. Secondary Metabolite*. 2018, 5 (4), 312–318. https://doi.org/10.21448/ijsm.478267
17. *Jefferson R. A.* Assaying chimeric genes in plants: The *gus* gene fusion system. *Plant Mol. Biol. Rep.* 1987, 5 (4), 387–405. https://doi.org/10.1007/bf02667740
18. *Wang F.-P., Wang X.-F., Zhang J.* Modulates Fe homeostasis by directly binding to the MdMATE43 promoter in plants. *Plant Cell Physiol.* 2018, V. 59, P. 2476–2489. https://doi.org/10.1093/pcp/pcy168
19. *Wang Y.-C., Yu M., Shih P.-Y., Wu H.-Y., Lai E.-M.* Stable pH suppresses defense signaling and is the key to enhance *Agrobacterium*-mediated transient expression in *Arabidopsis seedlings*. *Sci. Rep.* 2018, V. 8, P. 17071. https://doi.org/10.1038/s41598-018-34949-9
20. *Noman A., Liu Z., Yang S., Shen L., Hussain A., Ashraf M. F., Khan M. I., He S.* Expression and functional evaluation of CaZNF830 during pepper response to *Ralstonia solanacearum* or high temperature and humidity. *Microb. Pathog.* 2018, V. 118, P. 336–346. https://doi.org/10.1016/j.micpath.2018.03.044
21. *Kim N. H., Hwang B. K.* Pepper pathogenesis-related protein 4c is a plasma membrane-localized cysteine protease inhibitor that is required for plant cell death and defense signaling. *The Plant J.* 2015, V. 81, P. 81–94. https://doi.org/10.1111/tpj.12709
22. *Han J., Liu H.-T., Wang Sh.-Ch., Wang C.-R., Miao G.-P.* A class I TGA transcription factor from Tripterygium wilfordii Hook.f. modulates the biosynthesis of secondary metabolites in both native and heterologous hosts. *Plant Sci.* 2020, V. 290, P. 110293. https://doi.org/10.1016/j.plantsci.2019.110293
23. *Mertens J., Moerkercke A. V., Bossche R. V., Pollier J., Goossens A.* Clade IVa basic helix–loop–helix transcription factors form part of a conserved jasmonate signaling circuit for the regulation of bioactive plant terpenoid biosynthesis. *Plant Cell Physiol.* 2016, V. 57, P. 2564–2575. https://doi.org/10.1093/pcp/pcw168
24. *Lange M. J., Lange T.* Ovary-derived precursor gibberellin A9 is essential for female flower development in cucumber. *Development*. 2016, V. 143, P. 4425–4429. https://doi.org/10.1242/dev.135947
25. *Xie Y.-G., Ma Ya.-Ya, Bi P.-P., Wei W., Liu J., Hu Y., Gou Y.-J., Zhu D., Wen Y.-Q., Feng J.-Y.* Transcription factor FvTCP9 promotes strawberry fruit ripening by regulating the biosynthesis of abscisic acid and anthocyanins. *Plant Physiol. Biochem.* 2020, V. 146, P. 374–383. https://doi.org/10.1016/j.plaphy.2019.11.004
26. *Huang J., Gu L., Zhang Y., Yan T., Kong G., Kong L., Guo B., Qiu M., Wang Y., Jing M., Xing W., Ye W., Wu Z., Zhang Z., Zheng X., Gijzen M., Wang Y., Dong S.* An oomycete plant pathogen reprograms host pre-mRNA splicing to subvert immunity. *Nature Communications*. 2017, V. 8, P. 2051. https://doi.org/10.1038/s41467-017-02233-5
27. *Gascuel Q., Buendia L., Pecrix Ya., Blanchet N., Muños S., Vear F., Godiard L.* RXLR and CRN effectors from the sunflower downy mildew pathogen *Plasmopara halstedii* Induce hypersensitive-like responses in resistant sunflower lines. *Front Plant Sci.* 2016, V. 7, P. 1887. https://doi.org/10.3389/fpls.2016.01887
28. *Yang G., Gao X., Ma K., Li D., Jia C., Zhai M., Xu Z.* The walnut transcription factor JrGRAS2 contributes to high temperature stress tolerance involving in Dof transcriptional regulation and HSP protein expression. *BMC Plant Biol.* 2018, V. 18, P. 367. https://doi.org/10.1186/s12870-018-1568-y
29. *Yang G., Zhang W., Liu Z., Yi-Maer A.-Y., Zhai M., Xu Z.* Both JrWRKY2 and JrWRKY7 of *Juglans regia* mediate responses to abiotic stresses and abscisic acid through formation of homodimers and interaction. *Plant Biol. (Stuttg).* 2017, V. 19, P. 268–278. https://doi.org/10.1111/plb.12524
30. *Rosenthal S. H.* An intronless form of the tobacco extensin gene terminator strongly enhances transient gene expression in plant leaves. *Plant Mol. Biol.* 2018, V. 96, P. 429–443. https://doi.org/10.1007/s11103-018-0708-y
31. *Sakamoto S., Matsui K., Oshima Y., Mitsuda N.* Efficient transient gene expression system using buckwheat hypocotyl protoplasts for large-scale experiments. *Breed Sci.* 2020, 70 (1), 128–134. https://doi.org/10.1270/jsbbs.19082
32. *Mooney B. C., Graciet E.* A simple and efficient *Agrobacterium* — mediated transient expression system to dissect molecular processes in *Brassica rapa* and *Brassica napus*. 2020. https://doi.org/10.1002/pld3.237
33. *Situ J.* An RXLR effector PlAvh142 from Peronophythora litchii triggers plant cell death and contributes to virulence. *Mol.*

Plant Pathol. 2020, V. 21, P. 415–428. https://doi.org/10.1111/mpp.12905

34. *Grijalva-Manay R., Dorca-Fornell C., Enríquez-Villacreses W., Miño-Castro G., Oliva R., Ochoa V., Proaño-Tuma K., Armijos-Jaramilloc V.* DnaJ molecules as potential effectors in *Meloidogyne arenaria*. An unexplored group of proteins in plant parasitic nematodes. *Commun. Integr. Biol*. 2019, V. 12, P. 151–161. https://doi.org/10.1080/19420889.2019.1676138
35. *Santos C. M., Romeiro D., Silva J. P., Basso M. F., Molinari H. B. C., Centeno D. C.* An improved protocol for efficient transformation and regeneration of *Setaria italica*. *Plant Cell Rep*. 2020, V. 39, P. 501–510. https://doi.org/10.1007/s00299-019-02505-y
36. *Poborilova Z., Plchova H., Cerovska N., Gunter C. J., Hitzeroth I. I., Rybicki E. P., Moravec T.* Transient protein expression in tobacco BY-2 plant cell packs using single and multi-cassette replicating vectors. *Plant Cell Rep*. 2020, V. 39, P. 1115–1127. https://doi.org/10.1007/s00299-020-02544-w
37. *Juranić M. Nagahatenna D. S. K., Salinas-Gamboa R., Hand M. L., Sánchez-León N., Leong W. H., How T., Bazanova N., Spriggs A., Vielle-Calzada J.-P., Koltunow A. M. G.* A detached leaf assay for testing transient gene expression and gene editing in cowpea (*Vigna unguiculata* [L.] Walp.). *Plant Methods*. 2020, V. 16, P. 88. https://doi.org/10.1186/s13007-020-00630-4
38. *Castellanos-Arévalo A. P., Estrada-Luna A. A., Cabrera-Ponce J. L. Valencia-Lozano E., Herrera-Ubaldo H., de Folter S., Blanco-Labra A., Délano-Frier J. P.* *Agrobacterium rhizogenes*-mediated transformation of grain (*Amaranthus hypochondriacus*) and leafy (*A. hybridus*) amaranths. *Plant Cell Rep*. 2020, V. 39, P. 1143–1160. https://doi.org/10.1007/s00299-020-02553-9
39. *Burman N., Chandran D., Khurana J. P.* A rapid and highly efficient method for transient gene expression in rice plants. *Frontiers in Plant Science*. 2020, V. 11, P. 584011. https://doi.org/10.3389/fpls.2020.584011
40. *Sood P., Singh R. K., Prasad M.* An efficient Agrobacterium-mediated genetic transformation method for foxtail millet (*Setaria italica* L.). *Plant Cell Rep*. 2020, V. 39, P. 511–525. https://doi.org/10.1007/s00299-019-02507-w
41. *Torti S., Schlesier R., Thümmler A., Bartels D., Römer P., Koch B., Werner S., Panwar V., Kanyuka K., von Wirén N., Jones J. D. G., Hause G., Giritch A., Gleba Y.* Transient reprogramming of crop plants for agronomic performance. *Nat. Plants*. 2021, 7 (2), 159–171. https://doi.org/10.1038/s41477-021-00851-y
42. *Sorokin A., Yadav N., Gaudet D., Kovalchuk I.* Transient expression of the β-glucuronidase gene in *Cannabis sativa* varieties. *Plant Signaling & Behavior*. 2020, V. 15, P. 8. https://doi.org/10.1080/15592324.2020.1780037
43. *Yaroshko O., Vasylenko M., Gajdošová A., Morgun B.* "Floral-dip" transformation of *Amaranthus caudatus* L. and hybrids *A. caudatus* × *A. paniculatus* L. *Biologija*. 2019, 64 (4), 321–330. https://doi.org/10.6001/biologija.v64i4.3904
44. *Jasik Ja., Schiebold S., Rolletschek H., Denolf P., Van Adenhove K., Altmann T., Borisjuk L.* Subtissue-specific evaluation of promoter efficiency by quantitative fluorometric assay in laser microdissected tissues of rapeseed. *Plant Physiol*. 2011, 157 (2), 563–573. https://doi.org/10.1104/pp.111.180760
45. *Knoll K. A., Short K., Curtis I., Power B., Davey M. R.* Shoot regeneration from cultured root explants of spinach (*Spinacia oleracea* L.): a system for *Agrobacterium transformation*. *Plant Cell Rep*. 1997, 17 (2), 96–101 https://doi.org/10.1007/s002990050359
46. *Muthu T.* Establishment of an efficient *Agrobacterium tumefaciens*-mediated leaf disc transformation of spine gourd (*Momordica dioica* Roxb. Ex Willd). *African J. Biotechnol*. 2011, 10 (83) https://doi.org/10.5897/ajb11.2377
47. *Zhang H.-X., Zeevaart J. A. D.* An efficient *Agrobacterium tumefaciens*-mediated transformation and regeneration system for cotyledons of spinach (*Spinacia oleracea* L.). *Plant Cell Rep*. 1999, 18 (7–8), 640–645. https://doi.org/10.1007/s002990050635
48. *Yaacob J. S., Hwei L. C., Taha R. M.* Pigment analysis and tissue culture of *Amaranthus cruentus* L. *Acta horticulturae*. 2012, P. 54–64.

ТРАНЗІЄНТНА ЕКСПРЕСІЯ РЕПОРТЕРНИХ ГЕНІВ У СОРТАХ *Amaranthus caudatus* L.

О. М. Ярошко
М. В. Кучук

Інститут клітинної біології
та генетичної інженерії НАН України, Київ

E-mail: 90tigeryaroshko90@gmail.com

Як рослинний матеріал для дослідів використовували місцеві сорти *A. caudatus*: Геліос і Кармін. Амарант — нова сільськогосподарська культура для України. Рослинну біомасу, отриману з амаранту використовуть у медицині, харчовій промисловості та косметології.

Мета роботи — знайти оптимальні умови для транзієнтної експресії репортерних генів у сортах *Amaranthus caudatus*.

Методи. У роботі застосовували біохімічний та мікроскопічний методи. Проростки і дорослі рослини різного віку інфільтрували суспензіями агробактерій окремо (генетичний вектор pCBV19 з геном *uidA* і генетичний вектор pNMD2501 з геном *gfp* у штамі GV3101 *Agrobacterium tumefaciens*).

Результати. Після проведення серії експериментів досягнуто тимчасовох експресії гена *uidA* та *gfp* у рослинах амаранту. Найбільш інтенсивна транзієнтна експресія генів *gfp* і *uidA* спостерігали у проростків, інфільтрованих у віці 1 дня. Максимум флуоресценції протеїну GFP спостерігали на 5–6 добу.

Висновки. Показано, що сорт Геліос більш сприйнятливий до агробактеріальної інфекції, ніж сорт Кармін. Ефективність агробактеріальної трансформації становила від 16% до 95% для сорту Геліос і від 12% до 93% для сорту Кармін. Отримані результати свідчать про те, що досліджувані сорти амаранту, які досліджувалися, потенційно можуть бути використані для отримання в майбутньому транзієнтної експресії цільових генів та синтезу цільових протеїнів в їхніх тканинах.

Ключові слова: *Amaranthus; uidA; gfp; Agrobacterium*; транзієнтна експресія.

ТРАНЗИЕНТНАЯ ЭКСПРЕССИЯ РЕПОРТЕРНЫХ ГЕНОВ В СОРТАХ *Amaranthus caudatus* L.

О. Н. Ярошко
Н. В. Кучук

Иститут клеточной биологии
и генетической инженерии НАН Украины,
Киев

E-mail: *90tigeryaroshko90@gmail.com*

В качестве растительного материала для исследований использовались местные сорта *A. caudatus*: Гелиос и Кармин. Амарант — новая сельскохозяйственная культура для Украины. Растительная биомасса, полученная из амаранта, используется в медицине, пищевой промышленности и косметологии.

Цель работы — найти оптимальные условия для транзиентной экспрессии репортерных генов в сортах *Amaranthus caudatus*.

Методы. В работе были использованы биохимический и микроскопический методы. Проростки и взрослые растения разного возраста инфильтрировали суспензиями агробактерий (генетический вектор pCBV19 с геном *uidA* и генетический вектор pNMD2501 с геном *gfp* в штамме *Agrobacterium tumefaciens* GV3101).

Результаты. После проведения серии экспериментов была достигнута транзиентная экспрессия генов *uidA* и *gfp* в растениях амаранта. Наиболее интенсивную транзиентную экспрессию генов *gfp* и *uidA* наблюдали у проростков, инфильтрованных в возрасте 1 дня. Максимум флуоресценции потеина GFP наблюдали на 5–6 сутки.

Выводы. Было показано, что сорт Гелиос более восприимчив к агробактериальной инфекции, чем сорт Кармин. Эффективность агробактериальной трансформации составила от 16% до 95% для сорта Гелиос и от 12% до 93% для сорта Кармин. Полученные результаты свидетельствуют о том, что изучаемые сорта амаранта потенциально могут быть использованы для получения в будущем транзиентной экспрессии целевых генов и синтеза целевых протеинов в их тканях.

Ключевые слова: *Amaranthus; uidA; gfp; Agrobacterium;* транзиентная экспрессия.

UDC 616.13. 002+541.183 https://doi.org/10.15407.biotech14.04.064

ON THE POSSIBILITY OF USING CARBON ENTEROSORBENTS TO NORMALIZE CHOLESTEROL METABOLISM

N. V. Sych
L. I. Kotyns'ka
V. M. Vikarchuk
I. A. Farbun

Institute for Sorption and Endoecology Problems
of the National Academy of Sciences of Ukraine, Kyiv

E-mail: nataliya_sych@ukr.net

Received 19.06.2021
Revised 09.08.2021
Accepted 31.08.2021

The creation of effective drugs for the prevention and treatment of atherosclerosis is one of the urgent interdisciplinary tasks for modern chemistry and pharmacology. Given the role of hypercholesterolemia in the development of this disease, it is necessary to remove excess amounts of cholesterol from the body. As an alternative to means of lowering total cholesterol and low-density lipoprotein (LDL) cholesterol, the possibility of using carbon enterosorbents for efferent therapy is considered.

Aim. The purpose of the study was to evaluate the sorption capacity of the adsorbents developed by the authors in terms of the possibility of cholesterol adsorption.

Methods. Using the spectrophotometric method, the sorption of cholesterol on samples of adsorbents obtained by chemical activation of waste from the processing of lignocellulosic raw materials — dogwood and coffee residue has been studied.

Results. A comparison of sorption isotherms with the isotherm obtained on the industrial adsorbent SORBEX has been performed. It was shown that the adsorption capacity of carbon adsorbents is primarily determined by their porous structure. The highest sorption values (7.3 mg/g) have been revealed by the sorption material obtained by chemical activation of cornel seed, an intermediate position (6.3 mg/g) is occupied by the adsorbent obtained from the coffee residue. Industrial carbon SORBEX has the lowest sorption values (5.3 mg/g).

Conclusions. Calculations by Langmuir's and Freundlich's models testify about the accordance of the experimental data to Langmuir's model. The use of the obtained activated carbons may be one of the effective alternative ways to lower blood cholesterol.

Key words: cholesterol; atherosclerosis; low-density lipoprotein (LDL); enterosorbents; metabolism.

An increased concentration of cholesterol in the blood (i.e., hypercholesterolemia) is widely recognized as a risk factor for coronary artery disease. Cholesterol-LDL — one of the classes of lipoproteins, particles circulating in the blood, transporting cholesterol from the liver to other organs and tissues, a risk factor for the development of atherosclerosis and coronary heart disease — "bad cholesterol". This fraction of cholesterol refers to the so-called "bad cholesterol" because it contains a large amount of cholesterol. Deposited in the vessels, in the form of plaques, cholesterol, together with other metabolites, can lead to the development of atherosclerosis and the progression of coronary heart disease. Reducing plasma levels of total and low-density lipoprotein (LDL) cholesterol by diet, drugs or lifestyle modification is thus of principal importance in treating and preventing cardiovascular disease. In humans, blood cholesterol is derived from two sources. It is either absorbed from food by the intestine, or it is synthesized from precursor molecules in the liver [1].

Hepatic cholesterol synthesis can be pharmacologically regulated with statins by inhibiting 3-hydroxy-3-methylglutaryl-CoA reductase, the enzyme responsible for cholesterol synthesis. Statins are very potent lipid-lowering agents and they may significantly reduce significantly reduce coronary morbidity and mortality [2].

However many patients do not reach currently defined treatment goals and there is considerable interest in finding additional ways to reduce plasma and LDL cholesterol levels. This has led to the development of a new family of drugs that inhibits intestinal cholesterol absorption [3, 4]. Ezetimibe is a 2-azetidinone compound that reduces cholesterol absorption by inhibiting the protein responsible for cholesterol transport into enterocytes. As monotherapy, ezetimibe decreases LDL-C levels by 15–20 percent [2]; in combination with statins it reduces LDL-C by an additional 20–25% [3]. Increasing use of these therapeutic agents has refocussed interest on enterosorbents that have the potential to reduce intestinal cholesterol absorption. For this purpose, sorbents based on cellulose granules and modified cellulose [5, 6], alumina obtained by the sol-gel method [7], polyacrylate [8], a mixture of activated carbon and microcellulose [9], lignocellulose based activated carbons [10–13], are used for selective adsorption of LDL in order to prevent atherosclerosis. However, the elaboration of enterosorbents with high capacity for cholesterol is still topical. The oral intake of activated carbon may be helpful in therapy of atherosclerosis and diseases associated with an increased level of cholesterol and lipids.

The objective of the study was to evaluate the sorption capacity of the agricultural waste-based enterosorbents developed by the authors in terms of the possibility of cholesterol elimination.

Materials and Methods

Cholesterol was purchased from Sigma Chemical Co. (USA). Procaine hydrochloride solution was purchased from AO "Chemfarm" (Kazakhstan). Sodium nitrite was purchased from Co. "Stirol" (Ukraine). Hydrochloric acid ch. p. was purchased from Co. "Chemlaborreactive" (Ukraine).

Samples of adsorbents were prepared by chemical activation of waste from the processing of lignocellulosic raw materials — dogwood and coffee residue.

Spectrophotometric measurement of cholesterol for the purpose of sorption from alcoholic solution was determined according to the methodology of guidance [14].

Cholesterol solution was prepared by dissolving 0.05 g in ethanol and the volume was made up in 500 mL volumetric flask. Solutions of further dilute concentrations were prepared from this working standard solution.

Precisely weight of 0.0818 g of procaine hydrochloride was dissolved with less amount of distilled water, then 3 mL of $NaNO_2$ 0.1 M and 3 mL of HCl 1 M were added to the beaker. The solution was allowed to stand for 5 min at 5–10 °C, the solution was transferred into 50 mL volumetric flask and the volume was made up to mark with distilled water where temperature at 5–10 °C was kept.

1 mL of cholesterol solution (100 μg/mL) was added into 10 mL volumetric flask. 2 mL of the diazotized procaine hydrochloride solution and 2 mL of 2M NaOH were added to the volumetric flask. The solution was mixed thoroughly, the volume was made up to mark with distilled water and the solution allowed to stand for 5 min. Adsorbance of a colored product is proposed to measure at 428 nm in case of cholesterol against reagent blank.

Spectrophotometric measurements were carried out using the ultraviolet spectrophotometer Shimadzu UV-2500 with 1.00 cm glass cells.

Results and Discussions

Table 1 includes the characteristics of agro-based adsorbents, obtained with H_3PO_4 activation of dogwood stone (DS-AC) and coffee residue (CR-AC), and, for comparison, commercial sorbent SORBEX. It is seen that a rather high content of mesopores is typical for the considered sorbents.

In [14], the wavelength for measuring cholesterol was chosen mistakenly (for our opinion). To determine the optical density of the colored product, a blurred region of the spectrum (not having a peak) in the range of 360–430 nm was chosen.

In present work the solution was mixed thoroughly, the volume was made up to mark with distilled water and the solution allowed to stand for 24 hours to acquire permanent coloration. The wavelength of 318 nm has been chosen to determine cholesterol in a colored product. Obtained adsorption spectra of cholesterol are presented in Fig. 1. As it seen, the spectra are arranged in proportion to the concentration of the prepared solutions, the adsorption maxima are close, and the spectral shapes are similar. The adsorption maximum corresponds to the wavelength 318 nm.

The calibration curve obtained at different concentrations of cholesterol is presented in Fig. 2. It may be seen that solutions with different cholesterol content fit well along this straight line.

Table 1. **Characteristics of agro-based sorbents, obtained with H_3PO_4 activation of dogwood stone and coffee residue, and commercial sorbent SORBEX**

Characteristics	DS-AC	CR-AC	SORBEX
Granulometric composition, mm	0.5–1.0	0.25–1.0	0.25
Ash content,%	4.6	6	3.7
Yield,%	46	48	–
Bulk density, g/cm^3	0.35	0.36	0.40
S_{BET} specific surface area, m^2/g	2 169	1 480	1 228
S_{me} specific surface area, m^2/g	573	431	84
Total pore volum, VΣ, cm^3/g	1.0	0.84	0.58
Mesopore volume, V_{me} cm^3/g	0.67	0.32	0.12
Average pore radius, Å	10.6	9.8	9.5
MB sorption capacity	145	120	72

Note: DS-AC — dogwood stone activated carbon; CR-AC — coffee residue activated carbon; SORBEX — commercial activated carbon.

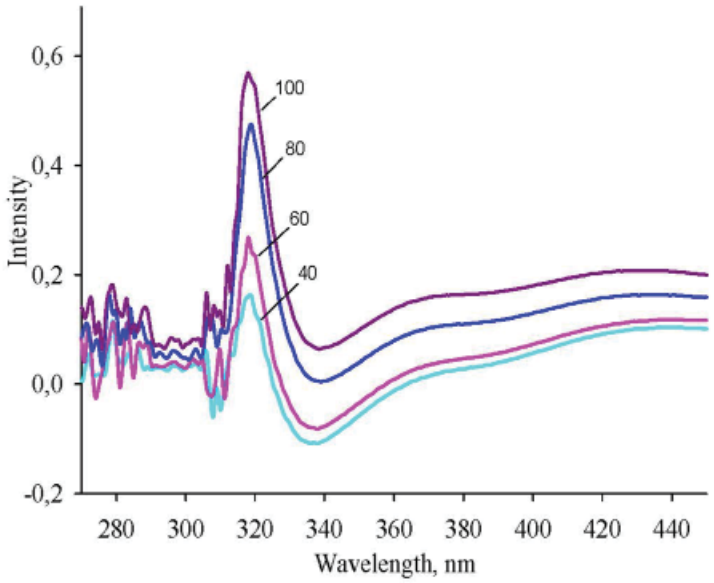

Fig. 1. **Adsorption spectra of cholesterol at different concentrations (mg/L)**

Photometric methods for determining cholesterol are based almost exclusively on the use of chemical reactions. Among the classical colorimetric methods, the Lieberman-Burkhard method is of the greatest importance, which is based on the measurement of the intensity of the greenish-blue color, which appears as a result of the treatment of cholesterol with a mixture of rather aggressive reagents — sulfuric acid and acetic anhydride. Toxic reagents such as acetic acid and chloroform are also used as solvents. In addition, the rate of color of the complex and its stability are strongly dependent on temperature, which significantly complicates the determination procedure. That is why, in this work, the method, described in [14], was chosen for the spectrophotometric determination of cholesterol on the obtained samples.

The corresponding adsorption isotherms are shown in Fig. 3. The best sorption ability is possessed by a sample of dogwood stone activated carbon (the maximum value

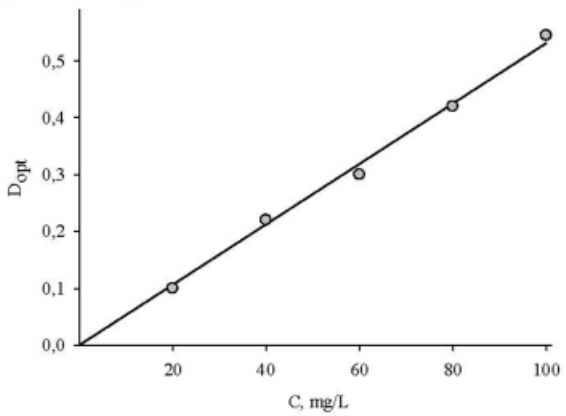

Fig. 2. **Calibration curve obtained at different concentrations of cholesterol**

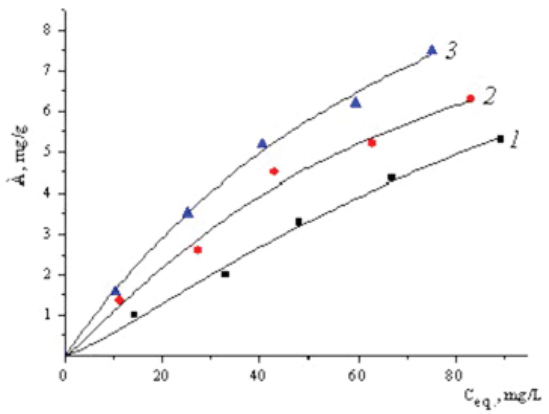

Fig. 3. **Cholesterol sorption isotherms by samples:** *1* — SORBEX; *2* — CR-AC; *3* — DS-AC

Table 2. **The parameters of the Langmuir and Freundlich isotherms calculated for isotherms of cholesterol sorption**

Samples	Langmuir isotherms			Freundlich isotherms		
	A_{∞}, mg/g	K_L, L/mg	r^2	K_F, mg/g	n	r^2
DS-AC	7.08	60.67	0.978	38.59	2.23	0.984
CR-AC	7.34	79.30	0.997	35.64	1.96	0.967
SORBEX	8.48	63.22	0.956	37.5	2.08	0.957

reaches 7.5 mg/g). An intermediate position is occupied by a sample of coffee residue activated carbon (the maximum value reaches 6.3 mg/g). SORBEX possesses the weakest adsorbing characteristics (the maximum value reaches 5.3 mg/g). It may be stated that the adsorption of cholesterol increases according to the growth of the specific surface area of mesopores.

With the help of the obtained isotherms, the parameters of the adsorption processes have been analyzed. Isotherms of adsorption were calculated by Langmuir and Freundlich equations:

$$a = a_0 \frac{KC_{eq}}{1 + KC_{eq}}, \quad (1)$$

where C_{eq} is equal concentration, mg/l; a_o — value of maximum adsorption, mg/g; K is a constant;

$$A_F = K_F \cdot C^{1/n}, \quad (2)$$

where A_F — adsorption value, mg/g; n — exponent index.

Table 2 shows the values of the maximum adsorption, Langmuir and Freundlich constants, as well as coefficients of correlation.

The characteristics of the correlation are quite high for all prepared samples that testified about the accordance of experimental data to Langmuir's model. It can be seen that the value of the maximum adsorption calculated using this equation also agrees well with the experimental data. Based on this, it is possible to make a guess about the potential mechanism of adsorption of cholesterol: adsorption is not carried on surfaces of the adsorbent, but on active centers, which are characterized by so-called free valency. Every active center is designed for interaction only with one molecule of the adsorbate; as a result, only one layer of adsorbed molecules may be installed on the surface. The process of adsorption is reversible and equally important — the adsorbed molecule is absorbed by the active center for a while, when it is desorbed; in this way, over time, a dynamic equilibrium will arise between the processes of adsorption and desorption.

Conclusions

A new method of spectrophotometric measurement of cholesterol in solutions has been mastered and improved. Using the spectrophotometric method, the isotherms of cholesterol adsorption on samples of adsorbents obtained by chemical activation of waste from the processing of lignocellulosic

raw materials — dogwood and coffee residue have been studied. It was proved the advantages of chosen methodology of determining cholesterol.

It was established that cholesterol adsorbtion grows proportionally to the mesopore specific surface area of enterosorbents.

Calculations by Langmuir's and Freundlich's models testify about the accordance of the experimental data to Langmuir's model. The value of the maximum adsorption, calculated with the help of this equation, fit well with experimental data.

With great probability it is possible to survive, that application of the obtained active carbons may be one of the effective alternative ways of lowering the level of cholesterol in blood and other biological solutions.

Funding. This research was conducted as a part of a fundamental topic of the Institute for Sorption and Endoecology Problems of the National Academy of Sciences of Ukraine 35NT "Modified synthetic carbons and pyrolyzed polymeric materials as a basis for the creation of medical sorbents of new generation and protonic catalysts of biomaterials processing" (State Registration 0115U002069, 2015–2019. Supervisor — prof. V.V. Strelko).

The authors declare that they have no conflict of interest.

REFERENCES

1. *Brugts J. J., Yetgin T., Hoeks S. E., Gotto A. M., Shepherd J., Westendorp R. G., de Craen A. J., Knopp R. H., Nakamura H., Ridker, P., van Domburg R., Deckers J. W.* The benefits of statins in people without established cardiovascular disease but with cardiovascular risk factors: metaanalysis of randomised controlled trials. *BMJ.* 2009, V. 338, P. b2376.
2. *Pandor A., Ara R. M., Tumur I., Wilkinson A. J., Paisley S., Duenas A., Durrington P. N., Chilcott J.* Ezetimibe monotherapy for cholesterol lowering in 2,722 people: systematic review and meta-analysis of randomized controlled trials. *J. Intern. Med.* 2009, V. 265, P. 568–580.
3. *Mikhailidis D. P., Sibbring G. C., Ballantyne C. M., Davies G. M., Catapano A. L.* Meta-analysis of the cholesterol-lowering effect of ezetimibe added to ongoing statin therapy. *Curr. Med. Res. Opin.* 2007, V. 23, P. 2009–2026.
4. *Jeffrey S. Cohn, Alvin Kamili, Elaine Wat, Rosanna W. S.* Chung and Sally Tandy Phospholipids and Intestinal Cholesterol Absorption. *Nutrients.* 2010, V. 2, P. 116–127. https://doi.org/10.3390/nu2020116
5. *Yu H., Fu G., Zhao J., Liu L., He B.* Synthesis and in vitro sorption properties of PAA-grafted cellulose beads for selective binding of LDL. *Artif Cells Blood Substit Immobil. Biotechnol.* 2006, 34 (5), 501–513. https://doi.org/10.1080/10731190600862795. PMID: 16893813
6. *Wang S., Guo X., Wang L., Wang W., Yu Y.* Effect of PEG spacer on cellulose adsorbent for the removal of low density lipoprotein-cholesterol. *Artif Cells Blood Substit Immobil. Biotechnol.* 2006, 34 (1), 99–110. PMID: 16519407
7. *Asano T., Tsuru K., Hayakawa S., Osaka A.* Low density lipoprotein adsorption on sol-gel derived alumina for blood purification therapy. *Biomed. Mater. Eng.* 2008, 18 (3), 161–170. PMID: 18725696
8. *Claus-Chr.* Heuck Polyacrylate adsorbents for the selective adsorption of cholesterol-rich lipoproteins from plasma or blood. *Ger. Med. Sci.* 2011, V. 9, Doc02. https://doi.org/10.3205/000125
9. *Lysenkova A. V., Filippova V. A., Prischepova L. V., Odintsova M. V.* Theoretical bases of adsorption therapy of atherosclerosis. *Problemy zdorovya i ecologii.* 2010, N 1, 101–104. (In Russian).
10. *Devi S., Singh R.* Antioxidant and antihypercholesterolemic potential of Vitis vinifera leaves. *Pharmacol. J.* 2017, 9 (4), 565–572. https://doi.org/10.5530/pj.2017.4.90
11. *Gunawan Pasaribu, Totok K. Waluyo, Gustan Pari, Novitri Hastuti.* The effectiveness of glucomannan and nano activated-carbon as hypercholesterollowering agents. *Indonesian J. Forestry Res.* 2020, 7 (2), 155–164.
12. *Liu Z., Tabakman S., Welsher K.* Carbon nanotubes in biology and medicine: in vitro and in vivo detection, imaging and drug delivery. *Nano Res.* 2010, 2 (2), 85–120. https://doi.org/10.1007/s12274-009-9009-8
13. *Shao W., Arghya P., Yiyong M., Rodes L., Prakash S.* Carbon nanotubes for use in medicine: Potentials and limitations. *Syntheses and Applications of Carbon Nanotubes and Their Composites.* 2013. https://doi.org/10.5772/51785
14. *Mashkour M. S., Alhassan-Almatori N. A., Brbber A. M.* Spectrophotometric determination of Cholesterol by using procaine as coupling reagent. *Int. J. ChemTech. Res.* 2017, 10 (2), 630–640.

ПРО МОЖЛИВОСТЬ ВИКОРИСТАННЯ ВУГЛЕЦЕВИХ ЕНТЕРОСОРБЕНТІВ ДЛЯ НОРМАЛІЗАЦІЇ ХОЛЕСТЕРОЛОВОГО МЕТАБОЛІЗМУ

Н. В. Сич
Л. Й. Котинська
В. М. Вікарчук
І.А. Фарбун

Інститут сорбції та проблем ендоекології
НАН України, Київ

E-mail: nataliya_sych@ukr.net

Створення ефективних препаратів для профілактики та лікування атеросклерозу є одним із актуальних міждисциплінарних завдань сучасної хімії та фармакології. З огляду на роль гіперхолестеринемії у розвиткові цієї хвороби необхідно виводити надлишки холестеролу з організму. Як альтернативу засобам зниження загального холестеролу та холестеролу ліпопротеїдів низької щільності (ЛПНЩ) розглядається можливість використання ентеросорбентів для еферентної терапії.

Метою дослідження було оцінити сорбційну здатність адсорбентів, розроблених авторами, з погляду можливості адсорбції холестеролу.

Методи. За допомогою спектрофотометричного методу досліджено сорбцію холестеролу на зразках адсорбентів, отриманих хімічною активацією відходів під час перероблення лігноцелюлозної сировини — кизилової кісточки та залишків кави.

Результати. Проведено порівняння ізотерм сорбції з ізотермою, отриманою на промисловому адсорбенті SORBEX. Показано, що поглинальна здатність вуглецевих адсорбентів визначається насамперед їхньою пористою структурою. Найвищі значення сорбції (7,3 мг/г) виявляє сорбційний матеріал, одержаний за допомогою хімічної активації кісточок кизилу, проміжне положення (6,3 мг/г) займає адсорбент, отриманий із кавових залишків. Промисловий вуглець SORBEX має найнижчі показники сорбції (5,3 мг/г).

Висновки. Розрахунки за моделями Ленгмюра та Фрейндліха свідчать про те, що експериментальні дані найбільш відповідають моделі Ленгмюра. Використання одержаного активованого вугілля може бути одним із ефективних альтернативних способів зниження холестеролу в крові.

Ключові слова: холестерол; атеросклероз; ліпопротеїди низької щільності (ЛПНЩ); ентеросорбенти; метаболізм.

О ВОЗМОЖНОСТИ ИСПОЛЬЗОВАНИЯ УГЛЕРОДНЫХ ЭНТЕРОСОРБЕНТОВ ДЛЯ НОРМАЛИЗАЦИИ ХОЛЕСТЕРОЛОВОГО МЕТАБОЛИЗМА

Н. В. Сыч
Л. И. Котинская
В. М. Викарчук
И. А. Фарбун

Институт сорбции и проблем эндоэкологии
НАН Украины, Киев

E-mail: nataliya_sych@ukr.net

Создание эффективных препаратов для профилактики и лечения атеросклероза является одной из актуальных междисциплинарных задач современной химии и фармакологии. Учитывая роль гиперхолестеринемии в развитии этой болезни, необходимо выводить излишки холестерола из организма. В качестве альтернативы средствам снижения общего холестерола и холестерола липопротеидов низкой плотности (ЛПНП) рассматривается возможность использования энтеросорбентов для эфферентной терапии.

Цель. Оценка сорбционной способности адсорбентов, разработанных авторами, с точки зрения возможности адсорбции холестерола.

Методы. С помощью спектрофотометрического метода исследованы сорбция холестерола на образцах адсорбентов, полученных химической активацией отходов при переработке лигноцеллюлозного сырья – кизиловой косточки и остатков кофе.

Результаты. Проведено сравнение изотерм сорбции с изотермой, полученной на промышленном адсорбенте SORBEX. Показано, что поглощающая способность углеродных адсорбентов определяется, прежде всего, их пористой структурой. Высокие значения сорбции (7,3 мг/г) обнаруживает сорбционный материал, полученный с помощью химической активации косточек кизила, промежуточное положение (6,3 мг/г) занимает адсорбент из кофейных остатков. Промышленный углерод SORBEX имеет самые низкие показатели сорбции (5,3 мг/г).

Выводы. Расчеты по моделям Ленгмюра и Фрейндлиха свидетельствуют о том, что экспериментальные данные наиболее соответствуют модели Ленгмюра. Использование полученного активированного угля может быть одним из эффективных альтернативных способов снижения холестерола в крови.

Ключевые слова: холестерол; атеросклероз; липопротеиды низкой плотности (ЛПНП); энтеросорбенты; метаболизм.

UDC 579.695 https://doi.org/10.15407.biotech14.04.070

TWO-STAGE DEGRADATION OF SOLID ORGANIC WASTE AND LIQUID FILTRATE

V. M. Hovorukha
O. A. Havryliuk
I. O. Bida
Ya. P. Danko
O. V. Shabliy
G. V. Gladka
L. S. Yastremska
O. B. Tashyrev

Zabolotny Institute of Microbiology and Virology
of the National Academy of Sciences of Ukraine, Kyiv

E-mail: vira-govorukha@ukr.net

Received 23.06.2021
Revised 29.07.2021
Accepted 31.08.2021

The accumulation of solid and liquid organic waste requires their treatment to develop energy biotechnologies and prevent environment pollution.

Aim. The goal of the work was to study the efficiency of the purification of the filtrate from dissolved organic compounds by aerobic oxidation and methane fermentation.

Methods. The standard methods were used to determine pH and redox potential (Eh), the gas composition, the content of short-chain fatty acids, the concentration of dissolved organic compounds counting to the total carbon. The efficiency of two types of microbial metabolism for the degradation of soluble organic compounds of filtrate was compared.

Results. The aerobic oxidation was established to provide 1.9 times more efficient removal of dissolved organic compounds, compared with the anaerobic methane fermentation. However, it provided CH_4 yield 1 L/dm^3 of filtrate (carbon concentration — 1071 mg/L). The necessity to optimize the methods for purifying filtrate to increase the efficiency of the process was determined.

Conclusions. The obtained results will be the basis to develop complex biotechnology providing not only the production of environmentally friendly energy H_2 via the fermentation of solid food waste, but also the purification of filtrate to solve the ecological and energy (CH_4 production) problem of society.

Key words: solid organic waste; soluble organic compounds; environmental biotechnologies; hydrogen; methane; fermentation; aerobic oxidation.

The development of food industries, intensification of agriculture and increasing yields are an indisputable positive aspect of the development of society and the improvement of life quality. However, the intensification of production and the processing of thousands of tons of organic products daily causes an increase in the amount of waste. The problem of degradation of both solid and liquid organic waste is urgent for most countries. Thus, up to 100 million tons is annually accumulated in European countries, and up to 600 million tons is reached in Asian countries [1–5]. They include a wide range of components: food waste, vegetables, fruits, meat, dairy, household, bakery products, agricultural waste (feed residues, crop waste, etc.), restaurant and culinary food residues, etc. [6, 7]. Irrational processing of raw materials and improper use of finished products causes the accumulation of surpluses that pose a threat to the environment and require proper disposal [6, 8, 9].

The accumulation of waste in landfills leads to uncontrolled decay, release of toxic gases and concentrated liquid filtrate polluting the environment [5, 10, 11]. Landfill filtrate is a concentrate of toxic products of microbial metabolism (fatty acids and alcohols), which inhibits plant growth, reduces soil fertility and is toxic to animals and humans [7, 8]. Liquid waste from food and canneries, livestock waste, alcohol bard, etc. are another examples

of dangerous for the environment waste. The volume of such waste is also constantly growing. For example, more than $5.5 \cdot 10^7$ m^3 of wastewater is generated annually in South Korea [12, 13].

Organic waste can be an alternative constantly renewable source for valuable products: molecular hydrogen, methane and purified water. Raw materials for hydrogen production can be food and culinary waste, vegetable residues, agricultural and industrial organic waste, rich in nutrients suitable for the growth of hydrogen-synthesizing bacteria [14]. High efficiency of hydrogen production is achieved by optimization of the process of fermentation of solid organic waste by a community of hydrogen-synthesizing microorganisms. H_2 yield depends on pH, temperature, fermentation time, mass transfer, concentration of organic compounds and microbiome used [3].

To increase the efficiency and profitability of the process, the filtrate formed as a result of fermentation of solid organic waste requires additional purification from dissolved organic compounds. Proper treatment of such waste is a serious environmental problem [6]. Existing physical and chemical methods of filtration, sorption, concentration, etc. are expensive, complex and do not provide effective purification [15, 16].

The liquid filtrate contains easily degradable organic compounds (fatty acids and alcohols), which is a promising substrate for oxidation by microorganisms of a wide range of physiological and taxonomic groups [5, 17].

Accelerated oxidation by aerobic microorganisms to obtain CO_2 and H_2O is the most promising among the biological methods of degradation of dissolved organic compounds [18–20]. Methane fermentation is an alternative to it. Fermentation provides not only the degradation of organic compounds, but also the synthesis of additional energy (CH_4) [18, 21].

To develop an optimal approach to solve the problem of purification of the filtrate, it is necessary to evaluate the efficiency of the aerobic and anaerobic methods, as well as to optimize the process to achieve maximum efficiency.

Therefore, the goal of the work was to study the efficiency of the purification of the filtrate from dissolved organic compounds by aerobic oxidation and methane fermentation.

Materials and Methods

For the purification of the filtrate formed after the fermentation of multicomponent food waste, modular installation with a volume of 40 L (linear dimensions 0.3×0.45×0.3 m) was used (Fig. 1).

The installation is made of plexiglass providing continuous visual inspection of the process dynamics. The installation is divided by two perforated plates (*1*) into three sections. On the one hand, they allowed separating the stages of purification, and, on the other hand, they did not interfere with mass transfer in the installation. Fittings for the sampling of the culture fluid (*2*) and the gas phase (*3*) are installed in the walls of the installation.

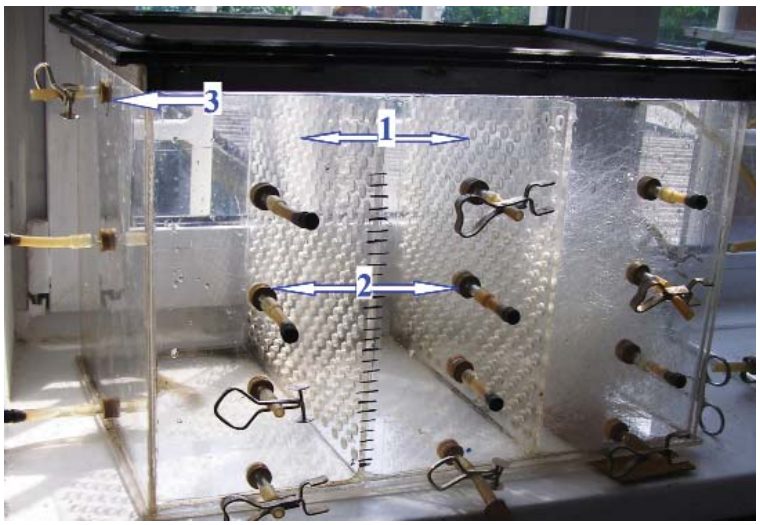

Fig. 1. **The modular plexiglass installation for purification of filtrate:**
1 — perforated plates for division of installation into sections; *2* — fittings for sampling of filtrate; *3* — fittings for sampling of the gas phase

To establish the efficiency of the filtrate purification, two pathways of degradation of dissolved organic compounds were investigated. In the first case, aerobic oxidation was performed. For this purpose, 10 L of the filtrate were added to the installation. The aerators were installed at the bottom of the installation to bubble air over the entire volume of the liquid. The lid was sealed, and air removal was carried out through a water seal. Hoses from the fittings were immersed into the water seal to prevent the spread of bacterial suspension.

In the second case, the anaerobic fermentation of the filtrate by a methanogenic microbial community of the fermented sludge (FS) of methane tank was used. For this, 30 L of the filtrate were added to the installation and 0.5 L of FS was added to the bottom. The installation was sealed and connected to the gasholder.

The dynamics of the process was monitored by changes in pH and redox potential (Eh), the content of dissolved organic compounds in the culture fluid counted on the concentration of total Carbon. The main criterion for completion of the process was the reduction of Carbon concentration, which indicated the purification of the filtrate from dissolved organic compounds. In addition, changes in the composition of the gas phase (CH_4 and CO_2) and the intensity of gas synthesis were evaluated in the anaerobic installation.

The pH and Eh were evaluated by the universal ionometer EZODO MP-103 with remote electrodes (models PY41 and PO50, respectively).

The volume of gas synthesized during the purification of filtrate from soluble organic compounds in the anaerobic installation was determined by the volume of water displaced under the gas pressure from the gasholder to the water seal. The gasholder was refilled with water after each measurement to avoid errors in calculating the composition of the gas phase.

The composition of the gas was analyzed according to the standard method on the gas chromatograph LHM-8-MD [22]. The sterile plastic syringes were used to sample the appropriate volume of gas. The gas composition was calculated by the square of the peaks of its components.

The chromatograph is equipped with two steel columns. The first one (I) in necessary for the analysis of H_2, O_2, N_2 and CH_4. The second column (II) is required for the analysis of CO_2. Column parameters are as follows. First column: l = 3 m, d = 3 mm, with molecular sieve 13X (NaX). Second column: l = 2 m, d = 3 mm, with Porapak-Q carrier. The column temperature is +60 °C. The evaporator temperature is +75 °C. The detector temperature (catharometer) is +60 °C. The detector current is 50 mA. Argon is used as a carrier gas. The gas flow rate is 30 cm^3/min.

The concentration of dissolved organic compounds counting to the total Carbon was determined using the permanganate method [23]. For this, a 5 mL sample of culture fluid was centrifuged in an OPn-8 centrifuge at 3 000 g for 15 min. The supernatant (1 mL) and 0.1 mL of 10% sulfuric acid (H_2SO_4) were added into a chemically pure test tube. The mixture was heated on a boiling water bath. Then 0.05 mL of 0.1% solution of $KMnO_4$ was added. The solution was titrated until a light purple color specific for the permanganate ion appeared. The concentration of Carbon in the sample correlates with the amount of oxidant $KMnO_4$ required for complete oxidation of dissolved organic compounds in the sample. The total content of dissolved organic compounds (mg/L) was calculated after determining the volume of the solution $KMnO_4$ spent for the titration of the test solution, according to the formula:

$$[C] = 0{,}11 \times V_{KMnO_4}\,(\mu L) - 12.168.$$

The content of short-chain fatty acids in the filtrate was determined by gas chromatomass spectrometry on the device Agilent 6890N/5973inert (Agilent Technologies, USA), capillary column DP-FFAP (30 m×0.25 mm×0.25 μm), (J&W Scientific, USA). The separation was performed with a temperature gradient of 10 °C/min from 60 °C to 230 °C. The flow rate through the column is 1 mL/min. The identification of the compounds of individual substances was performed using libraries of mass spectra NIST02 and standard solutions of short-chain fatty acids.

For the analysis, 5 mL of filtrate was sampled. Aliquots of samples were added to 1.5 mL Eppendorf microtubes and frozen at −20 °C. The batch of samples was given for analysis to Kharhota M. A. to the Laboratory of Biological Polymer Compounds of the Zabolotny Institute of Microbiology and Virology of the National Academy of Sciences of Ukraine.

The efficiency of the filtrate purification was evaluated by the duration of the process, the efficiency of degradation of soluble organic compounds, as well as the efficiency of methane synthesis by anaerobic purification.

The experiments were carried out in triplicate. Statistical analysis was conducted via

Excel and Origin 8.5.1 software determining the standard deviation of the data.

Results and Discussion

The study of the efficiency of molecular hydrogen obtaining by the fermentation of organic compounds has been attracting the attention of scientists and representatives of the industrial sector for several decades. The prospects and benefits of this area are in the opportunity to combine energy and environmental biotechnology increasing the efficiency and the profitability of the process [6, 24, 25]. To achieve the maximum yield of H_2, it is necessary to optimize the key fermentation parameters such as pH and Eh of the culture fluid, conditions of mass transfer, the ratio of solid and liquid phases, etc. Thus, the series of experiments resulted in the shortening of the fermentation duration (*T*) to 2–5 days. The yield of molecular hydrogen (VH_2) reached 50–100 L/kg of waste in terms of total solids (TS). The efficiency of waste destruction (*Kd*), i.e. the multiplicity of reduction of their weight, reached 85–95 [26–28].

The results of dark hydrogen fermentation of solid organic waste were promising. However, obtained fermentation filtrate required further purification. The filtrate formed after fermentation contained the following fatty acids: hexanoic (caproic), 3-methylbutanoic (isovaleric), butanoic (butyric), propane (propionic) and acetic. The concentration of dissolved organic compounds reached 1 071 mg/L. In high concentrations, they are toxic to the microbiome of soils, water reservoirs, and lead to the disruption of ecosystems [27, 29–32].

Therefore, the application of an effective method for the degradation of dissolved organic compounds is necessary to develop environmentally friendly biotechnology for hydrogen synthesis and waste degradation. In addition, the purified filtrate is suitable for the reuse for solid food waste fermentation, avoiding the need for new portions of water and increasing the profitability of the process.

To study the dynamics of the aerobic oxidation of organic compounds, 10 L of the filtrate after fermentation of solid food waste were loaded into the plexiglass installation. The initial parameters of the filtrate were as follows: Eh = +80 mV; pH = 6.32; carbon concentration [C] = 1 071 mg/L. To provide the continuous aeration, bubblers were installed at the bottom of the installation. Under such conditions, the filtrate microbiome oxidized organic compounds, providing purification of the culture fluid.

The dynamics of oxidation of organic compounds without regulation was performed. As a result, the concentration of total Carbon 19-fold decreased from 1071 to 56 mg/L (Fig. 2).

The following patterns were established

There was a decrease in pH values from 6.32 to 5.74 at the initial stages of oxidation (during the first 4 days). It could take place due to the hydrolysis of unfermented small solid particles of waste that may have been untreated. As

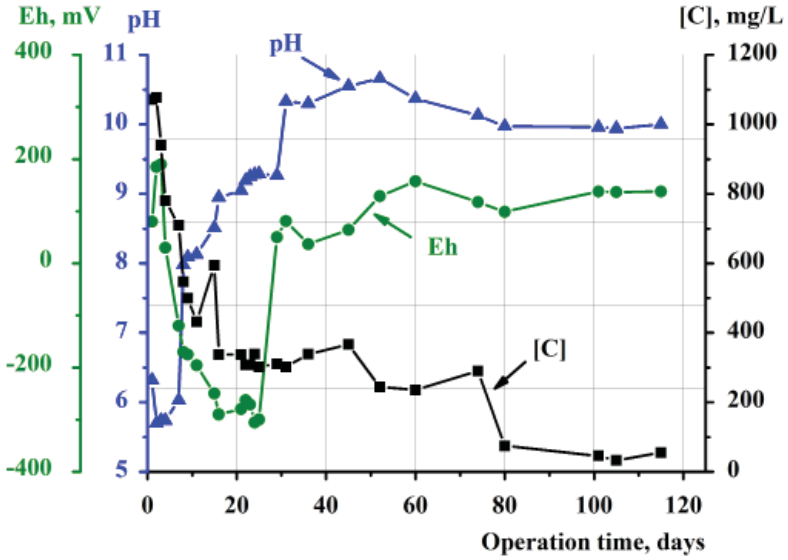

Fig. 2. **The dynamics of metabolic parameters during aerobic oxidation of dissolved organic compounds of filtrate**

a result, the accumulation of hydrolysis products (fatty acids and alcohols) appeared at the initial stages. Further, the pH values were shown to increase from 5.74 to 10.66 over the next 48 days of cultivation. This may indicate the stage of degradation of low molecular weight soluble organic compounds, such as organic acids, alcohols, amino acids, etc. The increase in pH may indicate complete oxidation of the compounds and accumulation of ammonium ions that alkalized the medium. Subsequently, the pH stabilized at about 10.0, which could indicate a decrease in the rate of degradation and completion of the process.

The dynamics of the Eh values also testified to the active growth of microorganisms. Thus, during the first 3 days, the microbiome adapted, as evidenced by the increase in Eh from +80 to +190 mV. Over the next 22 days, the Eh values decreased to −300 mV. Despite intense aeration, the redox potential reached negative values, indicating the growth of microorganisms and oxidation of the substrate. Further, growth and stabilization of Eh about +130 mV correlating with pH stabilization indicated the completion of the process.

The decrease in the concentration of dissolved organic compounds is the main criterion for the efficiency of the process. The concentration of carbon was decreased within 16 days from the beginning of cultivation the most intensively (3-fold from 1071 to 337 mg/L). Subsequently, from 16 to 80 days, the process slowed down, and the concentration of carbon decreased from 337 to 75 mg/L (4.5-fold decrease). Over the next 35 days, the concentration of soluble organic compounds decreased 1.3-fold (from 75 to 56 mg/L).

Thus, as the result of the conducted research aerobic oxidation was shown to be promissing for the purification of the filtrate after fermentation of solid food waste from the dissolved organic compounds. The study of the dynamics of the process distinguished 3 stages. During the first one, the microbiome adaptation and rapid degradation of organic compounds took place. It was evidenced by rapid changes in pH and Eh, as well as a rapid decrease in Carbon concentration. The second stage was characterized by a decrease in the efficiency of degradation of organic compounds and stabilization of pH and Eh. In the third stage, the oxidation of residual concentrations of organic compounds took place and the process was completed. The total duration of the process without optimization was 115 days.

The dynamics of the degradation of dissolved organic compounds of the filtrate due to methanogenic fermentation was investigated. For this purpose, 30 L of filtrate and 0.5 L of FS as inoculum were added to the installation.

As a result, methane fermentation of dissolved organic compounds was shown to 10-fold reduce the concentration of Carbon from 1071 to 105 mg/L (Fig. 3).

The decrease in pH during the first day of cultivation from 6.34 to 5.65 indicated the hydrolysis of unfermented detritus. During

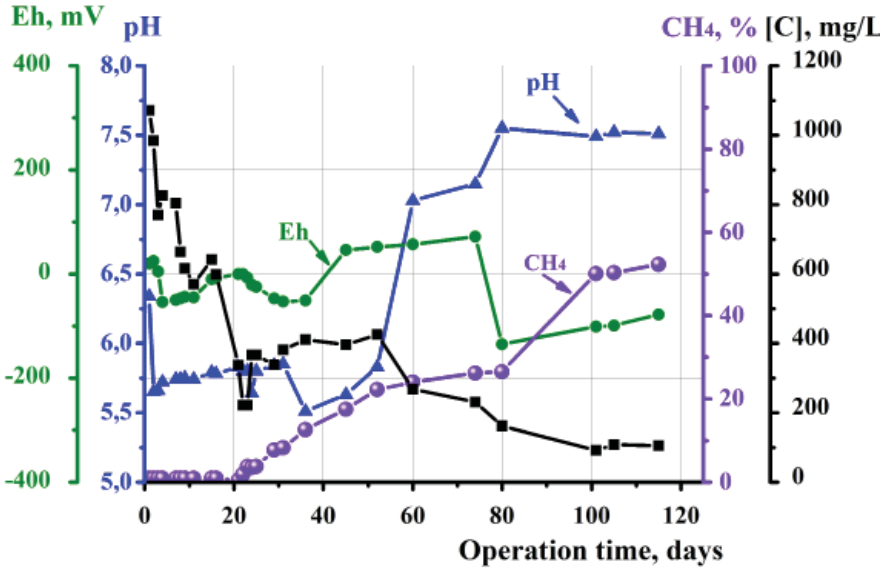

Fig. 3. **The dynamics of metabolic parameters during methane fermentation of dissolved organic compounds of filtrate**

the next 50 days of fermentation, the pH values remained in the range of 5.6–5.7. Subsequently, for 30 days, the pH increased to 7.5 and did not change until the end of the process. Such changes in the pH showed that the degradation of organic compounds and possible salinization of the medium due to the accumulation of alkaline NH_4^+ was achieved during methane fermentation.

The redox potential values remained in the range of −50...+70 mV for 74 days of fermentation. Subsequently, Eh decreased to -135 mV and remained within negative values. Since the regulation of microbial metabolism and optimization of cultivation conditions did not occur, this may indicate the adaptation of microorganisms to the created conditions.

The efficiency of complete degradation of dissolved organic compounds to gaseous products was evidenced by the release of methane after 21 days of cultivation. The most intensive accumulation of methane was observed after 80 days of cultivation. The concentration of CH_4 increased from 26 to 52% in the gas phase.

The most intensive degradation of organic compounds occurred within 23 days from the beginning of cultivation. Thus, the Carbon concentration 4.8-fold decreased from 1 071 to 221 mg/L. Over the next 92 days, the Carbon concentration was halved to 105 mg/L. As a result, the concentration of organic compounds during methane fermentation 10-fold decreased.

Thus, anaerobic degradation by methane fermentation was shown to be useful for effective purification of the filtrate. Two stages of the process were identified. During the first one, an intensive decrease in the Carbon concentration was observed. During the second stage, there was a gradual fermentation of organic compounds and methane synthesis. The total duration of the process was 115 days, with a CH_4 yield of 1 L/dm^3 of filtrate.

Therefore, methane fermentation of organic compounds can be effective for waste degradation. However, the speed of the process is low. It can cause an imbalance in the accumulation of waste and the rate of their treatment. In addition, further industrial implementation requires optimization of fermentation conditions, as methanogenic microorganisms are sensitive to cultivation conditions and competitive microbial communities [33, 34].

Hydrogen fermentation of multicomponent organic waste is a promising area for hydrogen production with simultaneous degradation of waste [24]. It is confirmed by the literature data. Thus, for the fermentation of a wide range of substrates, the yield of hydrogen varies: swine manure with the addition of glucose produces up to 26–30 L/kg of substrate [35], molasses — 585 L/L, dairy waste — 31.5 L/kg of solids [36], corn starch — 150 L/kg, sugars (hexose) — 311 L/kg [37, 38], multicomponent solid food waste — 50–100 L/kg [26–28]. Naturally, carbohydrate-rich foods and wastes (potatoes, cereals, etc.) are fermented faster and more efficiently than meat containing more protein and fat [6]. In addition, the use of hexoses increases the yield of hydrogen, but significantly increases the cost of biotechnology. Therefore, the optimization of the fermentation process of common cheap substrates (food waste) requiring the disposal is promising [24, 28].

The approach for treatment of solid waste is actively being developed and optimized. However, no information was found about the methods for treatment filtrate accumulated after fermentation. The paper compares the efficiency of two types of microbial metabolism for the degradation of soluble organic compounds of filtrate: aerobic oxidation and methane fermentation.

Based on theoretical calculations, aerobic oxidation of the substrate is more promising. Thus, the energy output reaches −2 877.0 kJ/M providing greater speed and efficiency of the process [18–20]:

$$C_6H_{12}O_6 + 6O_2 = 6CO_2 + 6H_2O,$$
$$\Delta G_o = -2\,877{,}0 \text{ kJ/M}.$$

Methanogenesis provides lower energy yield, so the degradation of organic compounds under such conditions can occur for a long time reducing the efficiency of biotechnology [18, 21]:

$$HCO_3^- + H^+ + 4H_2 = CH_4 + 3H_2O,$$
$$\Delta G_o = -135{,}6 \text{ kJ/M}.$$

Although aerobic oxidation of organic compounds is the most energy-efficient, its industrial application is limited due to the imbalance in the ratio of electron donor (organic compounds) and acceptor (molecular oxygen). During the oxidation of organic compounds, the rate of oxygen consumption by microorganisms in the liquid phase significantly exceeds the rate of its diffusion into solution. Therefore, to provide an efficient process, it is necessary to use compressors to inject air into a bioreactor. It causes the need to use additional equipment and increase the cost of biotechnology [18].

On the other hand, the use of obligate anaerobic methanogenic microorganisms does not require the application of additional electron acceptors and process equipment [39, 40]. Low molecular weight fatty acids and alcohols are the main products of the fermentation of solid food waste. They are the precursors of monocarbon compounds that serve as substrates for methanogenesis (formate, methanol, methylamine, etc.) [21, 41]:

$$4CH_3OH + 2H_2O \rightarrow 3CH_4 + CO_2 + 4H_2O;$$
$$4HCOO^- + 4H^+ \rightarrow CH_4 + 3CO_2 + 2H_2O;$$
$$4NH_2CH_3 + 2H_2O \rightarrow NH_3 + 3CH_4 + CO_2.$$

This method is common today for the degradation of polymeric organic waste, both agricultural (manure, plant residues) and industrial (excess biomass of activated sludge of aeration tank) [39, 40]. However, it is a complex process that requires control and regulation, as methanogenic microorganisms are sensitive to toxic metals (Cu^{2+}, Co^{2+}, Hg^{2+}, etc.) and competitive processes, including sulfate reduction [42, 33].

Thus, aerobic degradation of dissolved organic compounds can provide a high rate of oxidation of the substrate, but requires additional technological equipment. Methane fermentation is a longer process that can provide the degradation of organic compounds without the need of additional electron acceptors. But its application requires careful control and regulation of the process to maintain the efficient functioning of the methanogenic microbial community.

Two methods were used to purify the filtrate. According to thermodynamic calculations both of them are promising. These suggestions were confirmed experimentally. The efficiency of purification of the filtrate by aerobic method was shown to be higher than anaerobic for the same period of time (115 days). Thus, during aerobic oxidation the concentration of dissolved organic compounds 19-fold decreased from 1 071 to 56 mg/L. Methane fermentation provided 10-fold decrease of total Carbon concentration from 1 071 to 105 mg/L. However, it provided CH_4 yield 1 L/dm^3 of filtrate.

As a result of the conducted research, the fundamental opportunity to apply both aerobic and anaerobic methods to purify the filtrate was shown. The next step is to increase the efficiency of the process by the regulation of microbial metabolism and optimization of the parameters (pH, Eh, mixing, composition of microbial communitiess, etc.).

The heterogeneity of waste composition as a substrate hinders the development of stable and predictable biotechnologies for now [1, 6, 7]. The most efficient are carbohydrate-rich wastes of fruits, vegetables, bakery products, cereals, etc. [6]. However, despite the heterogeneity of the composition, food waste remains promising for industrial use, as it is a cheap, constantly renewable substrate.

Conclusions

The aerobic oxidation was established to provide 1.9 times more efficient removal of dissolved organic compounds of filtrate, compared with the anaerobic methane fermentation. The necessity to optimize the methods to purify filtrate to increase the efficiency of the process was determined. The obtained results will be the basis to develop complex biotechnology providing not only the production of environmentally friendly energy H_2 via the fermentation of solid food waste, but also the purification of filtrate to solve the ecological and energy (CH_4 production) problem of society.

The study was funded under the project No 1–20 (10.03.2021) “Obtaining of fermentation parameters of experimental-industrial technology for synthesis of biohydrogen” of the Target Program of Scientific Research of the National Academy of Sciences of Ukraine “Development of scientific foundations of obtaining, storage and application of hydrogen in autonomous energy supply systems” for 2019–2021. The authors declare no conflict of interests.

REFERENCES

1. *Curry N., Pillay P.* Biogas prediction and design of a food waste to energy system for the urban environment. *Renewable Energy.* 2012, V. 41, P. 200–209. https://doi.org/10.1016/j.renene.2011.10.019
2. *Pagliano G., Ventorino V., Panico A., Pepe O.* Integrated systems for biopolymers and bioenergy production from organic waste and by-products: a review of microbial processes. *Biotechnol. Biofuels.* 2017, 10 (1), 113–137. https://doi.org/10.1186/s13068-017-0802-4
3. *Algapani D., Wang J., Qiao W., Su M., Goglio A., Wandera S. M., Jiang M., Pan X., Adani F., Dong R.* Improving methane production and anaerobic digestion stability of food waste by extracting lipids and mixing it with sewage

sludge. *Biores. Technol.* 2017, V. 244. https://doi.org/10.1016/j.biortech.2017.08.087.
4. *Algapani D. E., Qiao W., Ricci M., Bianchi D., Wandera S. M., Adani F., Dong R.* Bio-hydrogen and bio-methane production from food waste in a two-stage anaerobic digestion process with digestate recirculation. *Renewable Energy.* 2019, V. 130, P. 1108–1115, https://doi.org/10.1016/j.renene.2018.08.079
5. *Pagliaccia P., Gallipoli A., Gianico A., Montecchio D., Braguglia C. M.* Single stage anaerobic bioconversion of food waste in mono and co-digestion with olive husks: Impact of thermal pretreatment on hydrogen and methane production. *Int. J. Hydrogen Energy.* 2016, 41 (2), 905–915. https://doi.org/10.1016/j.ijhydene.2015.10.061
6. *Paritosh K., Kushwaha S. K., Yadav M., Pareek N., Chawade A., Vivekanand V.* Food Waste to Energy: An Overview of Sustainable Approaches for Food Waste Management and Nutrient Recycling. *BioMed. Res. Int.* 2017, V. 2017, P. 1–19. https://doi.org/10.1155/2017/2370927
7. *Yasin N. H. M., Mumtaz T., Hassan M. A., Abd Rahman N.* Food waste and food processing waste for biohydrogen production: A review. *J. Environ. Management.* 2013, V. 130, P. 375–385. https://doi.org/10.1016/j.jenvman.2013.09.009
8. *Uçkun Kiran E., Trzcinski A. P., Ng W. J., Liu Y.* Bioconversion of food waste to energy: A review. *Fuel.* 2014, V. 134, P. 389–399, https://doi.org/10.1016/j.fuel.2014.05.074
9. *Cheng J., Ding L., Lin R., Yue L., Liu J., Zhou J., Cen K.* Fermentative biohydrogen and biomethane co-production from mixture of food waste and sewage sludge: Effects of physiochemical properties and mix ratios on fermentation performance. *Applied Energy.* 2016, V. 184, P. 1–8, https://doi.org/10.1016/j.apenergy.2016.10.003
10. *Meena R. A. A., Banu J. R., Kannah R. Y., Yogalakshmi K. N., Kumar G.* Biohythane production from food processing wastes — Challenges and perspectives. *Biores. Technol.* 2020, V. 298, P. 122449, https://doi.org/10.1016/j.biortech.2019.122449
11. *Hobbs S. R., Landis A. E., Rittmann B. E., Young M. N., Parameswaran P.* Enhancing anaerobic digestion of food waste through biochemical methane potential assays at different substrate: inoculum ratios. *Waste Manag.* 2018, V. 71, P. 612–617. https://doi.org/10.1016/j.wasman.2017.06.029
12. *Han W., Hu Y., Li S., Li F., Tang J.* Biohydrogen production in the suspended and attached microbial growth systems from waste pastry hydrolysate. *Biores. Technol.* 2016, V. 218, P. 589–594. https://doi.org/10.1016/j.biortech.2021
13. *Han M. J., Behera S. K., Park H.-S.* Anaerobic co-digestion of food waste leachate and piggery wastewater for methane production: statistical optimization of key process parameters. *J. Chem. Technol. Biotechnol.* 2012, 87 (11), 1541–1550. https://doi.org/10.1002/jctb.3786
14. *Polprasert C.* Organic Waste Recycling: Technology and Management — Third Edition. *IWA Publishing.* 2007. https://library.oapen.org/handle/20.500.12657/30981
15. *Levin D.* Biohydrogen production: prospects and limitations to practical application. *Int. J. Hydrogen Energy.* 2004, 29 (2), 173–185, https://doi.org/10.1016/S0360-3199(03)00094-6
16. *Show K. Y., Lee D. J., Tay J. H., Lin C. Y., Chang J. S.* Biohydrogen production: Current perspectives and the way forward. *Int. J. Hydrogen Energy.* 2012, 37 (20), 15616–15631, https://doi.org/10.1016/j.ijhydene.2012.04.109
17. *Nanda S., Berruti F.* A technical review of bioenergy and resource recovery from municipal solid waste. *J. Hazardous Materials.* 2021, V. 403, P. 123970. https://doi.org/10.1016/j.jhazmat.2020.123970
18. *Gottschalk G.* Bacterial metabolism, 2nd Edition. *New York: Springer-Verlag.* 1986, 359 p. http://dx.doi.org/10.1007/978-1-4612-1072-6
19. *Kleidon A., Lorenz R.D.* Non-equilibrium Thermodynamics and the Production of Entropy: Life, Earth, and Beyond. *Springer Science & Business Media.* 2005, 264 p. https://doi.org/10.1007/b12042
20. *Kekacs D., Drollette B. D., Brooker M., Plata D. L., Mouser P. J.* Aerobic biodegradation of organic compounds in hydraulic fracturing fluids. *Biodegradation.* 2015, 26 (4), 271–287, https://doi.org/10.1007/s10532-015-9733-6
21. *Thauer R.* Biochemistry of methanogenesis: a tribute to Marjory Stephenson. *Microbiol.* 1998, 144 (9), 2377–2406, https://doi.org/10.1099/00221287-144-9-2377
22. *Berezkin V. G., Drugov Y. S.* Gas Chromatography in Air Pollution Analysis. 1st Edition. *Elsevier.* 1991, 210 p. Available: https://www.elsevier.com/books/gas-chromatography-in-air-pollution-analysis/berezkin/978-0-444-98732-7
23. *Suslova O., Govorukha V., Brovarskaya O., Matveeva N., Tashyreva H., Tashyrev O.* Method for Determining Organic Compound Concentration in Biological Systems by Permanganate Redox Titration. *Int. J. Bioautomation.* 2014, 18 (1), 45–52. http://www.biomed.bas.bg/bioautomation/
24. *Ghimire A., Frunzo L., Pirozzi F., Trably E., Escudie R., Lens P., Esposito G.* A review on

dark fermentative biohydrogen production from organic biomass: Process parameters and use of by-products. *Applied Energy*. 2015, V. 144, P. 73–95, https://doi.org/10.1016/j.apenergy.2015.01.045
25. *Hovorukha V., Tashyrev O., Matvieieva N., Tashyreva H., Havryliuk O., Bielikova O., Sioma I.* Integrated Approach for Development of Environmental Biotechnologies for Treatment of Solid Organic Waste and Obtaining of Biohydrogen and Lignocellulosic Substrate. *Environ. Res., Engineering and Management*. 2018, 74 (4), 31–42. https://doi.org/10.5755/j01.erem.74.4.20723
26. *Hovorukha V., Tashyrev O., Havryliuk O., Iastremska L.* High Efficiency of Food Waste Fermentation and Biohydrogen Production in Experimental-industrial Anaerobic Batch Reactor. *The Open Agriculture J*. 2020, 14 (1), 174–186. https://doi.org/10.2174/1874331502014010174
27. *Tashyrev O., Govorukha V., Havryliuk O.* The effect of mixing modes on biohydrogen yield and spatial pH gradient at dark fermentation of solid food waste. *EEEP*. 2017, P. 53–62, https://doi.org/10.32006/eeep.2017.2.5362
28. *Hovorukha V., Havryliuk O., Gladka G., Tashyrev O., Kalinichenko A., Sporek M., Dolhanczuk-Srodka A.* Hydrogen Dark Fermentation for Degradation of Solid and Liquid Food Waste. *Energies*. 2021, 14 (7), https://doi.org/10.3390/en14071831
29. *Hovorukha V., Tashyrev O., Tashyreva H., Havryliuk O., Bielikova O., Iastremska L.* Increase in efficiency of hydrogen production by optimization of food waste fermentation parameters. *Energetika*. 2019, 65 (1), 85–94. https://doi.org/10.6001/energetika.v65i1.3977
30. *Ababouch L., Chaibi A., Busta F. F.* Inhibition of Bacterial Spore Growth by Fatty Acids and Their Sodium Salts. *J. Food Prot*. 1992, 55 (12), 980–984. https://doi.org/10.4315/0362-028X-55.12.980
31. *Herrero A. A.* End-product inhibition in anaerobic fermentations. *Trends in Biotechnol*. 1983, 1 (2), 49–53, https://doi.org/10.1016/0167-7799(83)90069-0
32. *Sivagurunathan P., Sen B., Lin C.-Y.* Overcoming propionic acid inhibition of hydrogen fermentation by temperature shift strategy. *Int. J. Hydrogen Energy*. 2014, 39 (33), 19232–19241, https://doi.org/10.1016/j.ijhydene.2014.03.260
33. *Ziemiński K., Frąc M.* Methane fermentation process as anaerobic digestion of biomass: Transformations, stages and microorganisms. *African J. Biotechnol*. 2012, 11 (18). https://doi.org/10.4314/ajb.v11i18
34. *Poeschl M., Ward S., Owende P.* Environmental impacts of biogas deployment — Part II: life cycle assessment of multiple production and utilization pathways. *J. Cleaner Production*. 2012, V. 24, P. 184–201. https://doi.org/10.1016/j.jclepro.2011.10.030
35. *Wu X., Zhu J., Dong Ch., Miller C., Li Y., Wang L., Yao W.* Continuous biohydrogen production from liquid swine manure supplemented with glucose using an anaerobic sequencing batch reactor. *Int. J. Hydrogen Energy*. 2009, 34 (16), 6636–6645, https://doi.org/10.1016/j.ijhydene.2009.06.058
36. *Ren N., Li J., Li B., Wang Y., Liu S.* Biohydrogen production from molasses by anaerobic fermentation with a pilot-scale bioreactor system. *Int. J. Hydrogen Energy*. 2006, 31 (15), 2147–2157, https://doi.org/10.1016/j.ijhydene.2006.02.011
37. *Zhang M.-L., Fan Y.-T., Xing Y., Pan C.-M., Zhang G.-S., Lay J.-J.* Enhanced biohydrogen production from cornstalk wastes with acidification pretreatment by mixed anaerobic cultures. *Biomass and Bioenergy*. 2007, 31 (4), 250–254, https://doi.org/10.1016/j.biombioe.2006.08.004
38. *Hawkes F. R., Hussy I., Kyazze G., Dinsdale R., Hawkes D. L.* Continuous dark fermentative hydrogen production by mesophilic microflora: Principles and progress. *Int. J. Hydrogen Energy*. 2007, 32 (2), 172–184. https://doi.org/10.1016/j.ijhydene.2006.08.014
39. *Ike M., Inoue D., Miyano T., Liu T. T., Sei K., Soda S., Kadoshin Sh.* Microbial population dynamics during startup of a full-scale anaerobic digester treating industrial food waste in Kyoto eco-energy project. *Biores. Technol*. 2010, 101 (11), 3952–3957, https://doi.org/10.1016/j.biortech.2010.01.028
40. *Kondusamy D., Kalamdhad A. S.* Pretreatment and anaerobic digestion of food waste for high rate methane production — A review. *J. Environ. Chem. Engineering*. 2014, 2 (3), 1821–1830, https://doi.org/10.1016/j.jece.2014.07.024
41. *Ferry J. G.* Enzymology of one-carbon metabolism in methanogenic pathways. *FEMS Microbiol. Rev*. 1999, 23 (1), 13–38. https://doi.org/10.1111/j.1574-6976.1999.tb00390.x
42. *Karhadkar P. P., Audic J.-M., Faup G. M., Khanna P.* Sulfide and sulfate inhibition of methanogenesis. *Water Res*. 1987, 21 (9), 1061–1066, https://doi.org/10.1016/0043-1354(87)90027-3

ДВОСТУПЕНЕВА ДЕГРАДАЦІЯ ТВЕРДИХ ОРГАНІЧНИХ ВІДХОДІВ ТА РІДКОГО ФІЛЬТРАТУ

В. М. Говоруха, О. А. Гаврилюк, І. О. Біда, Я. П. Данько, О. В. Шаблій, Г. В. Гладка, Л. С. Ястремська, О. Б. Таширев

Інститут мікробіології і вірусології ім. Д. К. Заболотного НАН України, Київ

E-mail: vira-govorukha@ukr.net

Накопичення твердих та рідких органічних відходів потребує їх перероблення для розвитку енергетичних біотехнологій та запобігання забрудненню довкілля.

Метою роботи було вивчити ефективність очищення фільтрату від розчинених органічних сполук за допомогою аеробного окиснення та метанової ферментації.

Методи. Для визначення pH та окисно-відновного потенціалу (Eh), складу газу, вмісту коротколанцюгових жирних кислот, концентрації розчинених органічних сполук за загальним карбоном використовували стандартні методи.

Результати. Порівнювали ефективність двох типів мікробного метаболізму для деградації розчинних органічних сполук фільтрату. Встановлено, що аеробне окиснення забезпечило в 1,9 раза більш ефективне видалення розчинених органічних сполук порівняно з анаеробною метановою ферментацією, однак вона створила умови для виходу CH_4 1 л/дм^3 фільтрату (концентрація за карбоном — 1 071 мг/л). Визначено необхідність оптимізації методів очищення фільтрату для підвищення ефективності процесу.

Висновки. Отримані результати становитимуть основу для розроблення комплексної біотехнології, що забезпечить не тільки виробництво екологічно чистого енергоносія H_2 шляхом зброджування твердих харчових відходів, але й очищення фільтрату для вирішення екологічної та енергетичної (продукування CH_4) проблеми суспільства.

Ключові слова: тверді органічні відходи; розчинні органічні сполуки; екологічні біотехнології; водень; метан; ферментація; аеробне окиснення.

ДВУХСТУПЕНЧАТАЯ ДЕГРАДАЦИЯ ТВЕРДЫХ ОРГАНИЧЕСКИХ ОТХОДОВ И ЖИДКОГО ФИЛЬТРАТА

В. М. Говоруха, О. А. Гаврилюк, И. А. Бида, Я. П. Данько, А. В. Шаблий, Г. В. Гладка, Л. С. Ястремская, А. Б. Таширев

Институт микробиологии и вирусологии им. Д. К. Заболотного НАН Украины, Киев

E-mail: vira-govorukha@ukr.net

Накопление твердых и жидких органических отходов требует их переработки для развития энергетических биотехнологий и предотвращения загрязнения окружающей среды.

Цель. Изучение эффективности очистки фильтрата от растворенных органических соединений с помощью аэробного окисления и метановой ферментации.

Методы. Для определения pH и окислительно-восстановительного потенциала (Eh), состава газа, содержания короткоцепочечных жирных кислот, концентрации растворенных органических соединений по общему карбону были использованы стандартные методы.

Результаты. Проведено сравнение эффективности двух типов микробного метаболизма для деградации растворимых органических соединений фильтрата. Установлено, что аэробное окисление обеспечило в 1,9 раза более эффективное удаление растворенных органических соединений по сравнению с анаэробной метановой ферментацией, однако она сделала возможным выход CH_4 1 л/дм^3 фильтрата (концентрация по карбону — 1 071 мг/л). Определена необходимость оптимизации методов очистки фильтрата для повышения эффективности процесса.

Выводы. Полученные результаты будут основой для разработки комплексной биотехнологии, обеспечивающей не только производство экологически чистого энергоносителя H_2 путем сбраживания твердых пищевых отходов, но также очистку фильтрата для решения экологической и энергетической (продуцирование CH_4) проблемы общества.

Ключевые слова: твердые органические отходы; растворимые органические соединения; экологические биотехнологии; водород; метан; ферментация; аэробное окисление.

UDC 628.331 https://doi.org/10.15407.biotech14.04.080

PROBLEMS OF SOAPSTOCK TREATMENT OF VEGETABLE OIL PRODUCTIONS AND THEIR SOLUTIONS

L. Sabliy[1]
V. Zhukova[1]
S. Konontsev[2]
O. Obodovych[3]
V. Sydorenko[3]

[1]National Technical University of Ukraine "Igor Sikorsky Kyiv Polytechnic Institute"
[2]National University of Water and Environmental Engineering, Rivne, Ukraine
[3]Institute of Engineering Thermophysics of the National Academy of Sciences of Ukraine, Kyiv

E-mail: verolis86@gmail.com

Received 28.06.2021
Revised 21.08.2021
Accepted 31.08.2021

Wastewater generated during vegetable oil production contains various pollutants that enter it during soapstock processing: fats and fatty acids and their salts (aqueous soap solutions), glycerin, phosphoglycerates, neutral fat, phosphatides, proteins, carbohydrates, dyes, unsaponifiable and waxy substances, salts, mechanical impurities, etc.

Aim. The purpose of the work was to study the processes of purification of industrial wastewater from oil production and to propose an effective technology for their treatment, taking into account the regulatory requirements for the discharge of treated wastewater into the city sewage system.

Methods. Chemical oxygen demand (COD) was determined by the dichromate method. The concentration of suspended solids was determined by gravimetric method.

Results. As a result of research, calcium carbonate was chosen as an alkaline reagent. After treatment of soapstock with calcium carbonate followed by flotation, the effect of removing the suspended particles was 70–75%, and COD decreased by 60%. On the basis of the research, a technology for processing soapstock was proposed, including sequential processes of physicochemical wastewater treatment — averaging, alkalization with calcium carbonate, stage I of flotation, coagulation, stage II of flotation, oxidation with hydrogen peroxide, filtration through quartz filters and adsorption on carbon filters.

Conclusion. An effective technology for preliminary cleaning of the soapstocks oil production has been developed. This will significantly reduce the concentration of organic matter and other pollutants in soapstocks, which will significantly reduce the impact of such effluents on the processes of biological wastewater treatment of urban wastewater treatment plants.

Key words: soapstock; vegetable oil; pollutants; technology; treatment; wastewater.

Wastewater generated during the production of vegetable oil contains various pollutants that enter it during the soapstock processing: fats and fatty acids and their salts (aqueous soap solutions), glycerin, phosphoglycerides, neutral fat, phosphatides, proteins, carbohydrates, dyes (carotene, carotenoids, chlorophyll, etc.), unsaponifiable and waxy substances, salts — sodium sulfate and chloride, mechanical impurities, etc.

Soap impurities have a complex and volatile composition, which depends on the nature and properties of their constituents, the amount of substances associated with fats and other factors. Wastewater is characterized by high concentrations of organic pollutants in terms of COD, high suspended solids, and low pH (Table 1).

In a phase-dispersed state, such wastewater is a stable emulsion with water. The presence in wastewater of phospholipids, which are emulsion stabilizers, leads to complications of phase separation. Wastewater contains suspended solids, colloidal substances and various organic and inorganic solutes as well. Soaps contained in wastewater had a high stabilizing and absorption capacity, due to which they absorbed a significant part of

Table 1. **Average value of indicators of wastewater from vegetable oil production**

No	Indicator	Units of measurement	Average value
1	pH	–	2
2	Suspended solids	mg/L	6 300
3	Non-volatile suspended solids	mg/L	700
4	Dry residue	mg/L	13 400
5	Ignited residue	mg/L	1 300
6	COD	mg/L	40 000

impurities such as phosphatides, proteins, mucus, dyes and others [1].

Wastewater color varies from chestnut brown to brown. Dyes can be divided into three groups: substances that are in the fat cells and turn into oil unchanged; substances that change composition and color during oil production; substances that are formed during oil production when heated.

Wastewater in terms of the content of pollutants exceeds the norms for discharge into city sewer systems. Therefore, before being discharged into city treatment facilities at local treatment facilities, they must be treated by physicochemical and biological methods.

Flotation combined with sedimentation has proven to be the most effective way to remove grease, soap, and suspended solids from water [2]. At the same time, there is a decrease in fat content by 10 or more times, soaps — by 4–5 times.

Comparison of the methods of coagulation-sedimentation and coagulation-flotation in terms of the efficiency of removing organic matter from wastewater due to COD, suspended solids showed that the use of coagulation and flotation enables to obtain a higher efficiency of removing organic matter, suspended particles due to effective adsorption of soap and fat on suspended solid particles, particles of metal hydroxides formed during coagulation, and flotation of these pollutants on the surface of the liquid and the formation of flotation sludge [3, 4].

For the treatment of soapstocks after physical and chemical treatment, it was proposed to use aerobic biological treatment [5]. The technology of such wastewater treatment using coagulation with the addition of coagulant $Al_2(SO_4)_3$, flotation and biological treatment in an aerotank is considered. When the COD of untreated wastewater is 1 800 mg/L, a decrease in the COD of 98% is achieved and the quality of treated wastewater is ensured, which is acceptable for discharge into a natural reservoir.

It was found that when using iron chloride $FeCl_3$ as a coagulant [6] in the treatment of soapstocks with an initial COD of 220,000 mg/L and high turbidity, the optimal pH value, which provides the best performance of wastewater treatment in terms of COD, is 8.5 for the pH range 2–13, the cleansing effect of COD reached 80% at a dose of coagulant $FeCl_3$ — 800 mg/L.

To clean soapstocks, absorption methods are also used, when choosing which it should be noted that when the temperature rises above 80 °C, the peroxide content of fatty acids increases significantly, and when the temperature drops below 50 °C, a mass is formed that is difficult to absorption purification [7].

Membrane methods are used for local cleaning of soapstocks. Fats are successfully separated from an aqueous solution by ultrafiltration at a pressure of up to 6 atm, since fats have practically no osmotic pressure. Low molecular weight fatty acids and other related substances with low osmotic release due to nanofiltration. Reverse osmosis is used at high osmotic pressure [2, 8].

The proposed technology includes cleaning of soapstocks by two-stage flotation in the presence of reagents under pressure and gravel filtration. The use of ultrafiltration made it possible to abandon the use of a reagent, the second stage of flotation and gravel filtration. The COD value after the first stage of flotation was 1 000 mg/L, and after ultrafiltration — 250 mg/L with the initial COD value up to 5 000 mg/L [9].

The use of ultrafiltration makes it possible to effectively use expensive ingredients contained in wastewater, as well as reuse purified water in production. The disadvantages of membrane methods are their high cost, the need for membrane regeneration and preliminary removal of substances that cause turbidity of water — suspended and colloidal, leading to clogging of the membranes. Consequently, membrane methods are difficult to operate, require complex equipment, and are very expensive [10].

The aim of the work was to study the processes of purification of industrial

wastewater from oil production and to propose an effective technology for their local treatment to regulatory requirements for the treated wastewater discharge into the city's sewerage system. To achieve these goals, a study was conducted using the actual production of soapstocks from vegetable oil in 2021.

Materials and Methods

COD was determined by the dichromate method (according to managing normative document in Ukraine — KND 211.1.4.021-95. "Method for determining the chemical oxygen demand (COD) in surface and wastewater". The concentration of suspended solids was determined by gravimetric method.

For the study, vegetable oil production soapstocks were used, which were characterized by the pollutants indicators given in the Table 1. The COD value of soapstocks was 40 000 mg/L, the pH value was 2.

For leaching, a comparison of the effect of two reagents on soapstock, namely NaOH and $CaCO_3$, was used. A 20% NaOH solution was added to the soapstock samples at a dose of 20 mL/L, which ensured an increase in pH to 7. When using $CaCO_3$, the dose was 2 g/L.

The following soapstock processing processes have been consistently studied:

1. Aeration using an aquarium compressor and aerator, installed with a capacity of 250 ml with the test soapstock, for 24 hours.

2. Chemical precipitation with calcium carbonate $CaCO_3$ at a dose of 1.8–2.0 g/L, pH 5.5, reaction time 10–15 min and flotation (stage I) with air supply through fine-porous aerators for 75 min, air flow rate was 8 $m^3/(m^2 \cdot h)$.

3. Coagulation was carried out with aluminum sulfate at a dose of 1–1.2 g/L at an optimum pH of 5.5. The soapstock sample was quickly mixed with the coagulant solution for 1–2 min and the stirring was continued for 15–20 min until the formation and compaction of flakes.

4. Flotation (stage II) of coagulated impurities was carried out for 75 min with air supply through fine-porous aerators.

5. The selection of purified water from the tank and the separation of the formed flotation sludge were carried out.

6. Oxidation of organic pollutants remaining in purified water at the outlet of the II stage flotation, hydrogen peroxide at a dose of 1.5–1.8 g/L, pH 4.5–5.5, process duration 2 hours with stirring laboratory magnetic stirrer.

7. Filtration of wastewater after oxidation through a sand filter. Sand for filtration was prepared as follows: thoroughly washed with running water to remove mechanical impurities; dried in an oven at 105 °C for 10 h; ignite in a muffle furnace at 600 °C for 2 hours to remove all residual contamination into ash; cooled and washed with distilled water. Thereafter, the sand was transferred to a filter and a filter layer was formed.

8. Filtration of wastewater after the sand filter through a carbon filter. Fine-grained activated carbon was used in the form of a filtering layer.

At each stage of the process, water samples were taken at the outlet, in which the indicators were determined: suspended particles and COD. The results of the analyses and the determined cleaning effects at each stage are shown in Table 2 and Fig. 1 and 2. The reliability of the obtained data was $P < 0.05$, i.e. statistically significant differences were found. To assess the significance of the difference between the averages of the two groups, *t*-test (Student's test) was used.

Results and Discussion

To alkalize the soapstock by adding 20% NaOH solution at a dose of 20 mL/L, the pH was raised to 7. The liquid became dark. There were some difficulties in setting the dose of NaOH to bring the pH of the wastewater to 5.5. With an increase in the alkali dose, the pH rose sharply above pH 7.

In the second variant, calcium carbonate $CaCO^3$ was used. To increase the pH of wastewater from 2 to 5.5, the dose of $CaCO_3$ was 2.4 g/L. In the process of alkalization, an intense formation of CO_2 gas was observed, the bubbles of which rose to the surface of the liquid with the formation of foam (about 10% of the volume). The amount of sediment was about 5%. The formation of gas promoted the flotation of pollutants — suspended particles, dissolved organic substances during their adsorption on the "bubble – solid particle" complexes. The use of $CaCO_3$ allowed the following flotation to be used to separate the flotation froth from the water. Therefore, $CaCO_3$ was chosen as the alkaline reagent, which made it possible to obtain the following positive results. When calcium carbonate reacted with water, insoluble calcium hydroxide was formed and carbon dioxide was liberated. The pH of the water increased, the

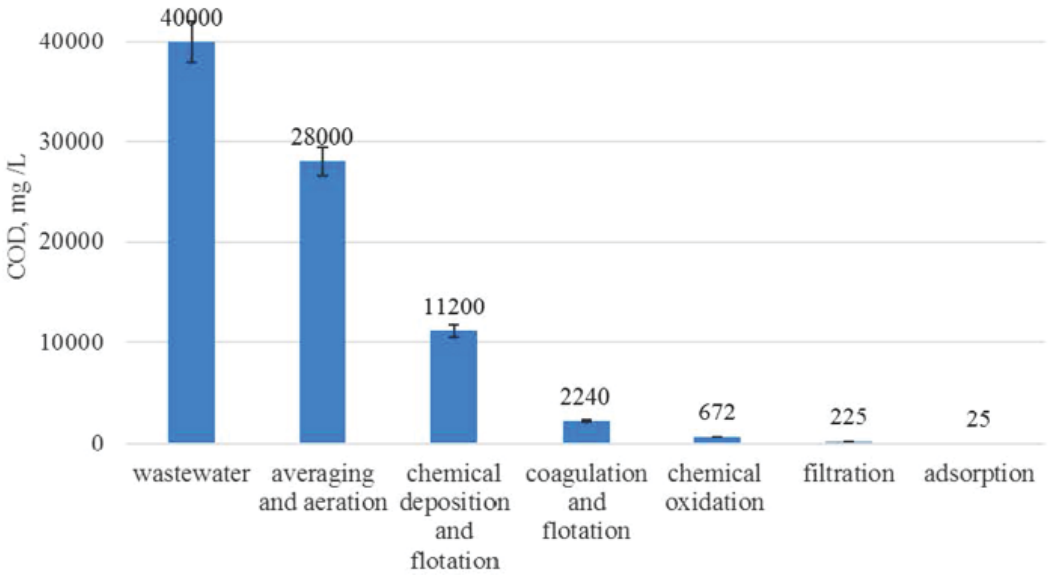

Fig. 1. **Change in the COD of the soap stock during treatment by technology:** averaging and aeration — chemical deposition and flotation — coagulation and flotation — chemical oxidation — filtration — adsorption

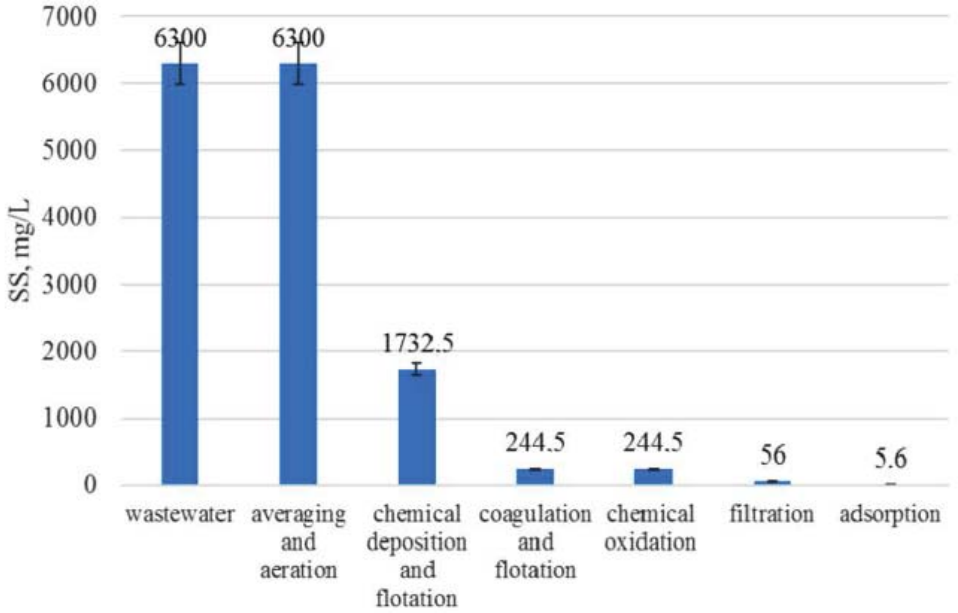

Fig. 2. **Change in the rate of suspended solids in soap stocks during treatment by technology:** averaging and aeration — chemical deposition, flotation — coagulation and flotation — chemical oxidation — filtration — adsorption

emulsion bonds between organic matter and water were destroyed, and the organic solution was destabilized. Due to the formation of small particles of calcium hydroxide with a large surface area, dissolved organic substances were adsorbed on their surface and precipitated. The release of carbon dioxide contributed to the saturation of water with gas bubbles, into which surfactants were released, which were released from the solution on the surface of the bubbles and float, forming foamy sediment on the surface of the water in the float. As a result of the processing of soapstock with calcium carbonate, followed by flotation, the effect of removing suspended solids of 70–75% was obtained, and the COD was reduced by 60%.

The research results on the processing of soapstock in some physical and chemical

processes of the technology given in the Table 1 showed the highest values of the effect of reducing COD — 80% with an initial COD of 40,000 mg/L, the effect of reducing the concentration of suspended solids — 70–75% with an initial 6 300 mg/L in the process of coagulation using $Al_2(SO_4)_3$ and flotation.

High effects were also observed for COD — 88–90% and suspended solids — 90% at the stage of soapstock adsorption. The use of other purification processes according to the investigated technological scheme made it possible to reduce the COD by 30% during aeration, by 60% during the chemical precipitation of $CaCO_3$ and flotation, by 70% during oxidation with hydrogen peroxide, by 65–68% during filtration on quartz filters. After all stages of sequential physical and chemical treatment according to the proposed technology, the obtained purified water was characterized by pollution indicators that did not exceed the permissible values for discharging to city treatment facilities with aeration tanks.

Based on the obtained results, the technology of local physical and chemical treatment of oil production soapstocks was developed (Fig. 3), process parameters were determined (aeration duration, reagent dose, flotation duration, oxidation, filtration rate, filtration loading height, amount of flotation sludge, and sediment formed, etc.).

The technology included the sequential processes of physical and chemical wastewater treatment — averaging, alkalization with calcium carbonate, stage I of flotation, coagulation, stage II of flotation, oxidation with hydrogen peroxide, filtration through quartz filters and absorption on carbon filters. Taking into account the uneven removal of the soap solution of oil production and fluctuations in the concentration of pollutants during a day, to equalize the quantitative and qualitative composition of wastewater when it entered the treatment plant for local treatment, it was required to use wastewater averaging, which was carried out using an aeration system.

The use of wastewater aeration in the balancing tank enabled up to 30% of organic substances contained in industrial wastewater to be oxidized with oxygen in the first stage.

At the first stage of wastewater treatment, it is recommended to use calcium carbonate $CaCO_3$ as a precipitating agent. When calcium carbonate reacts with water, poorly soluble calcium hydroxide is formed and carbon dioxide is liberated. The pH of the water increases, the emulsion bonds between organic matter and water are destroyed, and the organic solution is destabilized. Due to the formation of small particles of calcium hydroxide with a large surface area, dissolved organic substances were adsorbed on their surface and precipitated.

Table 2. **Change in soap stock indicators at certain stages of processing according to the proposed technology**

No	Stages of technology, indicators	At the inlet	At the outlet	E,%
1	Averaging and aeration COD, mgO_2/L Suspended solids, mg/L	 40 000 6 300	 28 000 6 300	 30 0
2	Chemical precipitation with $CaCO_3$ and flotation Suspended solids, mg/L COD, mgO_2/L	 6 300 28 000	 1 575–1 890 11 200	 70–75 60
3	Coagulation with $Al_2(SO_4)_3$ and flotation Suspended solids, mg/L COD, mgO_2/L	 1 575–1 890 11 200	 205–284 2 240	 85–87 80
4	Chemical oxidation with H_2O_2 Suspended solids, mg/L COD, mgO_2/L	 205–284 2 240	 205–284 672	 0 70
5	Filtration on quartz filters (2 stages) Suspended solids, mg/L COD, mgO_2/L	 205–284 672	 41–71 215–235	 75–80 65–68
6	Adsorption on pressure adsorption filters (2 stages) Suspended solids, mg/L COD, mgO_2/L	 41–71 215–235	 4.1–7.1 22–28	 90 88–90
7	Adsorption on pressure adsorption filters (2 stages) Suspended solids, mg/L COD, mgO_2/L	 41–71 215–235	 4.1–7.1 22–28	 90 88–90

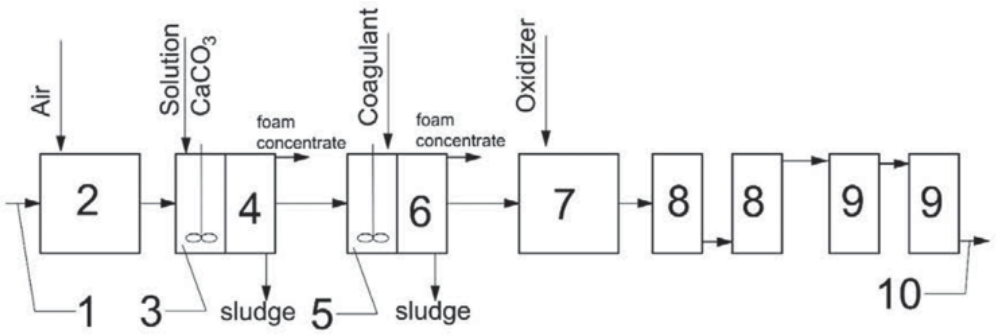

Fig. 3. **Technology scheme of the local physical and chemical vegetable oil production soapstock:**
1 — wastewater from the factory; *2* — averaging; *3* — alkalizing with calcium carbonate; *4* — flotation of the first stage; *5* — coagulation; *6* — flotation of the II stage; *7* — oxidation by hydrogen peroxide; *8* — filtration through quartz filters (2 stages); *9* — adsorption on carbon filters (2 stages); *10* — treated water in the city sewer

The release of carbon dioxide contributed to the water saturation with gas bubbles, which attached to the surfactants released from the solution on the surface of the bubbles and float, forming foamy sediment on the water surface at stage I of flotation with air supply through wonderful materials. The recommended dose of calcium carbonate is 1.8–2.0 g/L, pH 5.5. The air supply to the skimmer must provide the process with gas and could be carried out in case of insufficient amount of carbon dioxide formed as a result of the reaction, for example, in case of a decrease in the reaction temperature, etc. Duration of flotation was 75 minutes.

Removal of pollutants from wastewater by flotation occurred due to the adhesion of polluting particles to the carbon dioxide bubbles formed in the reaction chamber and the air that was introduced into the water by aerators with a porous surface. Surfactants and slurry fine particles attached to the gas bubbles. The resulting complexes "bubble — solid particle — surfactant" floated to the surface of the water, forming a layer of foam (flotation sludge). Flotation was considered as a molecular adhesion process of flotation material particles at the interface between two phases — gas (air) and water. Foam and sludge were periodically removed from the float for disposal.

The next wastewater treatment process was the coagulation of pollutants with a mineral coagulant, for example, aluminum sulfate — $Al_2(SO_4)_3$ at a dose of 1–1.2 g/L at an optimum pH of 5.5. It is possible to use flocculants, for example, polyacrylamide (PAA) at a dose of 10 mg/L to form large flocs and intensify the deposition of coagulant flocs.

Due to the large specific surface area of colloidal particles, they have significant surface energy and, as a consequence, high adsorption capacity, due to which there was an effective adsorption of substances dissolved in wastewater on the surface of the resulting colloidal particles.

The use of flocculants is based on the action of flocculants, which is based on the flocculant molecules adsorption on the surface of colloidal particles, the formation of a network structure of flocculants molecules and the adhesion of colloidal particles due to van der Waals forces. Under the action of flocculants, three-dimensional structures were formed between colloidal particles, capable of faster and more complete separation from the liquid phase. Flocculation was carried out to intensify the formation of aluminum hydroxide flakes in order to increase the rate of their deposition. The use of flocculants enables to reduce the dose of coagulants, reduce the duration of coagulation and increase the of deposition rate of the resulting flocs.

Thus, with the introduction of coagulant and flocculants into industrial wastewater due to coagulation and flocculation, contaminants were removed from wastewater — impurities of varying degrees of dispersion — finely dispersed, colloidal and molecularly soluble substances due to the adsorption of these substance on the surface of mineral coagulants flocs that were formed in water, providing the necessary conditions for coagulation. Stage II flotation with aeration through porous materials was used to separate the formed flocs with adsorbed pollutants from water. The duration of the flotation was taken as 75 min. Flotation sludge was periodically removed for disposal.

Then, according to the technology (Fig. 3), the wastewater after flotation of the II stage was directed to the oxidation of pollutants remaining in the wastewater at the outlet of the flotation of the II stage, using hydrogen peroxide H_2O_2 as an oxidizer at a dose of 1.5–1.8 g/L, pH 4.5–5.5 for 2 hours, and

contact of wastewater with an oxidizing agent under stirring conditions to carry out reactions between hydrogen peroxide and pollutants. The advantages of hydrogen peroxide using over other oxidizing reagents were the high oxidation efficiency of organic substances, the absence of residual concentrations of hydrogen peroxide in the treated wastewater due to its decomposition, the stability of the salinity of the treated wastewater, and reactions without toxic intermediate products.

The final process in the technology was wastewater filtration. For example, at first it was through loading a sand filter, the through coal. Due to filtration, small impurities were removed from the wastewater, which, after the settling stage, were removed by a stream of water: small coagulant flakes; colloidal substances that were retained on the surface of the grains of the filtering loaded due to the action of adhesion forces, mutual coagulation of colloids, adsorption on the surface of the load.

Conclusions

Experimental studies have determined rational parameters for processing soapstocks in the production of oils: efficiency at different stages of processing, duration of aeration, dose of reagents, duration of flotation and oxidation, filtration rate, height of filtering load, amount of formed flotation sludge and sediment.

A local treatment technology was proposed. The technology includes the following processes: wastewater averaging, reagent treatment of $CaCO_3$ with flotation using aeration through porous materials, reagent treatment with coagulant $Al_2(SO_4)_3$ with flotation, similarly, chemical oxidation with hydrogen peroxide H_2O_2, two-stage filtration on two-stage filtration on absorption filters.

When choosing a technology, the irregularity of industrial wastewater flow, the nature, concentration and phase-dispersed composition of pollutants in oil production soapstocks, the results of sample analysis according to the following indicators as pH, suspended particles, COD, etc., and the results of experimental studies of treatment were taken into consideration. The technology ensured high-quality processing of soapstocks. Purified water according to the proposed technology could be discharged into the city sewage system and would not interfere with the operation of city treatment facilities.

This study did not receive any financial support from a government, community or commercial organization. The authors state that they have no conflict of interest.

REFERENCES

1. *Abdel-Gawad S., Abdel-Shafy M.* Pollution control of industrial wastewater from soap and oil industries: a case study. *Water science and technology*: *a journal of the International Association on Water Pollution Research*. 2002, V. 46, P. 77–82. https://doi.org/10.2166/wst.2002.0556
2. *Liu J., Lien C.* Pretreatment of bakery wastewater by coagulation-flocculation and dissolved air flotation. *Water science and technology: a journal of the International Association on Water Pollution Research*. 2011, V. 43, P. 131–137. https://doi.org/10.2166/wst.2001.0482
3. *Chatoui M., Lahsaini S., Souabi S., Bahlaoui M., Amane J.* Removal of Wastewater Soaps by Coagulation Flocculation Process. *J. Colloid Sci. Biotechnol.* 2016, V. 5, P. 212–217. https://doi.org/10.1166/jcsb.2016.1148
4. *Drillia P., Kornaros M., Lyberatos G.* Wastewater treatment from a motor-oil reforming company using a sequencing batch reactor (SBR). *Water Sci. Technol*. 2003, 47 (10), 25–32. https://doi.org/10.2166/wst.2003.0529
5. *Antonic B., Dordević D., Jancikova S., Tremlová B., Kushkevych I.* Physicochemical Characterization of Home-Made Soap from Waste-Used Frying Oils. *Processes*. 2020, V. 8, P. 1219. https://doi.org/10.3390/pr8101219
6. *Tekade P. V., Mohabansi N. P., Patil V. B.* Study of physic-chemical properties of effluent from soap and detergent industry in Wardha. *Rasayan J*. 2011, 2 (4), 461–465.
7. *Martins Rui C., Quinta-Ferreira Rosa M.* Comparison of Advanced Oxidation Processes (AOPs) based on O_3 and H_2O_2 for the remediation of real wastewaters. *J. Advanced Oxidation Technol.* 2011, V. 14, P. 282–291. https://doi.org/10.1515/jaots-2011-0214
8. *Kiuri H.* Development of Dissolved Air Flotation Technology from the First Generation to the Newest (Third) one (DAF in Turbulent Flow Conditions). *Water science and technology: a journal of the International Association on Water Pollution Research*. 2001, 43 (8), 1–7. https://doi.org/10.2166/wst.2001.0450
9. *Saththasivam J., Loganathan K., Sarp S.* An overview of oil–water separation using gas flotation systems. *Chemosphere*. 2016, V. 144, P. 671–680. https://doi.org/10.1016/j.chemosphere.2015.08.087
10. *Kweinor Tetteh E., Rathilal S.* Effects of a polymeric organic coagulant for industrial mineral oil wastewater treatment using response surface methodology (RSM). *Water SA*. 2018, 44 (2), 155–161. https://doi.org/10.4314/wsa.v44i2.02

ПРОБЛЕМИ ОЧИЩЕННЯ СОАПСТОКІВ ОЛІЙНИХ ВИРОБНИЦТВ ТА ЇХ ВИРІШЕННЯ

Л. Саблій[1], *В. Жукова*[1], *С. Кононцев*[2], *О. Ободович*[3], *В. Сидоренко*[3]

[1]Національний технічний університет України «Київський політехнічний інститут імені Ігоря Сікорського»
[2]Національний університет водного господарства та природокористування, Рівне, Україна
[3]Інститут технічної теплофізики НАН України, Київ

E-mail: verolis86@gmail.com

Стічні води, які утворюються під час виробництва олії, містять різноманітні забруднювальні речовини, які переходять у стічні води під час перероблення соапстоків: жири й жирні кислоти та їхні солі (водні розчини мил), гліцерол, фосфогліцериди, нейтральний жир, фосфатиди, протеїни, вуглеводи, забарвлювальні речовини (каротин, каротиноїди, хлорофіл та ін.), речовини, які не омилюються, та воскоподібні, солі — сульфат і хлорид натрію, механічні домішки тощо.

Мета. Дослідити процеси очищення виробничих стічних вод олійного виробництва та запропонувати ефективну технологію їх локального очищення до нормативних вимог у процесі скидання очищених стічних вод у систему водовідведення міста.

Методи. Хімічне споживання кисню (ХСК) визначали біхроматним методом. Концентрацію завислих речовин — гравіметричним методом.

Результати. У процесі оброблення соапстоків карбонатом кальцію з подальшою флотацією було отримано ефект видалення завислих речовин на 70–75%, зниження ХСК — на 60%. На основі досліджень було запропоновано технологію очищення соапстоків, що включає послідовні процеси фізико-хімічного очищення стічних вод — усереднення, підлужування карбонатом кальцію, I ступінь флотації, коагуляція, II ступінь флотації, окиснення пероксидом водню, фільтрацію через кварцові фільтри та адсорбцію на вугільних фільтрах.

Висновки. Розроблено ефективну технологію попереднього очищення соапстоків олійного виробництва. Це дасть змогу значно знизити концентрації органічних речовин та інших забруднень у соапстоках, що суттєво знизить вплив таких стоків на процеси біологічного очищення стічних вод міських очисних станцій.

Ключові слова: соапстоки; рослинна олія; забруднювальні речовини; технологія очищення; стічні води.

ПРОБЛЕМЫ ОЧИСТКИ СОАПСТОКОВ МАСЛИЧНОГО ПРОИЗВОДСТВА И ИХ РЕШЕНИЕ

Л. Саблий[1], *В. Жукова*[1], *С. Кононцев*[2], *О. Ободович*[3], *В. Сидоренко*[3]

[1]Национальный технический университет Украины «Киевский политехнический институт имени Игоря Сикорского».
[2]Национальный университет водного хозяйства и природопользования, Ровно, Украина
[3]Институт технической теплофизики НАН Украины, Киев

E-mail: verolis86@gmail.com

Сточные воды, образующиеся при производстве масла, содержат различные загрязняющие вещества, которые переходят в сточные воды при переработке соапстоков: жиры и жирные кислоты и их соли (водные растворы мыл), глицерол, фосфоглицериды, нейтральный жир, фосфатиды, протеины, углеводы, окрашивающие вещества (каротин, каротиноиды, хлорофилл и др.), вещества, которые не омыляются, и воскообразные, соли — сульфат и хлорид натрия, механические примеси и т. п.

Цель. Исследовать процессы очистки производственных сточных вод масличного производства и предложить эффективную технологию их локальной очистки до нормативных требований в процессе сброса очищенных сточных вод в систему водоотведения города.

Методы. Химическое потребление кислорода (ХПК) определяли бихроматным методом. Концентрацию взвешенных веществ — гравиметрическим методом.

Результаты. В процессе обработки соапстоков карбонатом кальция с последующей флотацией был получен эффект удаления взвешенных веществ на 70–75%, снижение ХПК — на 60%. На основе исследований была предложена технология очистки соапстоков, включающая последовательные процессы физико-химической очистки сточных вод — усреднение, подщелачивание карбонатом кальция, I ступень флотации, коагуляция, II ступень флотации, окисление пероксидом водорода, фильтрацию через кварцевые фильтры и адсорбцию на угольных фильтрах.

Выводы. Разработана эффективная технология предварительной очистки соапстоков масляного производства. Это позволит значительно снизить концентрации органических веществ и других загрязнений в соапстоках, что существенно снизит влияние таких стоков на процессы биологической очистки сточных вод городских очистных станций.

Ключевые слова: соапстоки; растительное масло; загрязняющие вещества; технология очистки; сточные воды.